論文 / 著書情報
Article / Book Information

題目(和文)	
Title(English)	Optical second harmonic generation from phthalocyanine thin films
著者(和文)	山田俊樹
Author(English)	Toshiki Yamada
出典(和文)	学位:博士(工学), 学位授与機関:東京工業大学, 報告番号:甲第3327号, 授与年月日:1996年9月30日, 学位の種別:課程博士, 審査員:
Citation(English)	Degree:Doctor (Engineering), Conferring organization: Tokyo Institute of Technology, Report number:甲第3327号, Conferred date:1996/9/30, Degree Type:Course doctor, Examiner:
学位種別(和文)	博士論文
Type(English)	Doctoral Thesis

Optical Socond Harmonic Generation from Phthalocyanine Thin Films

by

Toshiki Yamada

A Thesis Submitted to
Tokyo Institute of Technology

Department of Organic and Polymeric Materials
Faculty of Engineering
Tokyo Institute of Technology

September, 1996

- Contents -

Chapter 1 Introduction

1-1 The second harmonic generation from higher order mechanisms

According to a symmetrical consideration, the second-harmonic generation (SHG) is forbidden for a centrosymmetric system under the electric dipole approximation. However, going beyond the electric dipole approximation and including multipole interactions, the SHG is also allowed in centrosymmetric systems. Theory in SHG including the higher order contributions was developed in 1960's [1-4]. Adler [2] classified the origin of sum frequency generation into five possible mechanisms (the electric dipole (ED) mechanism, the electric quadrupole coupling (EQC) mechanism, the magnetic dipole coupling (MDC) mechanism, the electric quadrupole (EQ) mechanism and the magnetic dipole (MD) mechanism), in which the last four mechanisms are also allowed in centrosymmetric systems, about which we will describe in chapter 2. In experimental, Terhune et al. [5] observed the SHG from a calcite which has an inversion symmetry for the first time. Subsequently, the SHG from inorganic insulators such as alkali halides and semiconductors such as Ge and Si and metals such as Au and Ag was observed [4,6]. In the measurements, not only the bulk contribution but also the surface contribution for the SHG were discussed. After that, many researchers pointed out the significant bulk contribution for the SHG from Si and Ge with well-controlled experiments [7-9]. They also observed the rotational anisotropy reflection SHG with various polarization conditions from Si(001) face, which implies the contribution of the bulk anisotropic term constructed from the

tensor components of EQ and EQC mechanisms, as will be described in chapter 2. Sipe et al. [10] presented the phenomenological theory of the SHG obtained in reflection from the surface and the bulk of cubic centrosymmetric single crystal with more general form.

Recently, the relatively strong SHG from C_{60} [11-18] and copper phthalocyanine (CuPc) [19-21] vacuum evaporation films has been observed and considerable attention has been paid to the origin of the SHG. Koopmans et al. [16] performed the thickness scan of SHG with various polarization conditions for C_{60} films using 689 nm fundamental wavelength and demonstrated that the resonant SHG in C_{60} films is of bulk character and is due to the MDC mechanism and the dominance originates from the resonant MD transition ($^1A_g \rightarrow {}^1T_{1g}$) at the fundamental frequency. They also obtained an effective value (1.8×10^{-8} esu) for a general $\chi^{(2)}$, which is an order of magnitude larger than the non-resonant $\chi^{(2)}$ value (1.9×10^{-9} esu) of quartz. Wilk et al. [18] indicated that the SHG in C_{60} films at 1064 nm fundamental wavelength originates from the ED transition and the vibration-assisted ED transition at SH frequency (the MDC mechanism and the EQC mechanism) and the EQ transition at the SH frequency (the EQ mechanism). Qin et al. [22] calculated the dispersion of the nonlinear susceptibilities for EQ mechanism in a C_{60} molecule on the basis of the Su-Schrieffer-Heeger (SSH) model, while Shuai and Brédas [23-25] calculated those for EQC and MDC mechanisms using a valence effctive Hamiltonian (VEH) method.

Chollet et al. [19] observed the relatively strong SHG for a CuPc film using 1064 nm fundamental wavelength for the first time. Kumagai et al. [21] also measured the thickness dependence of SHG for CuPc films using 1064 nm fundamental wavelength and obtained the $\chi^{(2)}$ value (4.5×10^{-8} (esu)). Then, they assumed that the film is

polar ($C_{\infty v}$) with respect to the surface normal as a bulk, and analyzed it on the basis of the electric dipole mechanism and considered no other possibilities.

Considerable attention [26-36] also has been paid to the SHG from systems consisted of chiral molecules apart from centrorsymmetric or noncentrosymmetric systems. Some of them have relation to higher order mechanisms (especially, MD and/or MDC mechanisms).

Recently, it has been possible to use wavelength-changeable coherent light sources due to the evolution of laser and the invention of many useful nonlinear optical crystals. Using these light sources, the nonlinear optical spectroscopy such as third-harmonic generation (THG), and two-photon absorption (TPA), sum-frequency generation (SFG) [37,38], was introduced in order to clarify the electronic structure including the electric dipole forbidden states for atomic vapors. For inorganic semiconductors and insulators, the nonlinear spectroscopy was used in order to investigate the various electronic excited states. Recently, considerable attention has been paid to the nonlinear spectroscopy which have relation to a magnetic dipole transition and an electric quadrupole transition [39-41]. For organic materials, nonlinear optical spectroscopy such as THG and TPA spectrum measurements has been ever used, while SFG (SHG) spectrum measurement have been little concerned as a means of probing electric dipole forbidden states.

In this study, we performed the SHG spectrum measurement in order to clarify the origin of the SHG from phthalocyanine films. The resonant enhancement was observed at an SH frequency due to the EQ mechanism and was used to investigate the electric dipole forbidden states. Thickness dependent SHG measurement was also

performed to support the assignment of the origin. The rotational angle dependent SHG measurement using the epitaxially grown phthalocyanine films on alkali halides also gives us useful informations on the origin of the SHG.

1-2 The electronic structure and linear absorption spectrum of phthalocyanines

Considerable attention has been paid to the electric properties and the optical properties of the phthalocyanines from fundamental and application viewpoints, about which many authors have written books [42,43] and review articles [44,45]. Here, we briefly describe the electronic structures and linear absorption spectra of phthalocyanines. The molecular structures of general phthalocyanines are illustrated in Figs. 1-2-1(a) and 1-2-1(b). Thus, phthalocyanines have a π-conjugate ring system and belong to D_{4h} or D_{2h} structure except some phthalocyanines. In phthalocyanines, π type, σ type and metal dominant d molecular orbitals construct the molecular levels. We show character tables and the correlation table for D_{4h} and D_{2h} system in Table 1-2-1, which are useful for the following discussion.

At first, we consider π type orbitals shown in Fig. 1-2-2. Electrons are occupied till a_{1u} and a_{2u} orbitals for D_{4h} systems and a_u and b_{1u} for the D_{2h} system, and e_g^*, b_{1u}^* and b_{2u}^* orbitals for D_{4h} systems and b_{2g}^*, b_{3g}^*, a_u^* and b_{1u}^* orbitals for the D_{2h} system are unoccupied. The strong absorption in visible region originates from the π-π^* transition ($a_{1u} \rightarrow e_g^*$) for D_{4h} systems or ($a_u \rightarrow b_{2g}^*$, b_{3g}^*) for the D_{2h} system, which is called by the name of Q-absorption band. The strong absorption in ultra-vioret region comes from the π-π^*

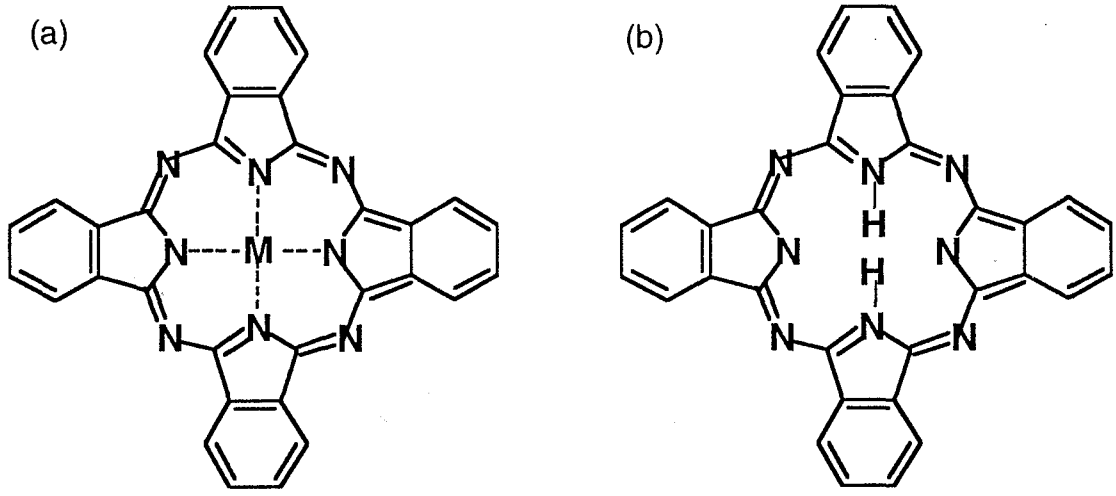

Fig. 1-2-1 The molecular structure of phthalocyanines. Here, the "M" and "Pc" in MPc mean a metal element and phthalocyanine, respectively.

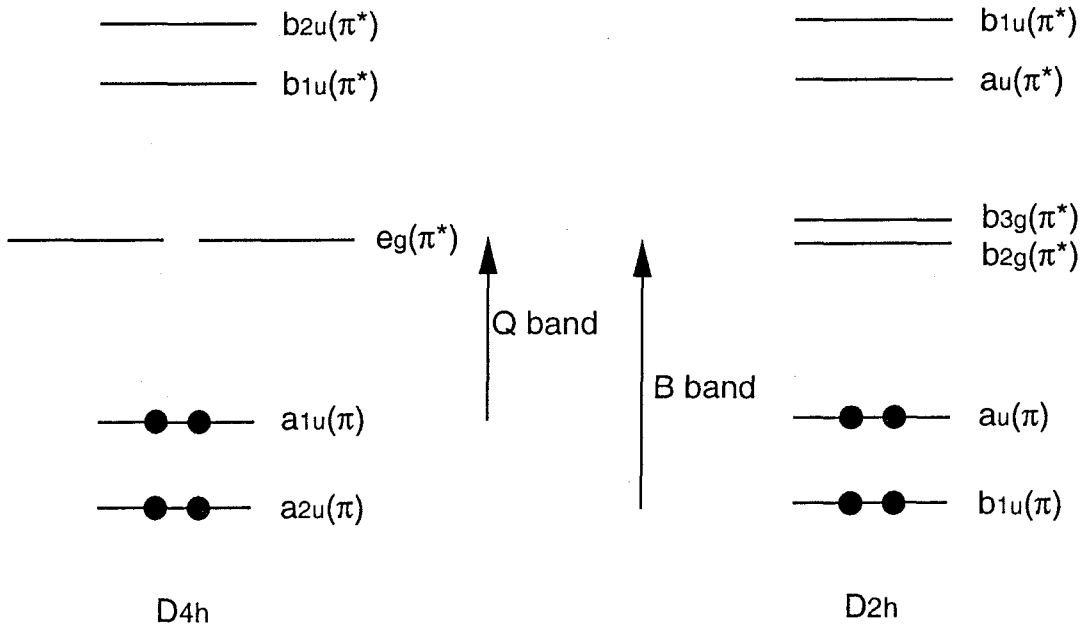

Fig. 1-2-2 π type orbitals of phthalocyanines.

D_{4h}	E	$2C_4$	C_2	$2C_2'$	$2C_2''$	i	$2S_4$	σ_h	$2\sigma_v$	$2\sigma_d$		[4/mmm]
A_{1g}	1	1	1	1	1	1	1	1	1	1		x^2+y^2, z^2
A_{2g}	1	1	1	-1	-1	1	1	1	-1	-1	R_z	
B_{1g}	1	-1	1	1	-1	1	-1	1	1	-1		x^2-y^2
B_{2g}	1	-1	1	-1	1	1	-1	1	-1	1		xy
E_g	2	0	-2	0	0	2	0	-2	0	0	(R_x, R_y)	(xz, yz)
A_{1u}	1	1	1	1	1	-1	-1	-1	-1	-1		
A_{2u}	1	1	1	-1	-1	-1	-1	-1	1	1	z	
B_{1u}	1	-1	1	1	-1	-1	1	-1	1	1		
B_{2u}	1	-1	1	-1	1	-1	1	-1	1	-1		
E_u	2	0	-2	0	0	-2	0	2	0	0	(x, y)	

D_{2h}	E	C_2	$C_2(y)$	$C_2(x)$	i	$\sigma(xy)$	$\sigma(xz)$	$\sigma(yz)$		[mmm]
A_g	1	1	1	1	1	1	1	1		x^2, y^2, z^2
B_{1g}	1	1	-1	-1	1	1	-1	-1	R_z	xy
B_{2g}	1	-1	1	-1	1	-1	1	-1	R_y	xz
B_{3g}	1	-1	-1	1	1	-1	-1	1	R_x	yz
A_u	1	1	1	1	-1	-1	-1	-1		
B_{1u}	1	1	-1	-1	-1	-1	1	1	z	
B_{2u}	1	-1	1	-1	-1	1	-1	1	y	
B_{3u}	1	-1	-1	1	-1	1	1	-1	x	

π type orbitals for phhtalocyanines change the sign for a σ_h operation.

D_{4h}	D_4	C_2' D_{2h}	C_2'' D_{2h}	C_2' D_{2d}	C_2'' D_{2d}	C_{4h}	C_{4v}	C_4	S_4
A_{1g}	A_1	A_g	A_g	A_1	A_1	A_g	A_1	A	A
A_{2g}	A_2	B_{1g}	B_{1g}	A_2	A_2	A_g	A_2	A	A
B_{1g}	B_1	A_g	B_{1g}	B_1	B_2	B_g	B_1	B	B
B_{2g}	B_2	B_{1g}	A_g	B_2	B_1	B_g	B_2	B	B
E_g	E	$B_{2g}+B_{3g}$	$B_{2g}+B_{3g}$	E	E	E_g	E	E	E
A_{1u}	A_1	A_u	A_u	B_1	B_1	A_u	A_2	A	B
A_{2u}	A_2	B_{1u}	B_{1u}	B_2	B_2	A_u	A_1	A	B
B_{1u}	B_1	A_u	B_{1u}	A_1	A_2	B_u	B_2	B	A
B_{2u}	B_2	B_{1u}	A_u	A_2	A_1	B_u	B_1	B	A
E_u	E	$B_{2u}+B_{3u}$	$B_{2u}+B_{3u}$	E	E	E_u	E	E	E

Table 1-2-1 Character tables for D_{4h} and D_{2h} symmetries and the correlation table.

transition ($a_{2u} \rightarrow e_g^*$) for D_{4h} systems or ($b_{1u} \rightarrow b_{2g}^*$, b_{3g}^*) for the D_{2h} system which is called by the name of B-absorption band. The results of Extended Hüchel calculations under one electron approximation for the various phthalocyanines are displayed in Fig. 1-2-3, which is quoted from refs. [46,47]. Thus, we find σ type and metal dominant d orbitals in addition to π type orbitals. Though there exist some σ orbitals near $a_{1u}(\pi)$ and $a_{2u}(\pi)$ for D_{4h} systems and $a_u(\pi)$ and $b_{1u}(\pi)$ for the D_{2h} system, these levels may be located lower than $a_{2u}(\pi)$ level according to the recent *ab-initio* calculations for magnesium phthalcyanine (MgPc) [48]. In fact, Schaffer et al. pointed out that the positions of these σ orbitals have poor reliability in ref. [46].

The samples studied were CuPc, metal-free phthalocyanine (H_2Pc) and vanadyl phthalocyanine (VOPc) which have D_{4h}, D_{2h} and C_{4v} symmetries, respectively. We used the vacuum evaporation films on the glass substarate or the alkali halide substrate of the phthalocyanines as the sample films. Such films are made of the polycrystals of phthalocyanine. In general, molecular crystals are molecular condensed matters in which molecules are connected weekly by van der Waals force and/or intermolecular dipole-dipole interaction. Therefore, electronic structure in a molecular crystal is some different from that in the orientation gas model due to the existence of interactions between molecules. States such as charge transfer excitons [49,50] have also been observed in phthalocyanine crystals [51,52]. However, the orientation gas model may be adequate to use as the first approximation.

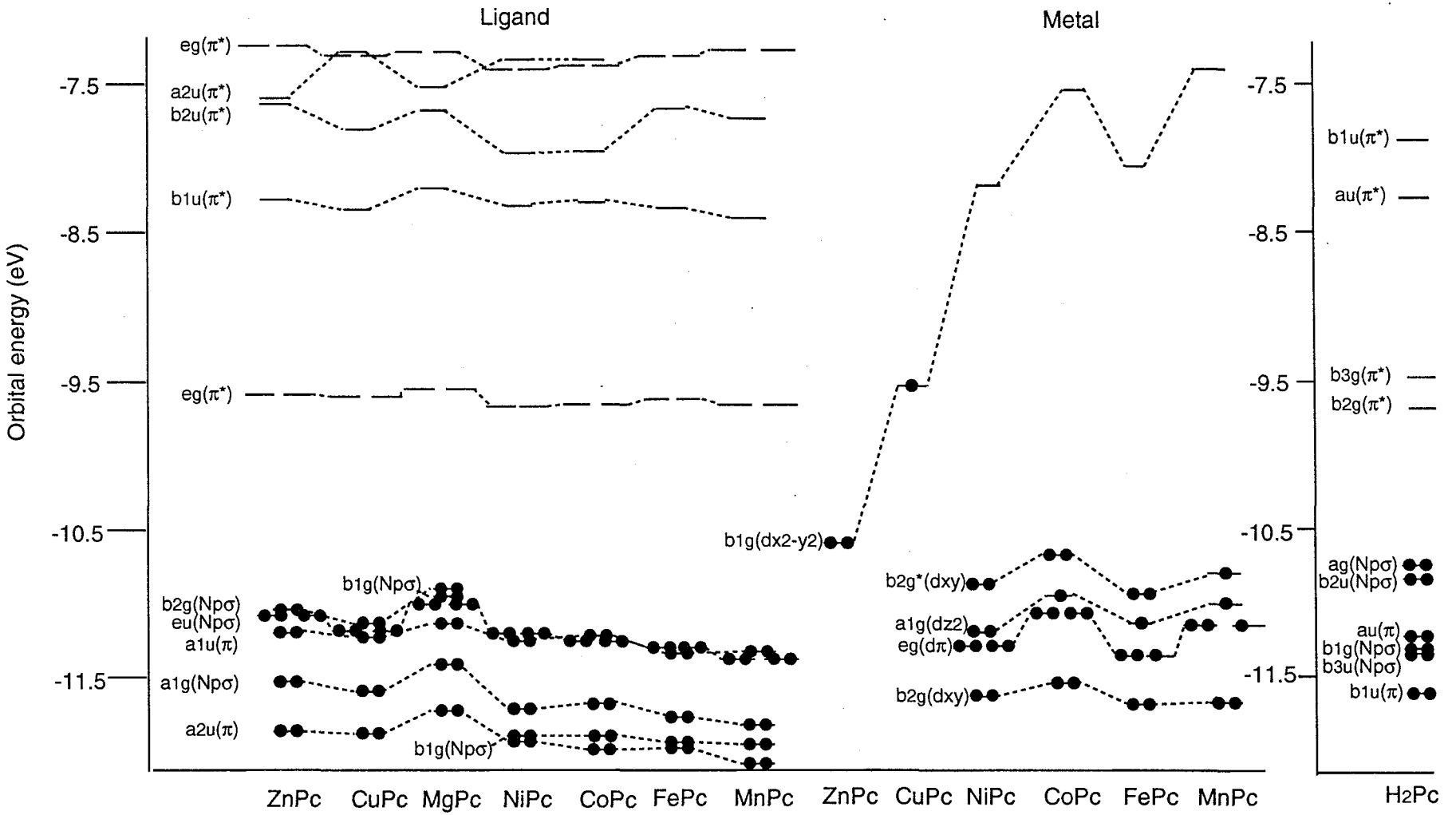

Fig. 1-2-3 Extended Hüchel caluculations under one electron approximation for phthalocyanines
This figure is quoted from refs. [46,47].

1-3 Purpose and outline of this thesis

This thesis was undertaken to clarify the origin of the relatively strong SHG from phthalocyanine thin films. For this purpose, we performed the thickness, rotational and spectral dependent SHG measurements for phthalocyanine films on glass substrates and epitaxially grown phthalocyanine films on alkali halides. Especially, we noticed that the SHG spectrum measurement provides us with a useful tool for studying electric-dipole-forbidden states and electric-quadrupole allowed and/or magnetic-dipole-allowed states.

In chapter 2, we described expressions of the nonlinear susceptibilities of SHG from higher order mechanisms and the analysis for various systems and geometries, which include systems used in this study.

In chapter 3, we mentioned experimental results of thickness dependent SHG for CuPc films on a glass substrate. Then, we found the deviation from the ED mechanism as a bulk which has ever been proposed. The experimental results were reproduced with higher order mechanisms except for the MD mechanism.

In chapter 4, in-plane anisotropic SHG was observed in CuPc films epitaxially grown on KCl and VOPc films epitaxially grown on KBr. The observed periodic signal indicates the significant contribution of EQ and EQC mechanisms.

In chapter 5, spectral dependent SHG for CuPc and H_2Pc films on a glass substrate and the epitaxially grown VOPc film were investigated. Then, a sharp peak was observed at the high-energy edge of the Q-absorption band for both CuPc and H_2Pc films on the glass substrate at 1100 nm fundamental wavelength, which implies the dominance of the EQ mechanism due to the EQ resonant

transition at SH frequency. We discussed the origin with the orientation gas model, which was supported by rotational anisotropic SHG described in chapter 4. We also observed a resonant peak at the high-energy edge of the Q-absorption band for the epitaxially grown VOPc film.

In chapter 6, the main results of previous chapters were summarized.

References

[1] P. S. Pershan, Phys. Rev. **130**, 919 (1963).

[2] E. Adler, Phys. Rev. **134**, A728 (1964).

[3] N. Bloembergen and Y. R. Shen, Phys. Rev. **141**, 298 (1966).

[4] N. Bloembergen, R. K. Chang, S. S. Jha, and C. H. Lee, Phys. Rev. **174**, 813 (1968).

[5] R. W. Terhune, P. D. Maker, and C. M. Savage, Phys. Rev. Lett. **8**, 404 (1962).

[6] F. Brown, R. E. Parks, and A. M. Sleeper, Phys. Rev. Lett. **14**, 1029 (1965).

[7] H. W. K. Tom, T. F. Heinz, and Y. R. Shen, Phys. Rev. Lett. **51**, 1983 (1983).

[8] J. A. Litwin, J. E. Sipe, and H. M. van Driel, Phys. Rev. B **31**, 5543 (1985).

[9] G. Lüpke and G. Marowsky, Appl. Phys. B **53**, 71 (1991).

[10] J. E. Sipe, D. J. Moss, and H. M. van Driel **35**, 1129 (1987).

[11] H. Hoshi, N. Nakamura, Y. Maruyama, T. Nakagawa, S. Suzuki, H. Shiromaru, and Y. Achiba, Jpn. J. Appl. Phys. **30**, 1397 (1991).

[12] X. K. Wang, T. G. Zhang, W. P. Lin, Sheng Zhong Liu, G. K. Wong, Manfred M. Kappes, R. P. H. Chang, and J. B. Ketterson, Appl. Phys. Lett. **60**, 810 (1992).

[13] T. G. Zhang, Z. Y. Xu, P. M. Lundquist, W. P. Lin, J. B. Ketterson, G. K. Wong, X. K. Wang, and R. P. H. Chang, Opt. Commun. **111**, 517 (1994).

[14] Y. Liu, H. Jiang, W. Wang, Y. Li, and J. Zheng, Phys. Rev. B **50**, 4940 (1994).

[15] B. Koopmans, A. Anema, H. T. Jonkman, G. A. Sawatzky, and F. van der Woude, Phys. Rev. B **48**, 2759 (1993).

[16] B. Koopmans, A. M. Janner, H. T. Jonkman, G. A. Sawatzky, and F. van der Woude, Phys. Rev. Lett. **71**, 3569 (1993).

[17] B. Koopmans, A. M. Janner, H. A. Wierenga, Th. Rasing, G. A. Sawatzky, F. van der Woude, Appl. Phys. A **60**, 103 (1995).

[18] D. Wilk, D. Johannsman, C. Stanners, and Y. R. Shen, Phys. Rev. B **51**, 10057 (1995).

[19] P. A. Chollet, F. Kajzar, and J. Le Moigne, Proc. SPIE, **1273**, 87 (1990).

[20] F. Kajzar, P. A. Chollet, I. Ledoux, J. Le Moigne, A. Lorin, and G. Gadret, in *Organic Molecules for Nonlinear Optics and Photonics*, edited by J. Messier et al. (Kluwer, Dordrecht, 1991), p.403.

[21] K. Kumagai, G. Mizutani, H. Tsukioka, T. Yamauchi, and S. Ushioda, Phys. Rev. B **48**, 14488 (1993).

[22] S. Qin, W. M. You, and Z. B. Su, Phys. Rev. B **48**, 17562 (1993).

[23] Z. Shuai and J. L. Brédas, Synth. Met. **55-57**, 2973 (1993).

[24] Z. Shuai and J. L. Brédas, Adv. Mater. **6**, 486 (1994).

[25] Z. Shuai and J. L. Brédas, Mol. Cryst. Liq. Cryst. **256**, 801 (1994).

[26] T. Petralli-mallow, T. M. Wang, J. D. Byers, H. I. Yee, J. M. Hicks, J. Phys. Chem. **97**, 1383 (1993).

[27] T. Verbiest, M. Kauranen, A. Persoons, M. Ikonen, J. Kurkela, H. Lemmetyinen, J. Am. Chem. Soc., **116**, 9203 (1994).

[28] M. Kauranen, T. Verbiest, J. J. Maki, A. Persoons, J. Chem. Phys. **101**, 8193 (1994).

[29] J. D. Byers, H. I. Yee, J. M. Hicks, J. Chem. Phys. **101**, 6233 (1994).

[30] J. D. Byers, H. I. Yee, T. Petralli-mallow, J. M. Hicks, Phys. Rev. B **49**, 14643 (1994).

[31] J. M. Hicks, T. Petralli-mallow, J. D. Byers, Faraday Discuss. **99**, 341 (1994).

[32] M. Kauranen, T. Verbiest, E. W. Meijer, E. E. Havinga, M. N. Teerenstra, A. J. Schouten, R. J. M. Nolte, A. Persoons, Adv. Mater. **7**, 641 (1995).

[33] J. D. Byers and J. M. Hicks, Chem. Phys. Lett. **231**, 216 (1994).

[34] J. J. Maki, M. Kauranen, and A. Persoons, Phys. Rev. B **51**, 1425 (1995).

[35] A. P. Shkurinov, A. V. Dubrovskii, and N. I. Koroteev, Phys. Rev. Lett. **70**, 1085 (1993).

[36] E. W. Meijer, E. E. Havinga and G. L. J. Rikken, Phys. Rev. Lett. **65**, 37 (1990).

[37] D. S. Bethune, R. W. Smith, and Y. R. Shen, Phys. Rev. Lett. **37**, 431 (1976).

[38] D. S. Bethune, R. W. Smith, and Y. R. Shen, Phys. Rev. A **17**, 277 (1978).

[39] D. Fröhlich, M. Itoh and Ch. Pahlke-Lerch, Phys. Rev. Lett. **72** 1001 (1994).

[40] F. Minami, K. Inoue, Y. Kato, K. Yoshida, K. Era, Phys. Rev. Lett. **67**, 3708 (1991).

[41] K. Inoue, K. Yoshida, F. Minami and Y. Kato, Phys. Rev. B **45**, 8807 (1992).

[42] M. Tanaka and S. Koma, *Futaroshianin*, (Bunshinshuppan, Tokyo, 1991).

[43] F. Moser, A. L. Thomas, *The Phthalocyanine* (CRC, Boca Raton, 1993).

[44] K. Kasuga and M. Tsutsui, Coord. Chem. Rev. **32**, 67 (1980).

[45] M. R. Willis, Mol. Cryst. Liq. Cryst. **171**, 217 (1989).

[46] A. M. Schaffer, M. Gouterman, and E. R. Davidson, Theoret. chim. Acta (Berl.) **30**, 9 (1973).

[47] A. M. Schaffer and M. Gouterman, Theoret. chim. Acta (Berl.) **25**, 62 (1972).

[48] M. G. Cory, H. Hirose, and M. C. Zerner, Inorg. Chem. **34**, 2969 (1995).

[49] J. P. Hernandez and S. Choi, J. Chem. Phys. **50**, 1524 (1969).

[50] W. L. Pollans and S. Choi, J. Chem. Phys. **52**, 3691 (1970).

[51] Y. Tokura, T. Koda, Y. Iyechika, and H. Kuroda, Chem. Phys. Letters **102**, 174 (1983).

[52] H. Yoshida, Y. Tokura, and T. Koda, Chem. Phys. **109**, 375 (1986).

Chapter 2 Theoretical Background

2-1 Microscopic origin of sum frequency generation

In order to clarify the microscopic origin of sum-frequency generation (SFG), including a centrosymmtric system [1], we describe the microscopic expressions of the nonlinear susceptibilities for SFG on the basis of the time dependent perturbation theory [2]. The modification of obtained results to second-harmonic generation (SHG) can be made easily.

We assume that all of the properties of the atomic or the molecular system can be described in terms of the wave function $\psi(\boldsymbol{r}, t)$, which is the solution to the time dependent Schrödinger equation

$$i\hbar\frac{\partial\psi}{\partial t} = \hat{H}\psi \quad . \tag{2-1-1}$$

Here $\hat{H}$ is the Hamiltonian operator

$$\hat{H} = \hat{H}_0 + \hat{V}(\boldsymbol{r}, t) \quad , \tag{2-1-2}$$

which is written as the sum of the Hamiltonian $\hat{H}_0$ for a free molecule (atom) and an interaction Hamiltonian $\hat{V}(\boldsymbol{r}, t)$, which describes the interaction of the molecule (atom) with the electromagnetic field. We take the interaction Hamiltonian as follows.

$$\hat{V}(\boldsymbol{r}, t) = -\boldsymbol{\mu}\cdot\tilde{\boldsymbol{E}}(\boldsymbol{r}, t) - \boldsymbol{m}\cdot\tilde{\boldsymbol{H}}(\boldsymbol{r}, t) - \hat{q}:\nabla\tilde{\boldsymbol{E}}(\boldsymbol{r}, t) \quad , \tag{2-1-3}$$

where $\hat{\mu}$, $\hat{q}$, and $\hat{m}$ are an electric dipole operator, an electric quadrupole operator which is symmetric and traceless tensor and a magnetic dipole operator, respectively. These components are described as

$$\hat{\mu}_\alpha = -e\,\hat{r}_\alpha \quad , \tag{2-1-4a}$$

$$\hat{q}_{\alpha\beta} = -\frac{1}{6}e(3\hat{r}_\alpha\hat{r}_\beta - \hat{r}^2\delta_{\alpha\beta}) \quad , \tag{2-1-4b}$$

$$\hat{m}_\alpha = -\frac{e}{2mc}\hat{L}_\alpha \quad , \tag{2-1-4c}$$

($\hat{L} = \hat{r} \times \frac{\hbar}{i}\frac{\partial}{\partial \hat{r}}$; the angular momentum operator).

The electric field and magnetic field are defined as

$$\tilde{E}(r, t) = \sum_i E(\omega_i)e^{-i\omega_i t} \quad , \quad E(\omega_i) = E^0(\omega_i)e^{ik_i r} \quad , \quad E(-\omega_i) = E(\omega_i)^* \quad , \tag{2-1-5a}$$

$$\tilde{H}(r, t) = \sum_i H(\omega_i)e^{-i\omega_i t} \quad , \quad H(\omega_i) = H^0(\omega_i)e^{ik_i r} \quad , \quad H(-\omega_i) = H(\omega_i)^* \quad , \tag{2-1-5b}$$

and the summation is to be taken over positive- and negative-frequency. Then, eq. (2-1-3) is rewritten as

$$\hat{V}(r, t) = \sum_i \hat{V}(\omega_i)e^{-i\omega_i t} \quad , \quad \hat{V}(-\omega_i) = \hat{V}(\omega_i)^\dagger \quad . \tag{2-1-6}$$

In order to solve eq. (2-1-1) in terms of a perturbation expansion, we replace the Hamiltonian (2-1-2) by

$$\hat{H} = \hat{H}_0 + \lambda\hat{V}(r, t) \quad , \tag{2-1-7}$$

where λ is a continuous varying parameter ranging from zero to unity which characterizes the strength of the interaction. To seek a solution in the Schrödinger equation, the wave function is expanded in the form of a power series in λ as follows.

$$\psi(\boldsymbol{r}, t) = \psi^{(0)}(\boldsymbol{r}, t) + \lambda\psi^{(1)}(\boldsymbol{r}, t) + \lambda^2\psi^{(2)}(\boldsymbol{r}, t) + \cdots \quad . \tag{2-1-8}$$

We substitute eq. (2-1-8) to eq. (2-1-1) and require that all terms proportional to $\lambda^{(N)}$ satisfy the equality, so that we obtain the set of equations

$$i\hbar\frac{\partial\psi^{(0)}}{\partial t} = \hat{H}_0\psi^{(0)} \quad , \tag{2-1-9a}$$

$$i\hbar\frac{\partial\psi^{(N)}}{\partial t} = \hat{H}_0\psi^{(N)} + \hat{V}\psi^{(N-1)}, \quad (N = 1, 2, 3, \cdots) \quad . \tag{2-1-9b}$$

We assume that when the fields causing perturbation are turned on slowly, the system is initially in state g (typically the ground), so that the solution for the Schrödinger equation under no applied field is

$$\psi^{(0)}(\boldsymbol{r}, t) = u_g(\boldsymbol{r})e^{-i\omega_g t/\hbar} \quad \left(\quad \omega_g = \frac{E_g}{\hbar} \quad \right), \tag{2-1-10}$$

where Eg is an energy eigenvalue of state g. In order to solve eq. (2-1-9b), we use the fact that the energy eigenfunctions of the system constitute a complete set of basis function and any wave functions are expanded in terms of them. Then, $\psi^{(N)}(\boldsymbol{r}, t)$ is described as

$$\psi^{(N)}(\boldsymbol{r}, t) = \sum_l a_l^{(N)}(t)u_l(\boldsymbol{r})e^{-i\omega_l t} \quad , \tag{2-1-11}$$

where $u_l(\boldsymbol{r})$ and $a_l^{(N)}(t)$ give the spatially varying part of the energy eigenfunction and the probability amplitude, respectively. The following relations between the probability amplitudes are obtained by substituting eq.(2-2-11) into eq. (2-1-9b).

$$i\hbar \sum_l \dot{a}_l^{(N)}(t) u_l(\boldsymbol{r}) e^{-i\omega_l t} = \sum_l a_l^{(N-1)}(t) \hat{V} u_l(\boldsymbol{r}) e^{-i\omega_l t} \quad . \tag{2-1-12}$$

If we multiply each side from the left by $u_m^*(\boldsymbol{r})$ and integrate the resulting equation over all space, we obtain the equation

$$\dot{a}_m^{(N)} = \frac{1}{i\hbar} \sum_l a_l^{(N-1)}(t) <u_m|\hat{V}|u_l> e^{i\omega_{ml} t} \quad , \tag{2-1-13}$$

where $\omega_{ml} = \omega_m - \omega_l$. In the calculation, we used the orthonormality condition of eigenfunctions

$$<u_m|u_l> = \delta_{ml} \quad . \tag{2-1-14}$$

Since we have assumed that the fields causing perturbation are turned on exponentially slowly at $t = -\infty$, when the system is in a state g, $a_m^{(N)}$ can be obtained by time integration of eq. (2-1-13) in successive orders.

$$a_m^{(1)}(t) = \frac{1}{\hbar} \sum_p \frac{<u_m|\hat{V}(\omega_p)|u_g>}{\omega_{mg} - \omega_p} e^{i(\omega_{mg} - \omega_p)t} \quad , \tag{2-1-15a}$$

$$a_m^{(2)}(t) = \frac{1}{\hbar^2} \sum_{pq} \sum_n \frac{<u_m|\hat{V}(\omega_q)|u_g> <u_n|\hat{V}(\omega_p)|u_g>}{(\omega_{ng} - \omega_p - \omega_q)\ (\omega_{mg} - \omega_p)} e^{i(\omega_{mg} - \omega_p - \omega_q)t} \quad , \tag{2-1-15b}$$

$\cdots$.

Here, we used the relation $a_l^{(0)} = \delta_{lg}$ on the basis of our assumption and described up to $a_m^{(2)}$ terms, which are needed to describe SFG (SHG). Hence, $\psi^{(0)}$, $\psi^{(1)}$, and $\psi^{(2)}$ were obtained. We seek the second-order contribution $<\tilde{G}^{(2)}>$ (i.e. the contribution of the second order in $\hat{V}$) in the expectation value $<\tilde{G}> = <\tilde{G}^{(0)}> + <\tilde{G}^{(1)}> + <\tilde{G}^{(2)}> + \cdots = <\psi|\hat{G}|\psi>$. Here, ψ is obtained with λ set equal to one in eq. (2-1-8). $<\tilde{G}^{(2)}>$ is described by the equation

$$<\tilde{G}^{(2)}> = <\psi^{(0)}|\hat{G}|\psi^{(2)}> + <\psi^{(1)}|\hat{G}|\psi^{(1)}> + <\psi^{(2)}|\hat{G}|\psi^{(0)}>$$

$$= \frac{1}{\hbar^2}\sum_{pq}\sum_{mn}\left(\frac{<u_g|\hat{G}|u_n><u_n|\hat{V}(\omega_q)|u_m><u_m|\hat{V}(\omega_p)|u_g>}{(\omega_{ng}-\omega_p-\omega_q)(\omega_{mg}-\omega_p)}e^{-i(\omega_p+\omega_q)t}\right.$$

$$+\frac{<u_n|\hat{V}(\omega_q)|u_g>^*<u_n|\hat{G}|u_m><u_m|\hat{V}(\omega_p)|u_g>}{(\omega_{ng}^*-\omega_q)(\omega_{mg}-\omega_p)}e^{-i(\omega_p-\omega_q)t}$$

$$\left.+\frac{<u_n|\hat{V}(\omega_q)|u_g>^*<u_m|\hat{V}(\omega_p)|u_n>^*<u_m|\hat{G}|u_g>}{(\omega_{ng}^*-\omega_p)(\omega_{mg}^*-\omega_p-\omega_q)}e^{i(\omega_p+\omega_q)t}\right) \quad . \text{ (2-1-16)}$$

If we replace ω_q by $-\omega_q$ in the second term in eq. (2-1-16) and, ω_q by $-\omega_q$ and ω_p by $-\omega_p$ in the third term in eq. (2-1-16), respectively, this equation can be rendered more transparent. These substitutions can be permitted because we take the summation over positive- and negative- frequency. Therefore, eq. (2-1-16) is expressed in the form

$$<\tilde{G}^{(2)}> = \frac{1}{\hbar^2}\sum_{pq}\sum_{mn}\left(\frac{<u_g|\hat{G}|u_n><u_n|\hat{V}(\omega_q)|u_m><u_m|\hat{V}(\omega_p)|u_g>}{(\omega_{ng}-\omega_p-\omega_q)(\omega_{mg}-\omega_p)}\right.$$

$$+\frac{<u_g|\hat{V}(\omega_q)|u_n><u_n|\hat{G}|u_m><u_m|\hat{V}(\omega_p)|u_g>}{(\omega_{ng}^*+\omega_q)(\omega_{mg}-\omega_p)}$$

$$\left.+\frac{<u_g|\hat{V}(\omega_q)|u_n><u_n|\hat{V}(\omega_p)|u_m><u_m|\hat{G}|u_g>}{(\omega_{ng}^*+\omega_p)(\omega_{mg}^*+\omega_p+\omega_q)}\right)e^{-i(\omega_p+\omega_q)t} \quad , \text{ (2-1-17a)}$$

$$<\tilde{G}^{(2)}> = \sum_{p+q} G(\omega_p+\omega_q)e^{-i(\omega_p+\omega_q)t} \quad , \text{ (2-1-17b)}$$

where,

$$G(\omega_p+\omega_q)=\frac{1}{\hbar^2}\sum_{mn}\Big(\frac{<u_g|\hat{G}|u_n><u_n|\hat{V}(\omega_q)|u_m><u_m|\hat{V}(\omega_p)|u_g>}{(\omega_{ng}-\omega_p-\omega_q)(\omega_{mg}-\omega_p)}$$
$$+\frac{<u_g|\hat{V}(\omega_q)|u_n><u_n|\hat{G}|u_m><u_m|\hat{V}(\omega_p)|u_g>}{(\omega^*_{ng}+\omega_q)(\omega_{mg}-\omega_p)}$$
$$+\frac{<u_g|\hat{V}(\omega_q)|u_n><u_n|\hat{V}(\omega_p)|u_m><u_m|\hat{G}|u_g>}{(\omega^*_{ng}+\omega_p)(\omega^*_{mg}+\omega_p+\omega_q)}$$
$$+\frac{<u_g|\hat{G}|u_n><u_n|\hat{V}(\omega_p)|u_m><u_m|\hat{V}(\omega_q)|u_g>}{(\omega_{ng}-\omega_q-\omega_p)(\omega_{mg}-\omega_q)}$$
$$+\frac{<u_g|\hat{V}(\omega_p)|u_n><u_n|\hat{G}|u_m><u_m|\hat{V}(\omega_q)|u_g>}{(\omega^*_{ng}+\omega_p)(\omega_{mg}-\omega_q)}$$
$$+\frac{<u_g|\hat{V}(\omega_p)|u_n><u_n|\hat{V}(\omega_q)|u_m><u_m|\hat{G}|u_g>}{(\omega^*_{ng}+\omega_q)(\omega^*_{mg}+\omega_q+\omega_p)}\quad . \qquad (2\text{-}1\text{-}18)$$

In this expression, the standard definition of the second-order susceptibility is introduced. Damping phenomena are treated with a crude way in these expressions. ω_{mg} and ω^*_{mg} are taken as

$$\omega_{mg}=\omega^0_{mg}-i\frac{\Gamma_m}{2}$$
$$\omega^*_{mg}=\omega^0_{mg}+i\frac{\Gamma_m}{2}\quad , \qquad (2\text{-}1\text{-}19)$$

where ω^0_{mg} and Γ_m are the real transition frequency and the population decay rate of the upper level m, respectively. We consider an equivalent polarization operator for $\hat{G}$ as follows.

$$\hat{G}=\hat{\mu}-\nabla\cdot\hat{q}-\frac{c}{i(\omega_p+\omega_q)}\nabla\times\hat{m}\quad , \qquad (2\text{-}1\text{-}20)$$

$G(\omega_p+\omega_q)$ can be obtained by collecting the contributions which come from the combinations of various terms in $\hat{V}(\omega_p)$, $\hat{V}(\omega_q)$ and $\hat{G}$. We describe the following five interesting contributions (a)~(e) and do not consider contributions from further higher order. Hereafter, we replace u_g, u_m and u_n as g, m and n for a simplification.

(a) Electric dipole mechanism (ED mechanism)

We choose the combination

$$\{\ \hat{G} = \boldsymbol{\mu},\ \hat{V}(\omega_q) = -\boldsymbol{\mu}\cdot\boldsymbol{E}(\omega_q),\ \hat{V}(\omega_p) = -\boldsymbol{\mu}\cdot\boldsymbol{E}(\omega_p)\ \} \tag{2-1-21}$$

for mechanism (a), so that we obtain

$$\mu_i(\omega_p+\omega_q) = \Sigma\,\beta_{ijk}E_j(\omega_q)E_k(\omega_p)\ , \tag{2-1-22}$$

$$\begin{aligned}\beta_{ijk} = \frac{1}{\hbar^2}\sum_{mn}\Bigg(&\frac{\langle g|\mu_i|n\rangle\langle n|\mu_j|m\rangle\langle m|\mu_k|g\rangle}{(\omega_{ng}-\omega_p-\omega_q)(\omega_{mg}-\omega_p)}\\ &+\frac{\langle g|\mu_j|n\rangle\langle n|\mu_i|m\rangle\langle m|\mu_k|g\rangle}{(\omega^*_{ng}+\omega_q)(\omega_{mg}-\omega_p)}\\ &+\frac{\langle g|\mu_j|n\rangle\langle n|\mu_k|m\rangle\langle m|\mu_i|g\rangle}{(\omega^*_{ng}+\omega_p)(\omega^*_{mg}+\omega_p+\omega_q)}\\ &+\frac{\langle g|\mu_i|n\rangle\langle n|\mu_k|m\rangle\langle m|\mu_j|g\rangle}{(\omega_{ng}-\omega_q-\omega_p)(\omega_{mg}-\omega_q)}\\ &+\frac{\langle g|\mu_k|n\rangle\langle n|\mu_i|m\rangle\langle m|\mu_j|g\rangle}{(\omega^*_{ng}+\omega_p)(\omega_{mg}-\omega_q)}\\ &+\frac{\langle g|\mu_k|n\rangle\langle n|\mu_j|m\rangle\langle m|\mu_i|g\rangle}{(\omega^*_{ng}+\omega_q)(\omega^*_{mg}+\omega_q+\omega_p)}\Bigg)\ .\end{aligned} \tag{2-1-23}$$

(b) Electric quadrupole coupling mechanism (EQC mechanism)

Similarly,

$$\{\ \hat{G} = \boldsymbol{\mu},\ \hat{V}(\omega_p) = -\boldsymbol{\mu}\cdot\boldsymbol{E}(\omega_p),\ \hat{V}(\omega_q) = -\hat{q}:\nabla\boldsymbol{E}(\omega_q)\ \}\ , \tag{2-1-24}$$

$$\mu_i(\omega_p+\omega_q) = \Sigma\,\delta^{\omega_p,\omega_q}_{ijkl}E_j(\omega_p)\,\partial_k E_l(\omega_q)\ , \tag{2-1-25}$$

$$\delta_{ijkl}^{\omega_p,\omega_q} = \frac{1}{\hbar^2}\sum_{mn}\left(\frac{\langle g|\Omega_i|n\rangle\langle n|\hat{q}_{kl}|m\rangle\langle m|\Omega_j|g\rangle}{(\omega_{ng}-\omega_p-\omega_q)(\omega_{mg}-\omega_p)}\right.$$
$$+\frac{\langle g|\hat{q}_{kl}|n\rangle\langle n|\Omega_i|m\rangle\langle m|\Omega_j|g\rangle}{(\omega_{ng}^*+\omega_q)(\omega_{mg}-\omega_p)}$$
$$+\frac{\langle g|\hat{q}_{kl}|n\rangle\langle n|\Omega_j|m\rangle\langle m|\Omega_i|g\rangle}{(\omega_{ng}^*+\omega_p)(\omega_{mg}^*+\omega_p+\omega_q)}$$
$$+\frac{\langle g|\Omega_i|n\rangle\langle n|\Omega_j|m\rangle\langle m|\hat{q}_{kl}|g\rangle}{(\omega_{ng}-\omega_q-\omega_p)(\omega_{mg}-\omega_q)}$$
$$+\frac{\langle g|\Omega_j|n\rangle\langle n|\Omega_i|m\rangle\langle m|\hat{q}_{kl}|g\rangle}{(\omega_{ng}^*+\omega_p)(\omega_{mg}-\omega_q)}$$
$$\left.+\frac{\langle g|\Omega_j|n\rangle\langle n|\hat{q}_{kl}|m\rangle\langle m|\Omega_i|g\rangle}{(\omega_{ng}^*+\omega_q)(\omega_{mg}^*+\omega_q+\omega_p)}\right) , \qquad (2\text{-}1\text{-}26)$$

and

$$\{\ \hat{G}=\Omega,\ \hat{V}(\omega_q)=-\boldsymbol{\mu}\cdot\boldsymbol{E}(\omega_q),\ \hat{V}(\omega_p)=-\hat{q}:\nabla\boldsymbol{E}(\omega_p)\ \} , \qquad (2\text{-}1\text{-}27)$$

$$\mu_i(\omega_q+\omega_p)=\Sigma\,\delta_{ijkl}^{\omega_q,\omega_p}E_j(\omega_q)\,\partial_k E_l(\omega_p) , \qquad (2\text{-}1\text{-}28)$$

$$\delta_{ijkl}^{\omega_q,\omega_p} = \frac{1}{\hbar^2}\sum_{mn}\left(\frac{\langle g|\Omega_i|n\rangle\langle n|\Omega_j|m\rangle\langle m|\hat{q}_{kl}|g\rangle}{(\omega_{ng}-\omega_p-\omega_q)(\omega_{mg}-\omega_p)}\right.$$
$$+\frac{\langle g|\Omega_j|n\rangle\langle n|\Omega_i|m\rangle\langle m|\hat{q}_{kl}|g\rangle}{(\omega_{ng}^*+\omega_q)(\omega_{mg}-\omega_p)}$$
$$+\frac{\langle g|\Omega_j|n\rangle\langle n|\hat{q}_{kl}|m\rangle\langle m|\Omega_i|g\rangle}{(\omega_{ng}^*+\omega_p)(\omega_{mg}^*+\omega_p+\omega_q)}$$
$$+\frac{\langle g|\Omega_i|n\rangle\langle n|\hat{q}_{kl}|m\rangle\langle m|\Omega_j|g\rangle}{(\omega_{ng}-\omega_q-\omega_p)(\omega_{mg}-\omega_q)}$$
$$+\frac{\langle g|\hat{q}_{kl}|n\rangle\langle n|\Omega_i|m\rangle\langle m|\Omega_j|g\rangle}{(\omega_{ng}^*+\omega_p)(\omega_{mg}-\omega_q)}$$
$$\left.+\frac{\langle g|\hat{q}_{kl}|n\rangle\langle n|\Omega_j|m\rangle\langle m|\Omega_i|g\rangle}{(\omega_{ng}^*+\omega_q)(\omega_{mg}^*+\omega_q+\omega_p)}\right) . \qquad (2\text{-}1\text{-}29)$$

(c) Magnetic dipole coupling mechanism (MDC mechanism)

Similarly,

$$\{\ \hat{G} = \hat{\mu},\ \hat{V}(\omega_p) = -\hat{\mu}\cdot \boldsymbol{E}(\omega_p),\ \hat{V}(\omega_q) = -\hat{\boldsymbol{m}}\cdot \boldsymbol{H}(\omega_q)\ \}\ , \qquad (2\text{-}1\text{-}30)$$

$$\mu_i(\omega_p + \omega_q) = \Sigma\, \gamma_{ijk}^{\omega_p,\,\omega_q} E_j(\omega_p)\, H_k(\omega_q)\ , \qquad (2\text{-}1\text{-}31)$$

$$\begin{aligned}\gamma_{ijk}^{\omega_p,\,\omega_q} = \frac{1}{\hbar^2}\sum_{mn}\Bigg(&\frac{\langle g|\hat{\mu}_i|n\rangle\langle n|\hat{m}_k|m\rangle\langle m|\hat{\mu}_j|g\rangle}{(\omega_{ng} - \omega_p - \omega_q)(\omega_{mg} - \omega_p)}\\ &+\frac{\langle g|\hat{m}_k|n\rangle\langle n|\hat{\mu}_i|m\rangle\langle m|\hat{\mu}_j|g\rangle}{(\omega_{ng}^* + \omega_q)(\omega_{mg} - \omega_p)}\\ &+\frac{\langle g|\hat{m}_k|n\rangle\langle n|\hat{\mu}_j|m\rangle\langle m|\hat{\mu}_i|g\rangle}{(\omega_{ng}^* + \omega_p)(\omega_{mg}^* + \omega_p + \omega_q)}\\ &+\frac{\langle g|\hat{\mu}_i|n\rangle\langle n|\hat{\mu}_j|m\rangle\langle m|\hat{m}_k|g\rangle}{(\omega_{ng} - \omega_q - \omega_p)(\omega_{mg} - \omega_q)}\\ &+\frac{\langle g|\hat{\mu}_j|n\rangle\langle n|\hat{\mu}_i|m\rangle\langle m|\hat{m}_k|g\rangle}{(\omega_{ng}^* + \omega_p)(\omega_{mg} - \omega_q)}\\ &+\frac{\langle g|\hat{\mu}_j|n\rangle\langle n|\hat{m}_k|m\rangle\langle m|\hat{\mu}_i|g\rangle}{(\omega_{ng}^* + \omega_q)(\omega_{mg}^* + \omega_q + \omega_p)}\Bigg)\end{aligned}\ , \qquad (2\text{-}1\text{-}32)$$

and

$$\{\ \hat{G} = \hat{\mu},\ \hat{V}(\omega_q) = -\hat{\mu}\cdot \boldsymbol{E}(\omega_q),\ \hat{V}(\omega_p) = -\hat{\boldsymbol{m}}\cdot \boldsymbol{H}(\omega_p)\ \}\ , \qquad (2\text{-}1\text{-}33)$$

$$\mu_i(\omega_q + \omega_p) = \Sigma\, \gamma_{ijk}^{\omega_q,\,\omega_p} E_j(\omega_q) H_k(\omega_p)\ , \qquad (2\text{-}1\text{-}34)$$

$$\begin{aligned}\gamma_{ijk}^{\omega_q,\,\omega_p} = \frac{1}{\hbar^2}\sum_{mn}\Bigg(&\frac{\langle g|\hat{\mu}_i|n\rangle\langle n|\hat{\mu}_j|m\rangle\langle m|\hat{m}_k|g\rangle}{(\omega_{ng} - \omega_p - \omega_q)(\omega_{mg} - \omega_p)}\\ &+\frac{\langle g|\hat{\mu}_j|n\rangle\langle n|\hat{\mu}_i|m\rangle\langle m|\hat{m}_k|g\rangle}{(\omega_{ng}^* + \omega_q)(\omega_{mg} - \omega_p)}\\ &+\frac{\langle g|\hat{\mu}_j|n\rangle\langle n|\hat{m}_k|m\rangle\langle m|\hat{\mu}_i|g\rangle}{(\omega_{ng}^* + \omega_p)(\omega_{mg}^* + \omega_p + \omega_q)}\\ &+\frac{\langle g|\hat{\mu}_i|n\rangle\langle n|\hat{m}_k|m\rangle\langle m|\hat{\mu}_j|g\rangle}{(\omega_{ng} - \omega_q - \omega_p)(\omega_{mg} - \omega_q)}\\ &+\frac{\langle g|\hat{m}_k|n\rangle\langle n|\hat{\mu}_i|m\rangle\langle m|\hat{\mu}_j|g\rangle}{(\omega_{ng}^* + \omega_p)(\omega_{mg} - \omega_q)}\\ &+\frac{\langle g|\hat{m}_k|n\rangle\langle n|\hat{\mu}_j|m\rangle\langle m|\hat{\mu}_i|g\rangle}{(\omega_{ng}^* + \omega_q)(\omega_{mg}^* + \omega_q + \omega_p)}\Bigg)\end{aligned}\ . \qquad (2\text{-}1\text{-}35)$$

(d) Electric quadrupole mechanism (EQ mechanism)

Similarly,

$$\{\ \hat{G} = -\nabla \cdot \hat{q},\ \hat{V}(\omega_q) = -\boldsymbol{\mu} \cdot \boldsymbol{E}(\omega_q),\ \hat{V}(\omega_p) = -\boldsymbol{\mu} \cdot \boldsymbol{E}(\omega_p)\ \}\ , \tag{2-1-36}$$

$$q_{ij}(\omega_p + \omega_q) = \lambda_{ijkl} E_k(\omega_q) E_l(\omega_p)\ , \tag{2-1-37}$$

$$\begin{aligned}\lambda_{ijkl} = \frac{1}{\hbar^2}\sum_{mn}\Bigg(&\frac{\langle g|\hat{q}_{ij}|n\rangle\langle n|\mu_k|m\rangle\langle m|\mu_l|g\rangle}{(\omega_{ng} - \omega_p - \omega_q)(\omega_{mg} - \omega_p)} \\ &+ \frac{\langle g|\mu_k|n\rangle\langle n|\hat{q}_{ij}|m\rangle\langle m|\mu_l|g\rangle}{(\omega^*_{ng} + \omega_q)(\omega_{mg} - \omega_p)} \\ &+ \frac{\langle g|\mu_k|n\rangle\langle n|\mu_l|m\rangle\langle m|\hat{q}_{ij}|g\rangle}{(\omega^*_{ng} + \omega_p)(\omega^*_{mg} + \omega_p + \omega_q)} \\ &+ \frac{\langle g|\hat{q}_{ij}|n\rangle\langle n|\mu_l|m\rangle\langle m|\mu_k|g\rangle}{(\omega_{ng} - \omega_q - \omega_p)(\omega_{mg} - \omega_q)} \\ &+ \frac{\langle g|\mu_l|n\rangle\langle n|\hat{q}_{ij}|m\rangle\langle m|\mu_k|g\rangle}{(\omega^*_{ng} + \omega_p)(\omega_{mg} - \omega_q)} \\ &+ \frac{\langle g|\mu_l|n\rangle\langle n|\mu_k|m\rangle\langle m|\hat{q}_{ij}|g\rangle}{(\omega^*_{ng} + \omega_q)(\omega^*_{mg} + \omega_q + \omega_p)}\Bigg)\end{aligned}\ . \tag{2-1-38}$$

i component of the equivalent electric polarization is obtained by

$$\sum_j -\partial_j q_{ij}(\omega_p + \omega_q)\ , \tag{2-1-39}$$

(e) Magnetic dipole mechanism (MD mechanism)

Similarly,

$$\{\ \hat{G} = -\frac{c}{i(\omega_p + \omega_q)}\nabla \times \hat{\boldsymbol{m}},\ \hat{V}(\omega_q) = -\boldsymbol{\mu} \cdot \boldsymbol{E}(\omega_q),\ \hat{V}(\omega_p) = -\boldsymbol{\mu} \cdot \boldsymbol{E}(\omega_p)\ \}\ , \tag{2-1-40}$$

$$m_i = \Sigma\, \xi_{ijk} E_j(\omega_q) E_k(\omega_p)\ , \tag{2-1-41}$$

$$\xi_{ijk} = \frac{1}{\hbar^2}\sum_{mn}\left(\frac{\langle g|\hat{m}_i|n\rangle\langle n|\Omega_j|m\rangle\langle m|\Omega_k|g\rangle}{(\omega_{ng}-\omega_p-\omega_q)(\omega_{mg}-\omega_p)}\right.$$
$$+\frac{\langle g|\Omega_j|n\rangle\langle n|\hat{m}_i|m\rangle\langle m|\Omega_k|g\rangle}{(\omega_{ng}^*+\omega_q)(\omega_{mg}-\omega_p)}$$
$$+\frac{\langle g|\Omega_j|n\rangle\langle n|\Omega_k|m\rangle\langle m|\hat{m}_i|g\rangle}{(\omega_{ng}^*+\omega_p)(\omega_{mg}^*+\omega_p+\omega_q)}$$
$$+\frac{\langle g|\hat{m}_i|n\rangle\langle n|\Omega_k|m\rangle\langle m|\Omega_j|g\rangle}{(\omega_{ng}-\omega_q-\omega_p)(\omega_{mg}-\omega_q)}$$
$$+\frac{\langle g|\Omega_k|n\rangle\langle n|\hat{m}_i|m\rangle\langle m|\Omega_j|g\rangle}{(\omega_{ng}^*+\omega_p)(\omega_{mg}-\omega_q)}$$
$$\left.+\frac{\langle g|\Omega_k|n\rangle\langle n|\Omega_j|m\rangle\langle m|\hat{m}_i|g\rangle}{(\omega_{ng}^*+\omega_q)(\omega_{mg}^*+\omega_q+\omega_p)}\right) \quad . \qquad (2\text{-}1\text{-}42)$$

The equivalent electric polarization is obtained by

$$-\frac{c}{i(\omega_p+\omega_q)}\nabla\times\boldsymbol{m} \quad . \qquad (2\text{-}1\text{-}43)$$

These microscopic quantities are related to macroscopic quantities (χ, Δ, Γ, Λ and Ξ), respectively, about which we will describe in the section 2-2, by considering orientation distribution functions of molecules (atoms) and the number (N) of molecules (atoms) per unit volume under week interactions. Most organic crystals are molecular condensed matters held together by van der Waals and dipole-dipole intermolecular forces. Therefore, we have to consider a local field correction more correctly [3].

In the case of SHG, we set ω_p, ω_q, and $\omega_p+\omega_q$ as ω, ω, and 2ω, respectively. In this case, the following relations exist in mechanisms (b) and (c).

$$\delta_{ijkl}^{\omega_p,\omega_q} = \delta_{ijkl}^{\omega_q,\omega_p} \quad , \qquad (2\text{-}1\text{-}44)$$

$$\gamma_{ijk}^{\omega_p,\omega_q} = \gamma_{ijk}^{\omega_q,\omega_p} \quad . \qquad (2\text{-}1\text{-}45)$$

Therefore, we take either $\delta_{ijkl}^{\omega_p,\omega_q}$ or $\delta_{ijkl}^{\omega_q,\omega_p}$ and either $\gamma_{ijk}^{\omega_p,\omega_q}$ or $\gamma_{ijk}^{\omega_q,\omega_p}$ and replace them as δ_{ijkl} and γ_{ijk}, respectively.

Crude order estimations of the SH amplitudes of the mechanisms (b)~(e) compared with that of the mechanism (a) can be done under the off-resonant condition and the condition that mechanisms (a)~(e) are allowed [1,4,5]. Mechanisms (b)~(e) include two electric dipole transitions and, an electric quadrupole transition or a magnetic dipole transition in each SH optical process, while mechanism (a) comes from three electric dipole transitions. If we take $\hat{r}$ as $a_0 \sim 10^{-8}(cm)$, the ratios of the SH amplitudes of the mechanisms (b)~(e) to that of the mechanism (a) in the optical region are estimated as follows,

$$\frac{ea_0^2k}{ea_0} = 10^{-3}\sim 10^{-4} \quad \text{(for mechanisms (b) and (d)),}$$

$$\frac{e\hbar}{\frac{mc}{ea_0}} = \sim 10^{-3} \quad \text{(for mechanism (c) and (e)),}$$

where k is the wavevector of the incident field.

Next, let us discuss the reason why mechanisms (b)~(e) are also allowed for centrosymmetric systems and their resonance conditions. We can define a parity for systems with an inversion symmetry. ED mechanism is not allowed for centrosymmetric systems as follows. The parity of electric dipole operator is odd, so that an electric dipole (ED) transition is allowed between states with different parity. We can not find any combinations of states g, m, and n which fulfill the condition $\langle g|\hat{\mu}|n\rangle\langle n|\hat{\mu}|m\rangle\langle m|\hat{\mu}|g\rangle \neq 0$ for ED mechanism. However, mechanisms (b)~(e) include an electric quadrupole (EQ) transition or an magnetic dipole (MD) transition, which is a transition between states with the same parity in each SH

optical process. Hence, mechanisms (b)~(e) are also allowed in centrosymmetric systems. We depict the resonance terms of the microscopic expressions for mechanisms (b)~(e) in the case of SHG. The EQC mechanism or the MDC mechanism is due to an EQ transition or a MD transition at one input field, respectively, and an ED transition at the other input field and an ED transition at the output field. The EQ mechanism or the MD mechanism is due to ED transitions at both input fields and an EQ transition or a MD transition at the output field, respectively. Such SH optical processes are schematically displayed in Fig. 2-1-1.

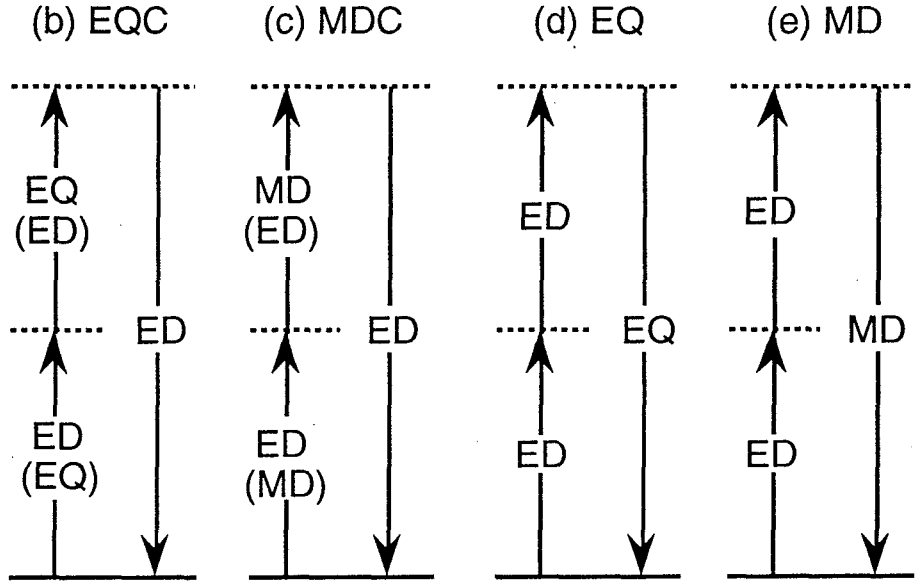

Fig. 2-1-1 Schematic illustration of microscopic views of four SHG processes, (b) the electric quadrupole coupling (EQC) mechanism, (c) the magnetic dipole coupling (MDC) mechanism, (d) the electric quadrupole (EQ) mechanism and (e) the magnetic dipole (MD) mechanism.

This figure implies that it is possible to probe the ED forbidden and the EQ and/or the MD allowed transition states for centrosymmetric systems, if SH spectra are measured. In this study, SH spectrum measurement is used to clarify the origin of SHG from

phthalocyanines and the electronic structures of them. Similar discussion can also be done for SFG.

So far, we have considered media made of molecules (atoms) under weak interaction. However, the SFG (SHG) spectrum measurement can be generally applied for media such as inorganic semiconductors and insulators in order to clarify the various electronic excited states.

2-2 Rotational angle dependent, polarization dependent and thickness dependent SHG from ED, EQC, MDC, EQ and MD mechanisms

The SHG of a bulk origin from EQC, MDC, EQ, and MD mechanisms show characteristic polarization and rotational angle dependences, which depend not only on the symmetry in each system but also on the geometry. The characteristic behaviors come from the form $P_i = g_{ijkl} E_j \partial_k E_l$ of the nonlinear electric polarization, where the forth rank tensor g is a gereralized nonlinear susceptibility as will be described later.

In this section, the bulk SHG from an effective nonlinear polarization including higher order mechanisms is considered. Here, we also treat the SHG from isotropic (K_h) system and O_h system such as Si and Ge cubic crystals about which a lot of studies [6-12] have been made both theoretically and experimentally, in addition to those from anisotropic point group systems ($D_{\infty h}$, $C_{\infty v}$, D_{4h}, and C_{4v} systems) which are relevant to the present study. Of course, the electric dipole mechanism should be dominant for the non-centrosymmetric systems ($C_{\infty v}$ and C_{4v}) in general. Analytical expressions of the SHG intensities were obtained under the three-layer model [13] illustrated in Fig. 2-2-1(a), in which a nonlinear active layer is embedded between two layers whose nonlinearity is negligible. Analytical expressions of the reflection SHG from the geometry shown in Fig. 2-2-1(b) can be also obtained by modifying those for the three layer model.

2-2A Sources of SHG

In general, sources of SHG are expressed as an effective polarization

$$P_{eff} = P - \nabla \cdot Q - \frac{c}{i2\omega} \nabla \times M \quad , \qquad (2\text{-}2A\text{-}1)$$

where **P** is the nonlinear electric polarization, Q the nonlinear electric quadrupole polarization, and **M** the nonlinear magnetization.

Following the previous section, we consider five possible mechanisms (the electric dipole, the electric quadrupole coupling, the magnetic dipole coupling, the electric quadrupole and the magnetic dipole mechanisms). The first term in eq. (2-2A-1) is related to the electric dipole, the electric quadrupole coupling, and the magnetic dipole coupling mechanisms. The second and the third terms bring about the electric qudrupole and the magnetic dipole mechanisms, respectively. Let us first describe the nonzero components of the nonlinear optical coefficients in the five mechanisms for systems with K_h, O_h, $D_{\infty h}$, $C_{\infty v}$, D_{4h}, or C_{4v} symmetry. The crystal axes are taken to be the standard axes for O_h system. The symmetry axis C_∞ coincides with axis 3 for $D_{\infty h}$ or $C_{\infty v}$ symmetries. For D_{4h} or C_{4v} symmetries, the symmetry axis C_4 is defined as axis 3 in the crystal axes.

(a) Electric dipole mechanism (ED mechanism)

The electric dipole mechanism is allowed only in polar systems like $C_{\infty v}$ and C_{4v} symmetries. The nonlinear electric polarization is expressed as

$$P_i = \Sigma \chi_{ijk} E_j E_k \quad , \qquad (2\text{-}2A\text{-}2)$$

where the nonzero components of the third rank tensor χ are;

$$\chi_{113} = \chi_{223} = \chi_{131} = \chi_{232}$$
$$\chi_{311} = \chi_{322}$$
$$\chi_{333} \quad , \qquad (2\text{-}2A\text{-}3)$$

for $C_{\infty v}$ and C_{4v} symmetries.

(b) Electric quadrupole coupling mechanism (EQC mechanism)

In this mechanism, both the electric dipole interaction and the electric quadrupole interaction perturb the system, and the following nonlinear electric polarization is produced.

$$P_i = \Sigma \Delta_{ijkl} E_j \partial_k E_l \quad , \qquad (2\text{-}2A\text{-}4)$$

where Δ is a forth rank tensor. In K_h, O_h, $D_{\infty h}$, $C_{\infty v}$, D_{4h} and C_{4v} symmetries, the nonzero components of Δ have the following forms, Δ_{iiii}, Δ_{ijij}, Δ_{ijji}, and Δ_{iijj}, ($i \neq j$). According to the quantum mechanical expression of Δ, index kl in Δ_{ijkl} originates from an electric quadrupolar operator that is a symmetric traceless tensor. Thus, the following relations should be satisfied.

$$\Delta_{ijkl} = \Delta_{ijlk} \qquad (2\text{-}2A\text{-}5)$$
$$\Delta_{ij11} + \Delta_{ij22} + \Delta_{ij33} = 0 \quad . \qquad (2\text{-}2A\text{-}6)$$

In K_h symmetry, there also exist the relations

$$\Delta_{iiii} = \Delta_{ijij} + \Delta_{ijji} + \Delta_{iijj} \ (i \neq j) \quad . \tag{2-2A-7}$$

Therefore, only one independent component exists as follows.

$$\Delta_{ijij} = \Delta_{ijji} = -\frac{3}{2}\Delta_{iijj} = \frac{3}{4}\Delta_{iiii} \ (i \neq j) \quad . \tag{2-2A-8}$$

In O_h symmetry, two independent components exist as follows.

$$\begin{aligned} &\Delta_{ijij} = \Delta_{ijji} \\ &\Delta_{iijj} = -\frac{1}{2}\Delta_{iiii} \ (i \neq j) \end{aligned} \quad . \tag{2-2A-9}$$

In $D_{\infty h}$ and $C_{\infty v}$ symmetries, there are five independent components.

$$\begin{aligned} &\Delta_{1212} = \Delta_{2121} = \Delta_{1221} = \Delta_{2112} \\ &\Delta_{1313} = \Delta_{2323} = \Delta_{1331} = \Delta_{2332} \\ &\Delta_{3131} = \Delta_{3232} = \Delta_{3113} = \Delta_{3223} \\ &\Delta_{1122} = \Delta_{2211} \\ &\Delta_{3311} = \Delta_{3322} \end{aligned} \quad . \tag{2-2A-10}$$

The other components are given by the above five components as follows.

$$\begin{aligned} &\Delta_{1111} = \Delta_{2222} = \Delta_{1122} + 2\Delta_{1212} \\ &\Delta_{1133} = \Delta_{2233} = -2\Delta_{1122} - 2\Delta_{1212} \\ &\Delta_{3333} = -2\Delta_{3311} \end{aligned} \quad . \tag{2-2A-11}$$

In D_{4h} and C_{4v} symmetries, there are six independent components.

$$\Delta_{1212} = \Delta_{2121} = \Delta_{1221} = \Delta_{2112}$$
$$\Delta_{1313} = \Delta_{2323} = \Delta_{1331} = \Delta_{2332}$$
$$\Delta_{3131} = \Delta_{3232} = \Delta_{3113} = \Delta_{3223}$$
$$\Delta_{1122} = \Delta_{2211}$$
$$\Delta_{3311} = \Delta_{3322}$$
$$\Delta_{1111} = \Delta_{2222} \quad . \qquad \text{(2-2A-12)}$$

The other nonzero components are determined by the above components,

$$\Delta_{1133} = \Delta_{2233} = -\Delta_{1111} - \Delta_{1122}$$
$$\Delta_{3333} = -2\Delta_{3311} \quad . \qquad \text{(2-2A-13)}$$

(c) Magnetic dipole coupling mechanism (MDC mechanism)

In this mechanism, the nonlinear electric polarization arises from the coupling product of an electric field and a magnetic field.

$$P_i = \Sigma \Gamma_{ijk} E_j H_k \quad . \qquad \text{(2-2A-14)}$$

Since a magnetic field is expressed as

$$\boldsymbol{H} = \frac{c}{i\omega} \nabla \times \boldsymbol{E} \quad , \qquad \text{(2-2A-15)}$$

the nonlinear electric polarization is expressed as

$$P_i = \Sigma \Gamma_{ijkl} E_j \partial_k E_l \quad , \qquad (2\text{-}2A\text{-}16)$$

where Γ is a forth rank tensor.

In K_h and O_h symmetries, we have only one independent component.

$$\Gamma_{ijj} = -\Gamma_{iji} \ (i \neq j) \quad . \qquad (2\text{-}2A\text{-}17)$$

In $D_{\infty h}$, $C_{\infty v}$, D_{4h} and C_{4v} symmetries, the nonzero components are;

$$\begin{aligned} &\Gamma_{1212} = \Gamma_{2121} = -\Gamma_{1221} = -\Gamma_{2112} \\ &\Gamma_{2323} = \Gamma_{1313} = -\Gamma_{2332} = -\Gamma_{1331} \\ &\Gamma_{3131} = \Gamma_{3232} = -\Gamma_{3113} = -\Gamma_{3223} \quad , \end{aligned} \qquad (2\text{-}2A\text{-}18)$$

and these three components are independent.

(d) Electric quadrupole mechanism (EQ mechanism)

The nonlinear electric quadrupole polarization Q_{ij} is expressed as

$$Q_{ij} = \Sigma \Lambda_{ijkl} E_k E_l \quad , \qquad (2\text{-}2A\text{-}19)$$

where Λ is a forth rank tensor. Since Q_{ij} is a symmetric and traceless tensor, the following relations exist.

$$\Lambda_{ijkl} = \Lambda_{jikl} \qquad (2\text{-}2A\text{-}20)$$

$$\Lambda_{11kl} + \Lambda_{22kl} + \Lambda_{33kl} = 0 \quad . \qquad (2\text{-}2A\text{-}21)$$

In SHG process, the following relation exist.

$$\Lambda_{ijkl} = \Lambda_{ijlk} \quad . \tag{2-2A-22}$$

In K_h symmetry, there also exists the relation

$$\Lambda_{iiii} = \Lambda_{iijj} + \Lambda_{ijji} + \Lambda_{iijj} \; (i \neq j) \quad . \tag{2-2A-23}$$

Therefore, the only one component exists as follows.

$$\Lambda_{ijij} = \Lambda_{ijji} = -\frac{3}{2}\Lambda_{iijj} = \frac{3}{4}\Lambda_{iiii} \; (i \neq j) \quad . \tag{2-2A-24}$$

In O_h symmetry, two independent components exist.

$$\Lambda_{iijj} = -\frac{1}{2}\Lambda_{iiii}$$
$$\Lambda_{ijji} = \Lambda_{ijij} \; (i \neq j) \quad . \tag{2-2A-25}$$

In $D_{\infty h}$ and $C_{\infty v}$ symmetries, there are four independent components as follows;

$$\Lambda_{1122} = \Lambda_{2211}$$
$$\Lambda_{1212} = \Lambda_{2121} = \Lambda_{1221} = \Lambda_{2112}$$
$$\Lambda_{1133} = \Lambda_{2233}$$
$$\Lambda_{1313} = \Lambda_{3131} = \Lambda_{1331} = \Lambda_{3113} = \Lambda_{2323} = \Lambda_{3232} = \Lambda_{2332} = \Lambda_{3223} \quad . \tag{2-2A-26}$$

The other components are described using the above four components;

$$\Lambda_{3311} = \Lambda_{3322} = -2\Lambda_{1122} - 2\Lambda_{1212}$$
$$\Lambda_{1111} = \Lambda_{2222} = \Lambda_{1122} + 2\Lambda_{1212}$$

$$\Lambda_{3333} = -2\Lambda_{1133} \quad . \qquad \text{(2-2A-27)}$$

In D_{4h} and C_{4v} symmetries, there are five independent components.

$$\Lambda_{1122} = \Lambda_{2211}$$
$$\Lambda_{1212} = \Lambda_{2121} = \Lambda_{1221} = \Lambda_{2112}$$
$$\Lambda_{1133} = \Lambda_{2233}$$
$$\Lambda_{1313} = \Lambda_{3131} = \Lambda_{1331} = \Lambda_{3113} = \Lambda_{2323} = \Lambda_{3232} = \Lambda_{2332} = \Lambda_{3223}$$
$$\Lambda_{1111} = \Lambda_{2222} \quad . \qquad \text{(2-2A-28)}$$

Other nonzero components are determined using the above components,

$$\Lambda_{3311} = \Lambda_{3322} = -\Lambda_{1111} - \Lambda_{1122}$$
$$\Lambda_{3333} = -2\Lambda_{1133} \quad . \qquad \text{(2-2A-29)}$$

This electric quadrupole polarization is equivalent to the nonlinear electric polarization of the following formation,

$$-\Sigma \partial_j Q_{ij} \quad . \qquad \text{(2-2A-30)}$$

(e) Magnetic dipole mechanism (MD mechanism)

The nonlinear magnetization **M** is produced as the square products of an electric field.

$$M_i = \Xi_{ijk} E_j E_k \quad . \qquad \text{(2-2A-31)}$$

Since the magnetization is proportional to a vector product of position **r** and momentum **p**, we define a forth rank tensor Ξ' as

$$-\frac{e}{2mc}r_i p_j = \Xi'_{ijkl}E_k E_l \quad . \qquad \text{(2-2A-32)}$$

Then, **M** is expressed as

$$\begin{aligned} M_1 &= (\Xi'_{2323} + \Xi'_{2332} - \Xi'_{3223} - \Xi'_{3232})E_2 E_3 \\ M_2 &= (\Xi'_{3113} + \Xi'_{3131} - \Xi'_{1313} - \Xi'_{1331})E_3 E_1 \\ M_3 &= (\Xi'_{1212} + \Xi'_{1221} - \Xi'_{2112} - \Xi'_{2121})E_1 E_2 \quad , \end{aligned} \qquad \text{(2-2A-33)}$$

where the nonzero components of the forth rank tensor Ξ' has the forms of Ξ'_{ijij} and Ξ'_{ijji} $(i \neq j)$ and should satisfy the relation, $\Xi'_{ijij}=\Xi'_{ijji}$ because of SHG process.

In K_h and O_h symmetries, all components of **M** vanish.

In $D_{\infty h}$, $C_{\infty v}$, D_{4h} and C_{4v} symmetries, this mechanism is described by only one independent parameter, $(\Xi'_{1313}-\Xi'_{3131})$. This magnetization is equivalent to the formation of the following nonlinear electric polarization.

$$-\frac{c}{i2\omega}\nabla \times M \quad . \qquad \text{(2-2A-34)}$$

(f) Relations between the mechanisms

As mentioned above, all the nonlinear electric polarizations produced by the electric quadrupole coupling, the magnetic dipole coupling, the electric quadrupole, the magnetic dipole mechanisms are expressed as

$$P_i = \Sigma\, g_{ijkl} E_j \partial_k E_l \quad . \qquad \text{(2-2A-35)}$$

Here, the forth rank tensor g has nonzero components, g_{iiii}, g_{iijj}, g_{ijij}, g_{ijji}. In K_h, O_h, $D_{\infty h}$, $C_{\infty v}$, D_{4h} and C_{4v} symmetries, we have the relations.

$$\begin{aligned} g_{iijj} &= \Delta_{iijj} - 2\Lambda_{ijij} + 2(\Xi_{ijij} - \Xi_{jiji}) \\ g_{ijij} &= \Delta_{ijij} + \Gamma_{ijij} - 2\Lambda_{iijj} \\ g_{ijji} &= \Delta_{ijji} + \Gamma_{ijji} - 2\Lambda_{ijij} + 2(\Xi_{ijij} - \Xi_{jiji}) \\ g_{iiii} &= \Delta_{iiii} - 2\Lambda_{iiii} \qquad (i \neq j) \end{aligned} \quad , \qquad \text{(2-2A-36)}$$

where the forth rank tensor Ξ is defined as $\Xi = -\frac{c}{i2\omega}\Xi'$. In fact, we can remove the term $2(\Xi_{ijij} - \Xi_{jiji})$ for K_h and O_h symmetries, since the magnetic dipole mechanism does not contribute to the SHG for those symmeties.

In K_h symmetry, we have three independent g tensor components as follows.

$$g_{iijj},\ g_{ijij},\ g_{ijji},\ g_{iiii} = g_{iijj} + g_{ijij} + g_{ijji} \qquad (i \neq j) \quad . \qquad \text{(2-2A-37)}$$

In O_h symmetry, there exist four independent g components of the forms,

$$g_{iijj},\ g_{ijij},\ g_{ijji},\ g_{iiii} \qquad (i \neq j) \quad . \qquad \text{(2-2A-38)}$$

In $D_{\infty h}$ and $C_{\infty v}$ symmetries, we have ten independent g tensor components.

$$g_{3311} = g_{3322},\ g_{1133} = g_{2233},\ g_{1122} = g_{2211}$$

$$g_{3131} = g_{3232},\ g_{1313} = g_{2323},\ g_{1212} = g_{2121}$$

$$g_{3113} = g_{3223},\ g_{1331} = g_{2332},\ g_{1221} = g_{2112}$$

$$g_{3333},\ g_{1111} = g_{2222} = g_{1122} + g_{1212} + g_{2121} \quad . \qquad \text{(2-2A-39)}$$

In D_{4h} and C_{4v} symmetries, we have eleven independent g tensor components.

$$g_{3311} = g_{3322},\ g_{1133} = g_{2233},\ g_{1122} = g_{2211}$$

$$g_{3131} = g_{3232},\ g_{1313} = g_{2323},\ g_{1212} = g_{2121}$$

$$g_{3113} = g_{3223},\ g_{1331} = g_{2332},\ g_{1221} = g_{2112}$$

$$g_{3333},\ g_{1111} = g_{2222} \quad . \qquad \text{(2-2A-40)}$$

On the basis of experimentals, we can determine g tensor components. Then, the form of g tensor components manifest the dominant mechanism.

2-2B SHG intensities under a three-layer model

Let us consider infinite media with K_h symmetry. When a fundamental wave of the plane wave form propagates in K_h symmetry, we define the direction of the wave vector as axis 3. The electric field of the fundamental wave has components of E_1 and E_2. We consider the nonlinear polarization from higher order mechanisms. In this coordinates, only the nonzero component ∂_k is ∂_3. Since all the components g_{1j31} and g_{2j31} are zero among all the g components in eq. 2-2A-37, both P_1 and P_2 components are zero, though P_3 component is not zero due to nonzero components in g_{3j31} components. Such a polarization can not radiate in the infinite media. However, for a finite media shown in Figs. 2-2-1(a) and 2-2-1(b), the nonlinear polarization from higher order mechanisms can radiate both into the media and out of the media, if we treat the boundary conditions properly as described below.

To calculate SH intensity, we use a three-layer model shown in Fig. 2-2-1(a), which is firstly treated by Bloembergen and Pershan. In this model, top and bottom layers are materials with isotropic dielectric tensors, in which nonlinear optical effect is negligible, and a middle layer with thickness d is treated as an uniaxial SH active materials whose optical axis is normal to the layer surface, since we deal with not only K_h and O_h systems but also anisotropic systems such as $D_{\infty h}$, $C_{\infty v}$, D_{4h} and C_{4v} point group symmetries.

For K_h, $C_{\infty v}$ and $D_{\infty h}$ symmetries, the coordinates are in accord with the laboratory coordinates about which we will state later, although the symmetry axis (C_∞ axis) must be coincided with the Z(3) axis in the laboratory coordinates for $C_{\infty v}$ and $D_{\infty h}$ symmetries. For O_h symmetry, one of the standard axes, which we call z(3) axis in

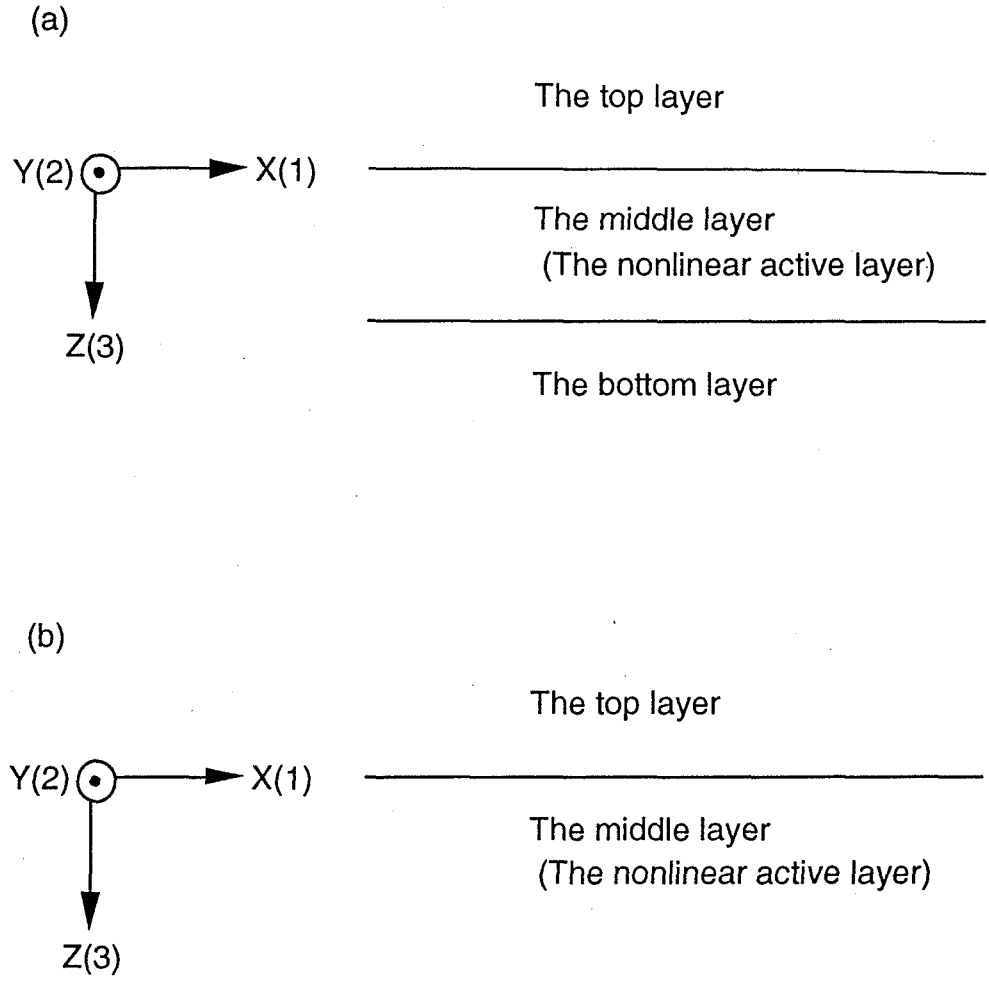

Fig. 2-2-1 The laboratory coordinates and the geometries

the crystal coordinates, coincide with Z(3) axis in the laboratory coordinates, though the other standard axes x(1) and y(2) are not in accord with X(1) and Y(2) axes in laboratory coordinate in general. This implys that the the SHG from (001) face for Si and Ge crystals with O_h symmetry is treated. The SHG gives us significant informations as for the bulk higher order mechanisms, if we rotate the crystal around the surface normal.

In this thesis, we use sample films grown epitaxially on KCl(001) or KBr(001) surface as well as those on a glass substrate. For such films with D_{4h} and C_{4v} symmetries, the symmetry axis C_4 also coincides with Z(3) axis in the laboratory coordinates, though the other axes x(1) and y(2) are not generally in accord with X(1) and Y(2) axes in laboratory coordinates. The SHG for such films also gives us significant informations as for the bulk higher order mechanisms, if we rotate the crystal around the surface normal.

We should notice that g tensor components in this section 2-2B are defined for the laboratory coordinates because the SH intensity is dependent on the orientation of the crystal for O_h, D_{4h} and C_{4v} symmetries. The g tensor components in the laboratory coordinates for those symmetries are described as g^L in order to distinguish from those in the crystal coordinates, which will be discussed in the section 2-2C.

The dielectric constants of the top, bottom, and middle layers at a fundamental angular frequency ω are denoted as ε_r, ε_t, $\tilde{\varepsilon}_{m1}$ (parallel to the surface) and $\tilde{\varepsilon}_{m3}$ (perpendicular to the surface), respectively. At a SH angular frequency 2ω, their dielectric constants are denoted as ε_R, ε_T, $\tilde{\varepsilon}_{M1}$ (parallel) and $\tilde{\varepsilon}_{M3}$ (perpendicular). In order to describe vector components, laboratory coordinates {X(1), Y(2), Z(3)} are introduced, where X is parallel to

the layer surface and Z is perpendicular to the surface. An incident light propagates in XZ plane toward the positive Z direction. The incident fundamental wave is assumed to be a linearly polarized plane wave. The polarization direction makes an angle γ_p with respect to the incident (XZ) plane and the electric field amplitude is E^{i0}. When it impinges on the top layer with the angle of incidence θ_0, the X and Y components of the amplitude are expressed by

$$E_1^{i0} = E^{i0} \cos\gamma_p \cos\theta_0$$
$$E_2^{i0} = E^{i0} \sin\gamma_p \quad , \qquad (2\text{-}2B\text{-}1)$$

respectively. The X component of the wavevector is given by

$$k_1 = \frac{\omega}{c} \sqrt{\varepsilon_r} \sin\theta_0 \quad . \qquad (2\text{-}2B\text{-}2)$$

Under the circumstance mentioned above, the wave equation in nonmagnetic system

$$\nabla \times \nabla \times \boldsymbol{E} + \frac{\varepsilon}{c^2} \frac{\partial^2 \boldsymbol{E}}{\partial t^2} + \frac{4\pi\sigma}{c^2} \frac{\partial \boldsymbol{E}}{\partial t} = 0 \qquad (2\text{-}2B\text{-}3)$$

is solved under electromagnetic boundary conditions at the top/middle and middle/bottom layers. The conductivity tensor σ appears in the middle layer to take account of absorption. It is assumed that the top layer and the bottom layer consist of materials with isotropic dielectric tensors whose dielectric constants are real.

The electric field in the middle layer is expressed as a sum of forward (mf) and backward (mb) waves, which also depend on the polarization directions (s and p). There are also a reflection (r) wave in the top layer and a transmission (t) wave in the bottom layer. The

X components of the wavevectors for these waves are equal to k_1 because of the boundary condition. The Z components of the wavevectors for r, t, mf and mb waves are determined by following dispersion relations.

$$
\begin{aligned}
r &= -\sqrt{\frac{\omega^2}{c^2}\varepsilon_r - k_1^2} \\
t &= \sqrt{\frac{\omega^2}{c^2}\varepsilon_t - k_1^2} \\
m_s^f &= \sqrt{\frac{\omega^2}{c^2}\tilde{\varepsilon}_{m1} - k_1^2} \\
m_p^f &= \sqrt{\frac{\omega^2}{c^2}\tilde{\varepsilon}_{m1} - \frac{\tilde{\varepsilon}_{m1}}{\tilde{\varepsilon}_{m3}}k_1^2}
\end{aligned}
\quad , \qquad \text{(2-2B-4)}
$$

where $\tilde{\varepsilon}_{m1}$ and $\tilde{\varepsilon}_{m3}$ are the X component (parallel to the surface) and the Z component (perpendicular to the surface) of the complex dielectric tensor ($\tilde{\varepsilon}_m = \varepsilon_m + i(4\pi\sigma_m/\omega)$) in the middle layer, respectively, and m_s^f and m_p^f are the Z components of the wavevectors for mf waves with s and p polarizations, respectively. The components for mb waves (m_s^b and m_p^b) are obtained by $m_s^b = -m_s^f$ and $m_p^b = -m_p^f$. The boundary conditions are expressed by the relations between the amplitudes of the waves (E^0). For the s component,

$$
\begin{pmatrix}
1 & -1 & -1 & 0 \\
r & -m_s^f & m_s^f & 0 \\
0 & e^{im_s^f d} & e^{-im_s^f d} & -1 \\
0 & m_s^f e^{im_s^f d} & -m_s^f e^{-im_s^f d} & -t
\end{pmatrix}
\begin{pmatrix}
E_2^{r0} \\ E_2^{mf0} \\ E_2^{mb0} \\ E_2^{t0}
\end{pmatrix}
=
\begin{pmatrix}
-E_2^{i0} \\ rE_2^{i0} \\ 0 \\ 0
\end{pmatrix}
\quad . \qquad \text{(2-2B-5)}
$$

For the p component,

$$\begin{pmatrix} 1 & -1 & -1 & 0 \\ \frac{\varepsilon_r}{r} & -\frac{\tilde{\varepsilon}_{m1}}{m_p^f} & \frac{\tilde{\varepsilon}_{m1}}{m_p^f} & 0 \\ 0 & e^{im_p^f d} & e^{-im_p^f d} & -1 \\ 0 & \frac{\tilde{\varepsilon}_{m1}}{m_p^f} e^{im_p^f d} & -\frac{\tilde{\varepsilon}_{m1}}{m_p^f} e^{-im_p^f d} & -\frac{\varepsilon_t}{t} \end{pmatrix} \begin{pmatrix} E_1^{r0} \\ E_1^{mf0} \\ E_1^{mb0} \\ E_1^{t0} \end{pmatrix} = \begin{pmatrix} -E_1^{i0} \\ \frac{\varepsilon_r}{r} E_1^{i0} \\ 0 \\ 0 \end{pmatrix} \quad . \quad \text{(2-2B-6)}$$

We can obtain the electric field amplitudes of the mf and mb waves by solving eqs. (2-2B-5) and (2-2B-6). The Z components are given by

$$E_3^{mf0} = -\frac{\tilde{\varepsilon}_{m1} k_1}{\tilde{\varepsilon}_{m3} m_p^f} E_1^{mf0}$$
$$E_3^{mb0} = \frac{\tilde{\varepsilon}_{m1} k_1}{\tilde{\varepsilon}_{m3} m_p^f} E_1^{mb0} \quad . \quad \text{(2-2B-7)}$$

The electric field in the middle layer is expressed as a sum of the mf and mb waves, namely,

$$E_i = E_i^{mf} + E_i^{mb} \quad . \quad \text{(2-2B-8)}$$

Consequently, the nonlinear electric polarization for higher order mechanisms is expressed as

$$P_\alpha = \Sigma\, g_{\alpha\beta\gamma\delta} E_\beta \partial_\gamma E_\delta = \Sigma_{\beta\gamma\delta\rho\rho'} g_{\alpha\beta\gamma\delta} E_\beta^\rho \partial_\gamma E_\delta^{\rho'} \quad , \quad \text{(2-2B-9)}$$

where the indices ρ and ρ' express mf and mb states. It must be noted that $g_{\alpha\beta\gamma\delta}$ in eq.(2-2B-9) is defined for the laboratory coordinates. For O_h, D_{4h} and C_{4v} symmetries, we describe it as

$g^{L}_{\alpha\beta\gamma\delta}$. Each term is of the plane wave form and the amplitude (P^0) is given by

$$P^0 = i\, k_\gamma(E_\delta^{\rho'})\, g_{\alpha\beta\gamma\delta}\, E_\beta^{\rho 0}\, E_\delta^{\rho' 0} \quad , \qquad \text{(2-2B-10)}$$

where $k_\gamma(E_\delta^{\rho'})$ is the γ component of the wavevector for $E_\delta^{\rho'}$. The wavevector (**K**) for this plane wave is given by

$$\begin{aligned} K_1 &= 2\, k_1 \\ K_2 &= 0 \\ K_3 &= k_3(E_\beta^{\rho}) + k_3(E_\delta^{\rho'}) \quad . \end{aligned} \qquad \text{(2-2B-11)}$$

We can also treat with the similar procedure for the electric dipole mechanism as follows.

$$P_\alpha = \Sigma\, \chi_{\alpha\beta\delta} E_\beta E_\delta = \Sigma_{\beta\delta\rho\rho'}\, \chi_{\alpha\beta\delta} E_\beta^{\rho} E_\delta^{\rho'} \quad . \qquad \text{(2-2B-12)}$$

$$P^0 = \chi_{\alpha\beta\delta}\, E_\beta^{\rho 0}\, E_\delta^{\rho' 0} \quad . \qquad \text{(2-2B-13)}$$

$$\begin{aligned} K_1 &= 2\, k_1 \\ K_2 &= 0 \\ K_3 &= k_3(E_\beta^{\rho}) + k_3(E_\delta^{\rho'}) \quad . \end{aligned} \qquad \text{(2-2B-14)}$$

The SH wave produced by the effective nonlinear polarization $\mathbf{P}_{eff}$ is given by solving the wave equation in a nonmagnetic system,

$$\nabla \times \nabla \times E + \frac{\varepsilon}{c^2}\frac{\partial^2 E}{\partial t^2} + \frac{4\pi\sigma}{c^2}\frac{\partial E}{\partial t} = -\frac{4\pi}{c^2}\frac{\partial^2 P_{eff}}{\partial t^2} \quad , \qquad \text{(2-2B-15)}$$

where the conductivity tensor σ appears in the middle layer in order to take the absorption effect into account. It is assumed that the top

layer and the bottom layer consist of materials with isotropic dielectric tensors whose dielectric constants at SH frequency are real. $\mathbf{P}_{eff}$ consists of the electric dipole, the electric quadrupole coupling, the magnetic dipole coupling, the electric quadrupole and magnetic dipole mechanisms. We use the form of eq (2-2B-9) for higher order mechanisms in $\mathbf{P}_{eff}$. Since $\mathbf{P}$ is expressed as linear combinations of the plane waves,

$$\boldsymbol{P} = \Sigma \boldsymbol{P}_a = \Sigma \boldsymbol{P}_a^0 \, e^{i(K_a \cdot r - 2\omega t)} \quad , \tag{2-2B-16}$$

the SH electric field is expressed as

$$E = \Sigma E_a = \Sigma \, E_a^0 \, e^{i(K_a \cdot r - 2\omega t)} \quad . \tag{2-2B-17}$$

Each component $\mathbf{E}a$ is obtained by solving

$$-\boldsymbol{K}_a \times \boldsymbol{K}_a \times \boldsymbol{E}_a - \frac{4\omega^2 \tilde{\varepsilon}_M}{c^2} \boldsymbol{E}_a = \frac{16\pi\omega^2}{c^2} \boldsymbol{P}_a \quad , \tag{2-2B-18}$$

where $\tilde{\varepsilon}_M = \varepsilon_M + i(2\pi\sigma_M / \omega)$ stands for the complex dielectric tensor in the middle layer at angular frequency 2ω. The magnetic field is obtained by

$$\boldsymbol{H}_a = \frac{c}{2\omega} \boldsymbol{K}_a \times \boldsymbol{E}_a \tag{2-2B-19}$$

using the Maxwell's equation.

We first solve eq. (2-2B-18) to obtain the inhomogeneous wave (I) $\mathbf{E}_a{}^I$ for $\mathbf{P}_a$. Then, the solution $\mathbf{E}=\Sigma\mathbf{E}_a$ is obtained. For the s wave, the inhomogeneous electric field E_2 and the corresponding H_1 component are given by

$$E^{I}_{a2} = \frac{4\pi P_{a2}}{\frac{c^2}{4\omega^2}(K_1^2 + K_{a3}^2) - \varepsilon_{M1}} \qquad (2\text{-}2B\text{-}20)$$

$$H^{I}_{a1} = -\frac{cK_{a3}E^{I}_{a2}}{2\omega} \quad . \qquad (2\text{-}2B\text{-}21)$$

For the p wave, E_1 component of the inhomogeneous electric field and the corresponding H_2 component are given by

$$E^{I}_{a1} = \frac{4\pi\{(K_1^2 - \frac{4\omega^2}{c^2}\varepsilon_{M3})P_{a1} + K_1 K_{a3} P_{a3}\}}{(\frac{4\omega^2}{c^2}\varepsilon_{M1}\varepsilon_{M3} - K_1^2\varepsilon_{M1} - K_{a3}^2\varepsilon_{M3})} \qquad (2\text{-}2B\text{-}22)$$

$$\frac{c}{2\omega}H^{I}_{a2} = \frac{4\pi(\varepsilon_{M1}K_1 P_{a3} - \varepsilon_{M3}K_{a3}P_{a1})}{(\frac{4\omega^2}{c^2}\varepsilon_{M1}\varepsilon_{M3} - K_1^2\varepsilon_{M1} - K_{a3}^2\varepsilon_{M3})} \quad . \qquad (2\text{-}2B\text{-}23)$$

To satisfy boundary conditions, homogeneous solution must be introduced. The homogeneous wave in the middle layer is obtained by solving eq. (2-2B-15) with $P_{eff}=0$, and is expressed as a sum of forward (MF) and backward (MB) waves, which also depend on the polarization directions (s and p). There are also a reflection (R) wave in the top layer, and a transmission (T) wave in the bottom layer. The X components of the wavevectors for these waves are equal to K_1. The following dispersion relations give the Z components for the R, T, MF, and MB waves.

$$\begin{aligned} R &= -\sqrt{\frac{4\omega^2}{c^2}\varepsilon_R - K_1^2} \\ T &= \sqrt{\frac{4\omega^2}{c^2}\varepsilon_T - K_1^2} \\ M_s^F &= \sqrt{\frac{4\omega^2}{c^2}\varepsilon_{M1} - K_1^2} \\ M_p^F &= \sqrt{\frac{4\omega^2}{c^2}\varepsilon_{M1} - \frac{\varepsilon_{M1}}{\varepsilon_{M3}}K_1^2} \end{aligned} \quad , \qquad (2\text{-}2B\text{-}24)$$

where M_s^F and M_p^F are the Z components of the wavevectors for the MF waves with s and p polarizations, respectively. Boundary conditions are written in the form of matrix equation. For the s wave,

$$\begin{pmatrix} 1 & -1 & -1 & 0 \\ R & -M_s^F & M_s^F & 0 \\ 0 & e^{iM_s^F d} & e^{-iM_s^F d} & -1 \\ 0 & M_s^F e^{iM_s^F d} & -M_s^F e^{-iM_s^F d} & -T \end{pmatrix} \begin{pmatrix} E_2^{R0} \\ E_2^{MF0} \\ E_2^{MB0} \\ E_2^{T0} \end{pmatrix} = \begin{pmatrix} \Sigma E_{a2}^{I0} \\ \Sigma K_{a3} E_2^{I0} \\ -\Sigma e^{iK_{a3}d} E_{a2}^{I0} \\ -\Sigma e^{iK_{a3}d} K_{a3} E_{a2}^{I0} \end{pmatrix} . \quad \text{(2-2B-25)}$$

For the p wave,

$$\begin{pmatrix} 1 & -1 & -1 & 0 \\ \frac{\varepsilon_R}{R} & -\frac{\tilde{\varepsilon}_{MI}}{M_p^F} & \frac{\tilde{\varepsilon}_{MI}}{M_p^F} & 0 \\ 0 & e^{iM_p^F d} & e^{-iM_p^F d} & -1 \\ 0 & \frac{\tilde{\varepsilon}_{MI}}{M_p^F} e^{iM_p^F d} & -\frac{\tilde{\varepsilon}_{MI}}{M_p^F} e^{-iM_p^F d} & -\frac{\varepsilon_T}{T} \end{pmatrix} \begin{pmatrix} E_1^{R0} \\ E_1^{MF0} \\ E_1^{MB0} \\ E_1^{T0} \end{pmatrix} = \begin{pmatrix} \Sigma E_{a1}^{I0} \\ \frac{c}{2\omega} \Sigma H_{a2}^{I0} \\ -\Sigma e^{iK_{a3}d} E_{a1}^{I0} \\ -\frac{c}{2\omega} \Sigma e^{iK_{a3}d} H_{a2}^{I0} \end{pmatrix} . \quad \text{(2-2B-26)}$$

Then, reflected and transmitted SH waves can be obtained by solving eqs. (2-2B-25) and (2-2B-26).

In our experimental geometry, an analyzer is located before the detector. When the polarization direction of the analyzer makes an angle γ_a with respect to the incident plane, the amplitudes of the electric field components that pass the analyzer are given by

$$E_{\gamma a}^{R0} = \sin\gamma_a E_2^{R0} - \cos\gamma_a \frac{2\omega\sqrt{\varepsilon_R}}{cR} E_1^{R0} \quad \text{(2-2B-27)}$$

$$E_{\gamma a}^{T0} = \sin\gamma_a E_2^{T0} + \cos\gamma_a \frac{2\omega\sqrt{\varepsilon_T}}{cT} E_1^{T0} . \quad \text{(2-2B-28)}$$

Finally, the intensity of SHG are obtained by

$$I_{\gamma\alpha}^{R} = | E_{\gamma\alpha}^{R0} |^2 \qquad \text{(2-2B-29)}$$

$$I_{\gamma\alpha}^{T} = | E_{\gamma\alpha}^{T0} |^2 \ . \qquad \text{(2-2B-30)}$$

In the case of K_h and O_h symmetries, an isotropic dielectric tensor should be taken into consideration, so that we make the substitutions

$$\tilde{\varepsilon}_m = \tilde{\varepsilon}_{m1} = \tilde{\varepsilon}_{m3} \qquad \text{(2-2B-31)}$$

$$\tilde{\varepsilon}_M = \tilde{\varepsilon}_{M1} = \tilde{\varepsilon}_{M3} \ , \qquad \text{(2-2B-32)}$$

Using above relations, the following replacements can be also made.

$$m^f = m_s^f = m_p^f = \sqrt{\frac{\omega^2}{c^2}\tilde{\varepsilon}_m - k_1^2} \qquad \text{(2-2B-33)}$$

$$m^b = m_s^b = m_p^b = -m^f \qquad \text{(2-2B-34)}$$

$$M^f = M_s^f = M_p^f = \sqrt{\frac{\omega^2}{c^2}\tilde{\varepsilon}_M - k_1^2} \qquad \text{(2-2B-35)}$$

$$M^b = M_s^b = M_p^b = -M^f \ . \qquad \text{(2-2B-36)}$$

The analytical expressions for the reflection SHG from the geometry shown in Fig. 2-2-1(b) can be obtained as follows. There exist the r wave in addition to the incident wave in the top layer and mf waves, which depend on the polarization directions (s and p) in the middle layer, at the angular frequency ω. Hence, we pick up the terms concerning with these waves in eqs. (2-2B-1)~(2-2B-14), although we need to modify eqs. (2-2B-5) and (2-2B-6) to the forms

$$\begin{pmatrix} 1 & -1 \\ r & -m_s^f \end{pmatrix} \begin{pmatrix} E_2^{r0} \\ E_2^{mf0} \end{pmatrix} = \begin{pmatrix} -E_2^{i0} \\ rE_2^{i0} \end{pmatrix} \qquad \text{(2-2B-37)}$$

$$\begin{pmatrix} 1 & -1 \\ \frac{\varepsilon_r}{r} & -\frac{\varepsilon_{m1}}{m_p^f} \end{pmatrix} \begin{pmatrix} E_1^{r0} \\ E_1^{mf0} \end{pmatrix} = \begin{pmatrix} -E_1^{i0} \\ \frac{\varepsilon_r}{r} E_1^{i0} \end{pmatrix} . \qquad \text{(2-2B-38)}$$

At the angular frequency 2ω, we pick up the terms concerning with the nonlinear electric polarization produced by the mf waves and the corresponding inhomogeneous waves in eqs. (2-2B-15)~(2-2B-23). In this geometry, there exist the R wave in the top layer and the homogeneous MF waves, which depend on the polarization directions (s and p) in the middle layer. Therefore we pick up the terms accompanied with these waves in eqs. (2-2B-24)~(2-2B-30). Here, we need to modify eqs. (2-2B-25) and (2-2B-26) to the forms

$$\begin{pmatrix} 1 & -1 \\ R & -M_s^F \end{pmatrix} \begin{pmatrix} E_2^{R0} \\ E_2^{MF0} \end{pmatrix} = \begin{pmatrix} \Sigma E_{a2}^{I0} \\ \Sigma K_{a3} E_2^{I0} \end{pmatrix} \qquad \text{(2-2B-39)}$$

$$\begin{pmatrix} 1 & -1 \\ \frac{\varepsilon_R}{R} & -\frac{\varepsilon_{M1}}{M_p^F} \end{pmatrix} \begin{pmatrix} E_1^{R0} \\ E_1^{MF0} \end{pmatrix} = \begin{pmatrix} \Sigma E_{a1}^{I0} \\ \frac{c}{2\omega} \Sigma H_{a2}^{I0} \end{pmatrix} . \qquad \text{(2-2B-40)}$$

For K_h and O_h system in this geometry, the substitutions (eq. (2-2B-31), (2-2B-32), (2-2B-33) and (2-2B-35)) are also effective. The expressions of P components in the labratory coordinates for each system in each geometry will be described in the section 2-2C.

2-2C Rotational angle dependence and polarization angle dependence in SHG

In this section, we describe the rotational angle and the polarization angle dependences of the SHG for systems argued in the previous section.

For K_h, $D_{\infty h}$ and $C_{\infty v}$ symmetries, the polarization dependence of the SHG are listed in Table 2-2-1. We can further transfigure the expressions in Table 2-2-1 for K_h symmetry, so that we find some important informations. The P_1, P_2 and P_3 components for the polarization conditions (p→p, s→p and 45°→s) in the geometries shown in Fig. 2-2-1(a) and 2-2-1(b) are described as follows.

For p→p condition,

$$\begin{aligned}
P_1 &= g_{1111}E_1\partial_1E_1 + g_{1133}E_1\partial_3E_3 + g_{1313}E_3\partial_1E_3 + g_{1331}E_3\partial_3E_1 \\
&= (g_{iijj} + g_{ijij} + g_{ijji})E_1\partial_1E_1 + g_{iijj}E_1\partial_3E_3 + g_{ijij}E_3\partial_1E_3 + g_{ijji}E_3\partial_3E_1 \\
&= g_{iijj}E_1(\partial_1E_1 + \partial_3E_3) + \frac{1}{2}g_{ijij}\partial_1(E_1^2 + E_3^2) + g_{ijji}(E_1\partial_1 + E_3\partial_3)E_1 \\
P_3 &= g_{3113}E_1\partial_1E_3 + g_{3131}E_1\partial_3E_1 + g_{3311}E_3\partial_1E_1 + g_{3333}E_3\partial_3E_3 \\
&= g_{ijji}E_1\partial_1E_3 + g_{ijij}E_1\partial_3E_1 + g_{iijj}E_3\partial_1E_1 + (g_{ijji} + g_{ijij} + g_{iijj})E_3\partial_3E_3 \\
&= g_{iijj}E_3(\partial_1E_1 + \partial_3E_3) + \frac{1}{2}g_{ijij}\partial_3(E_1^2 + E_3^2) + g_{ijji}(E_1\partial_1 + E_3\partial_3)E_3
\end{aligned} \qquad \text{(2-2C-1)}$$

For s→p condition,

$$\begin{aligned}
P_1 &= g_{1212}E_2\partial_1E_2 \\
&= \frac{1}{2}g_{ijij}\partial_1(E_2^2) \\
P_3 &= g_{3232}E_2\partial_3E_2 \\
&= \frac{1}{2}g_{ijij}\partial_3(E_2^2)
\end{aligned} \qquad \text{(2-2C-2)}$$

For 45°→s condition,

Table 2-2-1 Expressions of nonlinear polarizations in higher order mechanisms for K_h and $D_{\infty h}$ and $C_{\infty v}$ systems and those in the electric dipole mechanism for $C_{\infty v}$ system. Here, only the elements which contribute to SHG in each polarization condition are listed.

p→p	$P_1 = g_{1111}E_1\partial_1 E_1 + g_{1133}E_1\partial_3 E_3 + g_{1313}E_3\partial_1 E_3 + g_{1331}E_3\partial_3 E_1$ $P_3 = g_{3113}E_1\partial_1 E_3 + g_{3131}E_1\partial_3 E_1 + g_{3311}E_3\partial_1 E_1 + g_{3333}E_3\partial_3 E_3$
	$P_1 = (\chi_{113} + \chi_{131})E_1E_3$ $P_3 = \chi_{311}E_1^2 + \chi_{333}E_3^2$
s→p	$P_1 = g_{1212}E_2\partial_1 E_2$ $P_3 = g_{3232}E_2\partial_3 E_2$
	$P_3 = \chi_{322}E_2^2$
45°→s	$P_2 = g_{2112}E_1\partial_1 E_2 + g_{2211}E_2\partial_1 E_1 + g_{2233}E_2\partial_3 E_3 + g_{2332}E_3\partial_3 E_2$
	$P_2 = (\chi_{223} + \chi_{232})E_2E_3$
p→s	$P_2 = 0$
	$P_2 = 0$
s→s	$P_2 = 0$
	$P_2 = 0$

The electric field **E** in nonlinear active layer is described as

$E_i = E_i^{mf} + E_i^{mb}$ (for the geometry shown in Fig. 2-2-1(a)),
$E_i = E_i^{mf}$ (for the geometry shown in Fig. 2-2-1(b)).

For K_h symmetry, the following relations between g components should be satisfied.

$$g_{iijj},\ g_{ijij},\ g_{ijji},\ g_{iiii} = g_{iijj} + g_{ijij} + g_{ijji} \qquad (i \neq j)$$

We should consider an isotropic dielectric tensor for K_h symmetry. Therefore, the relations also exist.

$\varepsilon_m = \varepsilon_{m1} = \varepsilon_{m3}$
$\varepsilon_M = \varepsilon_{M1} = \varepsilon_{M3}$

We can perform further transformation for K_h symmetry using the relations, so that we obtain some important informations as described in the section 2-2C.

For $D_{\infty h}$ and $C_{\infty v}$ symmetry, the following relations between g components should be satisfied.

$g_{3311} = g_{3322}$, $g_{1133} = g_{2233}$, $g_{1122} = g_{2211}$
$g_{3131} = g_{3232}$, $g_{1313} = g_{2323}$, $g_{1212} = g_{2121}$
$g_{3113} = g_{3223}$, $g_{1331} = g_{2332}$, $g_{1221} = g_{2112}$
g_{3333}, $g_{1111} = g_{2222} = g_{1122} + g_{1212} + g_{2121}$.

For $C_{\infty v}$ symmetry, the relation between χ components should be satisfied.

$\chi_{113} = \chi_{131} = \chi_{223} = \chi_{232}$
$\chi_{311} = \chi_{322}$
χ_{333} .

$$P_2 = g_{2112}E_1\partial_1 E_2 + g_{2211}E_2\partial_1 E_1 + g_{2233}E_2\partial_3 E_3 + g_{2332}E_3\partial_3 E_2$$
$$= g_{ijji}(E_1\partial_1 + E_3\partial_3)E_2 + g_{iijj}E_2(\partial_1 E_1 + \partial_3 E_3) \quad . \qquad (2\text{-}2C\text{-}3)$$

In the caluculation, we used the relations which are satisfied in K_h symmtry as described in Table 2-2-1. The results can be directly obtained according to the Appendix. For the geometry shown in Fig. 2-2-1(b), the electric field in nonlinear active layer is $E_i = E_i^{mf}$. Then, the P_1, P_2 and P_3 for the polarization conditions (p→p, s→p and 45°→s) in the geometry are described as follows.

For p→p condition,

$$P_1 = \frac{1}{2}g_{ijij}(i2k_1)(E_1^{mf2} + E_3^{mf2})$$
$$P_3 = \frac{1}{2}g_{ijij}(i2m^f)(E_1^{mf2} + E_3^{mf2}) \quad . \qquad (2\text{-}2C\text{-}4)$$

For s→p condition,

$$P_1 = \frac{1}{2}g_{ijij}(i2k_1)E_2^{mf2}$$
$$P_3 = \frac{1}{2}g_{ijij}(i2m^f)E_2^{mf2} \quad . \qquad (2\text{-}2C\text{-}5)$$

For 45°→s condition,

$$P_2 = 0 \quad . \qquad (2\text{-}2C\text{-}6)$$

In the calculation, we used the relation $E_1^{mf0}k_1 + E_3^{mf0}m^f = 0$. We find s-polarized SH light of the bulk origin from higher order mechanisms can not be observed and only the term g_{ijij} appears for K_h system in the geometry (Fig. 2-2-1(b)).

For the geometry shown in Fig. 2-2-1(a), the electric field in the nonlinear active layer is described as $E_i = E_i^{mf} + E_i^{mb}$. Then, the P_1, P_2 and P_3 components are described for each polarization as follows.

For p→p condition,

$$\begin{aligned} P_1 &= \frac{1}{2} g_{ijij}(i2k_1)(E_1^{mf2} + E_3^{mf2} + 2E_1^{mf0}E_1^{mb} + 2E_3^{mf}E_3^{mb} + E_1^{mb2} + E_3^{mb2}) \\ &+ g_{ijji}(ik_1(2E_1^{mf}E_1^{mb}) - im^f E_3^{mf}E_1^{mb} + im^f E_3^{mb}E_1^{mf}) \\ P_3 &= \frac{1}{2} g_{ijij}((i2m^f)(E_1^{mf2} + E_3^{mf2}) - (i2m^f)(E_1^{mb2} + E_3^{mb2})) \\ &+ g_{ijji}ik_1(E_1^{mf}E_3^{mb} + E_1^{mb}E_3^{mf}) \end{aligned} \quad . \qquad (2\text{-}2C\text{-}7)$$

For s→p condition,

$$\begin{aligned} P_1 &= \frac{1}{2} g_{ijij}(i2k_1)(E_2^{mf2} + 2E_2^{mf}E_2^{mb} + E_2^{mb}) \\ P_3 &= \frac{1}{2} g_{ijij}((i2m^f)E_2^{mf2} - (i2m^f)E_2^{mb2}) \end{aligned} \quad . \qquad (2\text{-}2C\text{-}8)$$

For 45°→s condition,

$$P_2 = g_{ijji}(ik_1(E_1^{mf}E_2^{mb} + E_1^{mb}E_2^{mf}) + im^f E_3^{mf}E_2^{mb} - im^f E_3^{mb}E_2^{mf}) \quad . \qquad (2\text{-}2C\text{-}9)$$

In this calculation, we used the relations $E_1^{mf0}k_1 + E_3^{mf0}m^f = 0$, $E_1^{mb0}k_1 + E_3^{mb0}m^b = 0$ and $m^b = -m^f$. For K_h symmetry, the nonlinear polarization due to the g_{ijji} terms arises only from the product of the fields of forward and backward waves in the nonlinear active layer for all polarization conditions. This fact is consistent with no existence of g_{ijji} terms in eqs. (2-2C-4), (2-2C-5) and (2-2C-6) for the geometry (Fig. 2-2-1(b)) where the backward wave do not exist. Moreover, the bulk SHG comes only from the g_{ijji} terms for the

polarization condition (45°→s). Thus, both g_{ijji} and g_{ijij} components are evaluated in the geometry (Fig 2-2-1(b)). In fact, Koopmans et al. [14,15] clarified the dominant origin of SHG from vacuum evaporated C_{60} films by measuring the thickness and the polarization dependent SHG and evaluating the ratio g_{ijji}/g_{ijij}. They obtained $g_{ijji}/g_{ijij}=-1$ which indicates the dominance of the magnetic dipole coupling mechanism (see eqs. (2-2A-17) and (2-2A-36)) and concluded that the dominance comes from the resonant magnetic dipole transition ($^1A_g \rightarrow {}^1T_{1g}$) at a fundamental frequency.

Further transfiguration is not so effective for $C_{\infty v}$ and $D_{\infty h}$ symmetries as for K_h symmetry since we have many independent tensor components and an anisotropic dielectric tensor. In these symmetries, the SHG in the polarization condition (45°→s) should be observed for both geometries (Figs. 2-2-1(a) and 2-2-1(b)).

For O_h, D_{4h} and C_{4v} symmetries, the relation between the crystal coordinates and the laboratory coordinates is the same one, about which we described in the section 2-2B. We define the rotational angle φ which is the one between X(1) axis in the laboratory coordinates and x(1) axis in the crystal coordinates. By using the tansformation matrix,

$$\begin{pmatrix} a_{11} & a_{12} & a_{13} \\ a_{21} & a_{22} & a_{23} \\ a_{31} & a_{32} & a_{33} \end{pmatrix} = \begin{pmatrix} \cos\varphi & \sin\varphi & 0 \\ -\sin\varphi & \cos\varphi & 0 \\ 0 & 0 & 1 \end{pmatrix}, \qquad (2\text{-}2C\text{-}10)$$

the tensor components in the laboratory coordinates are calculated by

$$g^{L}_{\alpha\beta\gamma\delta} = \Sigma\, a_{\omega} a_{\beta j} a_{\gamma k} a_{\delta l} g_{ijkl} \quad . \qquad (2\text{-}2C\text{-}11)$$

Here, the g components with the superscript L stand for those in the laboratory coordinates. The polarization and rotational angle dependences of the SHG are summarized in Table 2-2-2.

In O_h system, we can perform further transfiguration for the expressions. The P_1, P_2 and P_3 components for the polarization conditions (p→p, s→p, 45°→s, p→s and s→s) are described as follows.

For p→p condition,

$$
\begin{aligned}
&P_1 = g^L_{1111}E_1\partial_1E_1 + g^L_{1133}E_1\partial_3E_3 + g^L_{1313}E_3\partial_1E_3 + g^L_{1331}E_3\partial_3E_1 \\
&= (\frac{1}{4}(\cos 4\varphi + 3)(g_{iiii} - g_{iijj} - g_{ijij} - g_{ijji}) + (g_{iijj} + g_{ijij} + g_{ijji}))E_1\partial_1E_1 \\
&+ g_{iijj}E_1\partial_3E_3 + g_{ijij}E_3\partial_1E_3 + g_{ijji}E_3\partial_3E_1 \\
&= \frac{1}{4}(\cos 4\varphi + 3)g^aE_1\partial_1E_1 \\
&+ g_{iijj}E_1(\partial_1E_1 + \partial_3E_3) + \frac{1}{2}g_{ijij}\partial_1(E_1^2 + E_3^2) + g_{ijji}(E_1\partial_1 + E_3\partial_3)E_1 \\
&P_3 = g^L_{3333}E_3\partial_3E_3 + g^L_{3311}E_3\partial_1E_1 + g^L_{3131}E_1\partial_3E_1 + g^L_{3113}E_1\partial_1E_3 \\
&= ((g_{iiii} - g_{iijj} - g_{ijij} - g_{ijji}) - (g_{iijj} + g_{ijij} + g_{ijji}))E_3\partial_3E_3 + g_{iijj}E_3\partial_1E_1 + g_{ijij}E_1\partial_3E_1 + g_{ijji}E_1\partial_1E_3 \\
&= g^aE_3\partial_3E_3 + g_{iijj}E_3(\partial_1E_1 + \partial_3E_3) + \frac{1}{2}g_{ijij}\partial_3(E_1^2 + E_3^2) + g_{ijji}(E_1\partial_1 + E_3\partial_3)E_3
\end{aligned}
\qquad \text{(2-2C-12)}
$$

For s→p condition,

$$
\begin{aligned}
&P_1 = g^L_{1212}E_2\partial_1E_2 \\
&= (\frac{1}{4}(1 - \cos 4\varphi)(g_{iiii} - g_{iijj} - g_{ijij} - g_{ijji}) + g_{ijij})E_2\partial_1E_2 \\
&= \frac{1}{4}(1 - \cos 4\varphi)g^aE_2\partial_1E_2 + \frac{1}{2}g_{ijij}\partial_1(E_2^2) \\
&P_3 = g^L_{3232}E_2\partial_3E_2 \\
&= g_{ijij}E_2\partial_3E_2 \\
&= \frac{1}{2}g_{ijij}\partial_3(E_2^2)
\end{aligned}
\qquad \text{(2-2C-13)}
$$

For 45°→s condition,

Table 2-2-2 Expressions of nonlinear polarizations in higher order mechanisms for O_h, C_{4v} and D_{4h} systems and those in the electric dipole mechanism for C_{4v} system in the laboratory coordinates. The relation between the crystal coordinates and the laboratory coordinates is defined in the section 2-2B. Here, only the elements which contribute to SHG in each polarization condition are listed.

p→p	$P_1 = g^L_{1111}E_1\partial_1E_1 + g^L_{1133}E_1\partial_3E_3 + g^L_{1313}E_3\partial_1E_3 + g^L_{1331}E_3\partial_3E_1$ $P_3 = g^L_{3333}E_3\partial_3E_3 + g^L_{3311}E_3\partial_1E_1 + g^L_{3131}E_1\partial_3E_1 + g^L_{3113}E_1\partial_1E_3$
	$P_1 = (\chi_{113} + \chi_{131})E_1E_3$ $P_3 = \chi_{311}E_1^2 + \chi_{333}E_3^2$
s→p	$P_1 = g^L_{1212}E_2\partial_1E_2$ $P_3 = g^L_{3232}E_2\partial_3E_2$
	$P_3 = \chi_{322}E_2^2$
45°→s	$P_2 = g^L_{2111}E_1\partial_1E_1 + g^L_{2112}E_1\partial_1E_2 + g^L_{2211}E_2\partial_1E_1 + g^L_{2212}E_2\partial_1E_2$ $+ g^L_{2332}E_3\partial_3E_2 + g^L_{2233}E_2\partial_3E_3$
	$P_2 = (\chi_{223} + \chi_{232})E_2E_3$
p→s	$P_2 = g^L_{2111}E_1\partial_1E_1$
	$P_2 = 0$
s→s	$P_2 = g^L_{2212}E_2\partial_1E_2$
	$P_2 = 0$

The components for the fundamental electric field **E** and the nonlinear polarization **P** in the nonlinear active layer and the g^L tensor components are defined for the laboratory coordinates. We removed the superscript L for χ components, since χ in C_{4v} system does not change under the transformation (eq. 2-2C-10). The electric field in the nonlinear active layer is described as

$E_i = E_i^{mf} + E_i^{mb}$ (for the geometry shown in Fig. 2-2-1(a)),
$E_i = E_i^{mf}$ (for the geometry shown in Fig. 2-2-1(b)).

We should consider an isotropic dielectric tensor for O_h symmetry. Therefore, the following relations also exist.

$\varepsilon_m = \varepsilon_{m1} = \varepsilon_{m3}$
$\varepsilon_M = \varepsilon_{M1} = \varepsilon_{M3}$

The independent g tensor components in crystal coordinates are described as

g_{iijj}, g_{ijij}, g_{ijji}, g_{iiii} $(i \neq j)$

for O_h symmetry, and

$g_{3311} = g_{3322}$, $g_{1133} = g_{2233}$, $g_{1122} = g_{2211}$
$g_{3131} = g_{3232}$, $g_{1313} = g_{2323}$, $g_{1212} = g_{2121}$
$g_{3113} = g_{3223}$, $g_{1331} = g_{2332}$, $g_{1221} = g_{2112}$
g_{3333}, $g_{1111} = g_{2222}$

for D_{4h} and C_{4v} symmetries.

The independent χ tensor components in crystal coordinates are described as

$\chi_{113} = \chi_{131} = \chi_{223} = \chi_{232}$
$\chi_{311} = \chi_{322}$
χ_{333}

for C_{4v} symmetry.

The g^L tensor components are related to the g tensor component using the transformation matrix defined in the section 2-2-C as follows.

$$g^L_{1111} = \frac{1}{4}(\cos 4\varphi + 3)(g_{1111} - g_{1122} - g_{1212} - g_{1221}) + (g_{1122} + g_{1212} + g_{1221}) ,$$
$$g^L_{1133} = g_{1133} , \quad g^L_{1313} = g_{1313} , \quad g^L_{1331} = g_{1331} ,$$
$$g^L_{3333} = g_{3333} , \quad g^L_{3311} = g_{3311} , \quad g^L_{3131} = g_{3131} , \quad g^L_{3113} = g_{3113} ,$$
$$g^L_{1212} = \frac{1}{4}(1 - \cos 4\varphi)(g_{1111} - g_{1122} - g_{1212} - g_{1221}) + g_{1212} ,$$
$$g^L_{3232} = g_{3131} ,$$
$$g^L_{2111} = -\frac{1}{4}\sin 4\varphi\,(g_{1111} - g_{1122} - g_{1212} - g_{1221}) ,$$
$$g^L_{2112} = \frac{1}{4}(1 - \cos 4\varphi)(g_{1111} - g_{1122} - g_{1212} - g_{1221}) + g_{1221} ,$$
$$g^L_{2211} = \frac{1}{4}(1 - \cos 4\varphi)(g_{1111} - g_{1122} - g_{1212} - g_{1221}) + g_{1122} ,$$
$$g^L_{2212} = \frac{1}{4}\sin 4\varphi\,(g_{1111} - g_{1122} - g_{1212} - g_{1221}) ,$$
$$g^L_{2332} = g_{1331} , \quad g^L_{2233} = g_{1133} .$$

Here, we used the relations which are satisfied in both O_h, D_{4h} and C_{4v} symmetries in the caluculation. For O_h symmetry, further transfiguration are made in order to obtain some significant informations as described in section 2-2C.

$$
\begin{aligned}
P_2 &= g^L_{2111}E_1\partial_1E_1 + g^L_{2112}E_1\partial_1E_2 + g^L_{2211}E_2\partial_1E_1 + g^L_{2212}E_2\partial_1E_2 \\
&+ g^L_{2332}E_3\partial_3E_2 + g^L_{2233}E_2\partial_3E_3 \\
&= (-\frac{1}{4}\sin 4\varphi\,(g_{iiii} - g_{iijj} - g_{ijij} - g_{ijji}))E_1\partial_1E_1 \\
&+ (\frac{1}{4}(1-\cos 4\varphi)(g_{iiii} - g_{iijj} - g_{ijij} - g_{ijji}) + g_{ijji})E_1\partial_1E_2 \\
&+ (\frac{1}{4}(1-\cos 4\varphi)(g_{iiii} - g_{iijj} - g_{ijij} - g_{ijji}) + g_{iijj})E_2\partial_1E_1 \\
&+ (\frac{1}{4}\sin 4\varphi\,(g_{iiii} - g_{iijj} - g_{ijij} - g_{ijji}))E_2\partial_1E_2 + g_{ijji}E_3\partial_3E_2 + g_{iijj}E_2\partial_3E_3 \\
&= g^a(-\frac{1}{4}\sin 4\varphi E_1\partial_1E_1 + \frac{1}{4}(1-\cos 4\varphi)E_1\partial_1E_2 + \frac{1}{4}(1-\cos 4\varphi)E_2\partial_1E_1 + \frac{1}{4}\sin 4\varphi E_2\partial_1E_2) \\
&+ g_{ijji}(E_1\partial_1 + E_3\partial_3)E_2 + g_{iijj}E_2(\partial_1E_1 + \partial_3E_3)
\end{aligned}
\qquad \text{(2-2C-15)}
$$

For p→s condition,

$$
\begin{aligned}
P_2 &= g^L_{2111}E_1\partial_1E_1 \\
&= -\frac{1}{4}\sin 4\varphi\,(g_{iiii} - g_{iijj} - g_{ijij} - g_{ijji})E_1\partial_1E_1 \\
&= -\frac{1}{4}\sin 4\varphi\, g_a E_1\partial_1E_1
\end{aligned}
\qquad \text{(2-2C-16)}
$$

For s→s condition,

$$
\begin{aligned}
P_2 &= g^L_{2212}E_2\partial_1E_2 \\
&= \frac{1}{4}\sin 4\varphi\,(g_{iiii} - g_{iijj} - g_{ijij} - g_{ijji})E_2\partial_1E_2 \\
&= \frac{1}{4}\sin 4\varphi\, g_a E_2\partial_1E_2
\end{aligned}
\qquad \text{(2-2C-17)}
$$

Here, we introduced a parameter $g^a = g_{iiii} - g_{iijj} - g_{ijij} - g_{ijji}$. The same results can be directly obtained according to Appendix.

For the geometry shown in Fig. 2-2-1(b), the electric field in nonlinear active layer is $E_i = E_i^{mf}$. Then, the P_1, P_2 and P_3 for the polarization conditions (p→p, s→p, 45°→s, p→s and s→s) in this geometry are described as follows.

For p→p condition,

$$
P_1 = \frac{1}{4}(\cos 4\varphi + 3)g^a(ik_1)E_1^{mf2} + \frac{1}{2}g_{ijij}(i2k_1)(E_1^{mf2} + E_3^{mf2})
$$

$$P_3 = g^a(im^f)E_3^{mf2} + \frac{1}{2}g_{ijij}(im^f)(E_1^{mf2} + E_3^{mf2}) \quad . \qquad (2\text{-}2C\text{-}18)$$

For s→p condition,

$$P_1 = \frac{1}{4}(1 - \cos 4\varphi)g^a(ik_1)E_2^{mf2} + \frac{1}{2}g_{ijij}(i2k_1)E_2^{mf2}$$
$$P_3 = \frac{1}{2}g_{ijij}(i2m^f)E_2^{mf2} \quad . \qquad (2\text{-}2C\text{-}19)$$

For 45°→s condition,

$$P_2 = g^a(-\frac{1}{4}\sin 4\varphi\ (ik_1)E_1^{mf2} + 2(\frac{1}{4}(1-\cos 4\varphi)(ik_1)E_1^{mf}E_2^{mf}) + \frac{1}{4}\sin 4\varphi(ik_1)E_2^{mf2}) \quad .$$

(2-2C-20)

For p→s condition,

$$P_2 = -\frac{1}{4}\sin 4\varphi\ g^a\ (ik_1)E_1^{mf2} \quad . \qquad (2\text{-}2C\text{-}21)$$

For s→s condition,

$$P_2 = \frac{1}{4}\sin 4\varphi\ g^a\ (ik_1)E_2^{mf2} \quad . \qquad (2\text{-}2C\text{-}22)$$

In this calculation, we used the relations $E_1^{mf0}k_1 + E_3^{mf0}m^f = 0$. At first, we note that the bulk SHG can be observed even for the polarizations (45°→s), (p→s) and (s→s) in contrast to K_h system in the same geometry and the g^a terms are added for all polarization conditions. Especially, the polarization conditions (45°→s, p→s and s→s) possess only the g^a terms. It is also noted that all the rotational angle dependent terms are multiplied by a parameter $g^a = g_{iiii} - g_{iijj} - g_{ijij} - g_{ijji}$.

We can perform further calculation for O_h symmetry using eqs. (2-2A-9), (2-2A-17), (2-2A-25) and (2-2A-36), so that we obtain the relation

$$g^a = g_{iiii} - g_{iijj} - g_{ijij} - g_{ijji} = (\frac{1}{2}\Delta_{iiii} - 2\Delta_{ijij}) + (-\Lambda_{iiii} + 4\Lambda_{ijij}) \quad . \qquad (2\text{-}2C\text{-}23)$$

Thus, the g^a comes from only the EQC and EQ mechanisms. This is important from the viewpoint that we can distinguish the origin of higher order SHG of EQC and EQ mechanisms from that of MDC and MD mechanism. The g_{ijij} and g^a terms are evaluated in the geometry (Fig. 2-2-1(b)).

So far, we have not considered the SHG from the effective surface polarization [11]. Here, we also briefly discuss such contribution in order to recognize the significance of the rotational dependent SHG. If we treat the SHG from (001) surface in O_h systems such as Si and Ge crystals, the surface have C_{4v} symmetry [11], in which the symmetry axis is parallel to the surface normal direction. The surface contribution appears at the polarization conditions (p→p, s→p and 45°→s). However, the SHG due to such a surface contribution does not show the rotational angle dependence, since $\chi^{(2)}$ does not distinguish C_{4v} symmetry from $C_{\infty v}$ symmetry. Thus, the rotational angle dependence in the SHG implies the contribution from the bulk EQ and EQC mechanisms. Moreover, the rotational angle dependent SHG from the polarization conditions (p→s) and (s→s) is entirely caused by the bulk EQC and EQ mechanisms, since both the surface contribution and the contribution from the isotropic terms which comes from EQ, EQC and MDC mechanisms as a bulk are not included in these polarization conditions. Many researchers [6-11] observed the rotational anisotropy of the reflection SHG from Si(001) face with various polarization conditions and pointed out the significance of the bulk contribution. Figs. 2-2-2(a) and 2-2-2(b) show the rotational angle

(a)

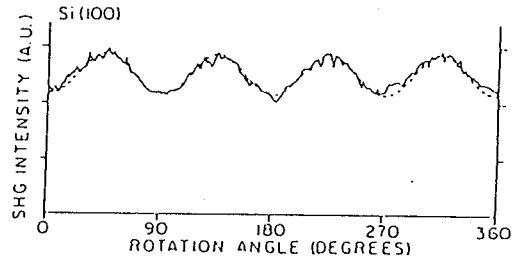

(b)

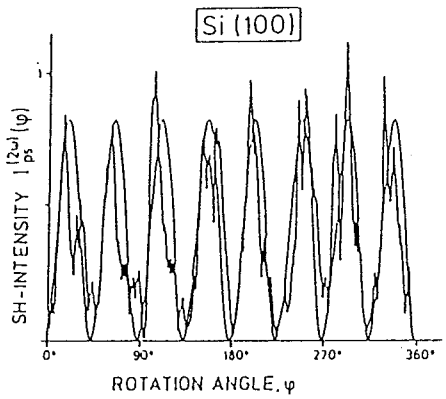

Fig. 2-2-2 Rotational angle depedence of SHG from Si(001) face in (a) p→p polarization condition and (b) p→s polarization condition, which are quoted from refs. [6,10]. In the experiments, pump radiation of a wavelength of 532 nm was used.

dependence of SHG from Si(001) face, which are quoted from refs [6,10].

For the geometry shown in Fig. 2-2-1(a), the electric field in the nonlinear active layer is described as $E_i = E_i^{mf} + E_i^{mb}$. Then, the P_1, P_2 and P_3 components are described for each polarization as follows.

For p→p condition,

$$
\begin{aligned}
&P_1 = \frac{1}{4}(\cos 4\varphi + 3)g^a(ik_1)(E_1^{mf2} + 2E_1^{mf}E_1^{mb} + E_1^{mb2}) \\
&+ \frac{1}{2}g_{ijij}(i2k_1)(E_1^{mf2} + E_3^{mf2} + 2E_1^{mf}E_1^{mb} + 2E_3^{mf}E_3^{mb} + E_1^{mb2} + E_3^{mb2}) \\
&+ g_{ijji}(ik_1(2E_1^{mf}E_1^{mb}) - im^{fa}E_3^{mf}E_1^{mb} + im^fE_3^{mb}E_1^{mf}) \\
&P_3 = g^a((im^f)E_3^{mf2} - (im^f)E_3^{mb2}) \\
&+ \frac{1}{2}g_{ijij}((i2m_f)(E_1^{mf2} + E_3^{mf2}) - (i2m_f)(E_1^{mb2} + E_3^{mb2})) + g_{ijji}(ik_1)(E_1^{mf}E_3^{mb} + E_1^{mb}E_3^{mf})
\end{aligned}
\qquad \text{(2-2C-24)}
$$

For s→p condition,

$$
\begin{aligned}
&P_1 = \frac{1}{4}(1 - \cos 4\varphi)g^a(ik_1)(E_2^{mf2} + 2E_2^{mf}E_2^{mb} + E_2^{mb2}) \\
&+ \frac{1}{2}g_{ijij}(i2k_1)(E_2^{mf2} + 2E_2^{mf0}E_2^{mb0} + E_2^{mb2}) \\
&P_3 = \frac{1}{2}g_{ijij}((i2m^f)E_2^{mf2} - (i2m^f)E_2^{mb2})
\end{aligned}
\qquad \text{(2-2C-25)}
$$

For 45°→s condition,

$$
\begin{aligned}
&P_2 = g^a(-\frac{1}{4}\sin 4\varphi\ (ik_1)(E_1^{mf2} + 2E_1^{mf}E_1^{mb} + E_1^{mb2})) \\
&+ 2(\frac{1}{4}(1 - \cos 4\varphi)(ik_1)(E_1^{mf}E_2^{mf} + E_1^{mf}E_2^{mb} + E_1^{mb}E_2^{mf} + E_1^{mb2})) \\
&+ \frac{1}{4}\sin 4\varphi\ (ik_1)(E_2^{mf2} + 2E_2^{mf}E_2^{mb} + E_2^{mb2})
\end{aligned}
\qquad \text{(2-2C-26)}
$$

For p→s condition,

$$
P_2 = -\frac{1}{4}\sin 4\varphi\ g^a\ (ik_1)(E_1^{mf2} + 2E_1^{mf}E_1^{mb} + E_1^{mb2}) \qquad \text{(2-2C-27)}
$$

For s→s condition,

$$P_2 = \frac{1}{4}\sin 4\varphi \, g^a (ik_1)(E_2^{mf2} + 2E_2^{mf}E_2^{mb} + E_2^{mb2}) \quad . \qquad \text{(2-2C-28)}$$

In this calculation, we used the relations $E_1^{mf0}k_1 + E_3^{mf0}m^f = 0$ and $E_1^{mb0}k_1 + E_3^{mb0}m^b = 0$, $m^b = -m^f$. The g_{ijij}, g_{ijji} and g^a terms are included in this geometry. Of cource, we can make the same discussion as described above.

Further transfiguration is not so effective for C_{4v} and D_{4h} symmetries as for O_h symmetry, since we have many independent tensor components and an anisotropic dielectric tensor. In these symmetries, rotational dependent tensor components in g^L are also characterized by a parameter

$$(g_{1111} - g_{1122} - g_{1212} - g_{1221}) = (\Delta_{1111} - \Delta_{1122} - 2\Delta_{1212}) + (-2\Lambda_{1111} + 2\Lambda_{1122} + 4\Lambda_{1212}) \quad .$$

In the calculation, we used eqs. (2-2A-12), (2-2A-18), (2-2A-28), and (2-2A-36). It is also noted that $(g_{1111} - g_{1122} - g_{1212} - g_{1221})$ comes only from EQC and EQ mechanisms in these symmetries. Similar discussion to the case of O_h symmetry can also be made as for the rotational anisotropy of SHG. We can add an significant information in C_{4v} system. In C_{4v} system, the bulk itself is also non-centrosymmetric, so that the contribution of electric dipole mechanism as a bulk may be large in general and the contribution appears at the polarization conditions (p→p, s→p, 45°→s). Again, we recognize the significance of the rotational anisotropy of the polarization conditions (p→s, s→s), because EQ and EQC mechanisms can be probed even in the non-centrosymmetric system such as C_{4v} symmetry.

References

[1] E. Adler, Phys. Rev. **134**, A728 (1964).

[2] R. W. Boyd, *Nonlinear Optics*, (ACADEMIC PRESS, INC, San Diego, 1992).

[3] V. Mizrahi and J. E. Sipe, Phys. Rev. B **34**, 3700 (1986).

[4] Z. Shuai and J. L. Brédas, Adv. Mater. **6**, 486 (1994).

[5] Z. Shuai and L. J. Brédas, Mol. Cryst. Liq. Cryst. **256**, 801 (1994).

[6] H. W. K. Tom, T. F. Heinz, and Y. R. Shen, Phys. Rev. Lett. **21**, 1983 (1983).

[7] J. A. Litwin, J. E. Sipe, and H. M. van Driel, Phys. Rev. B **31**, 5543 (1985).

[8] H. W. K. Tom, G. D. Aumiller, and C. H. Brito-Cruz, Phys. Rev. Lett. **60**, 1438 (1988).

[9] G. Mizutani, Y. Sonoda, S. Ushioda, T. Maeda, and J. Murota, Jpn, J. Appl. Phys. **34**, L119 (1995).

[10] G. Lüpke and G. Marowsky, Appl. Phys. B **53**, 71 (1991).

[11] J. E. Sipe, D. J. Moss, and H. M. van Driel, Phys. Rev. B **35**, 1129 (1987).

[12] W. Daum, H.-J. Krause, U. Reichel, and H. Ibach, Phys. Rev. Lett. **71**, 1234 (1993).

[13] N. Broembergen and P. S. Pershan, Phys. Rev. **128**, 606 (1962).

[14] B. Koopmans, A. M. Janner, H. T. Jonkman, and G. A. Sawatzky, F. van der Woude, Phys. Rev. Lett. **71**, 3569 (1993).

[15] B. Koopmans, A. M. Janner, H. A. Wierenga, Th. Rasing, G. A. Sawatzky, and F. van der Woude, Appl. Phys. A **60**, 103 (1995).

Chapter 3 Thickness Dependence of SHG in Vacuum Deposited Phthalocyanine Films

3-1 Introduction

Recently, the relatively strong SHG from CuPc vacuum evaporation films has been observed by Chollet et al. [1] and Kumagai et al. Kumagai et al. [2] performed the thickness dependent SHG for CuPc films and confirmed that the SH intensity is proportional to the square of the thickness in the thin film region. Then, they ascribed the SHG to the contribution from electric dipole mechanism, which is caused by the breaking of the inversion symmetry to the surface normal direction produced during the film growth. Here, we also have performed the thickness scan of the SHG from a CuPc film. Then, we took advantages of *in situ* observation of the SH intensity during vacuum evaporation. The main advantages are: (1) The precise thickness dependent SHG can be observed using a sample film. (2) The SHG measurement can be performed without exposing it to the atmosphere. As for the advantage (2), however, we confirmed that the change of the SH intensity from CuPc films due to exposing it to the atmosphere is negligible.

3-2 Experiment

Fig. 3-2-1(a) shows the optical arrangement around a vacuum chamber (Kitano Seiki Co. Ltd.) which has optical viewports. A substrate glass plate (Matsunami micro slide glass) was placed in a Cu mount at room temperature without special temperature regulation. CuPc after purification by sublimation was evaporated in a vacuum of

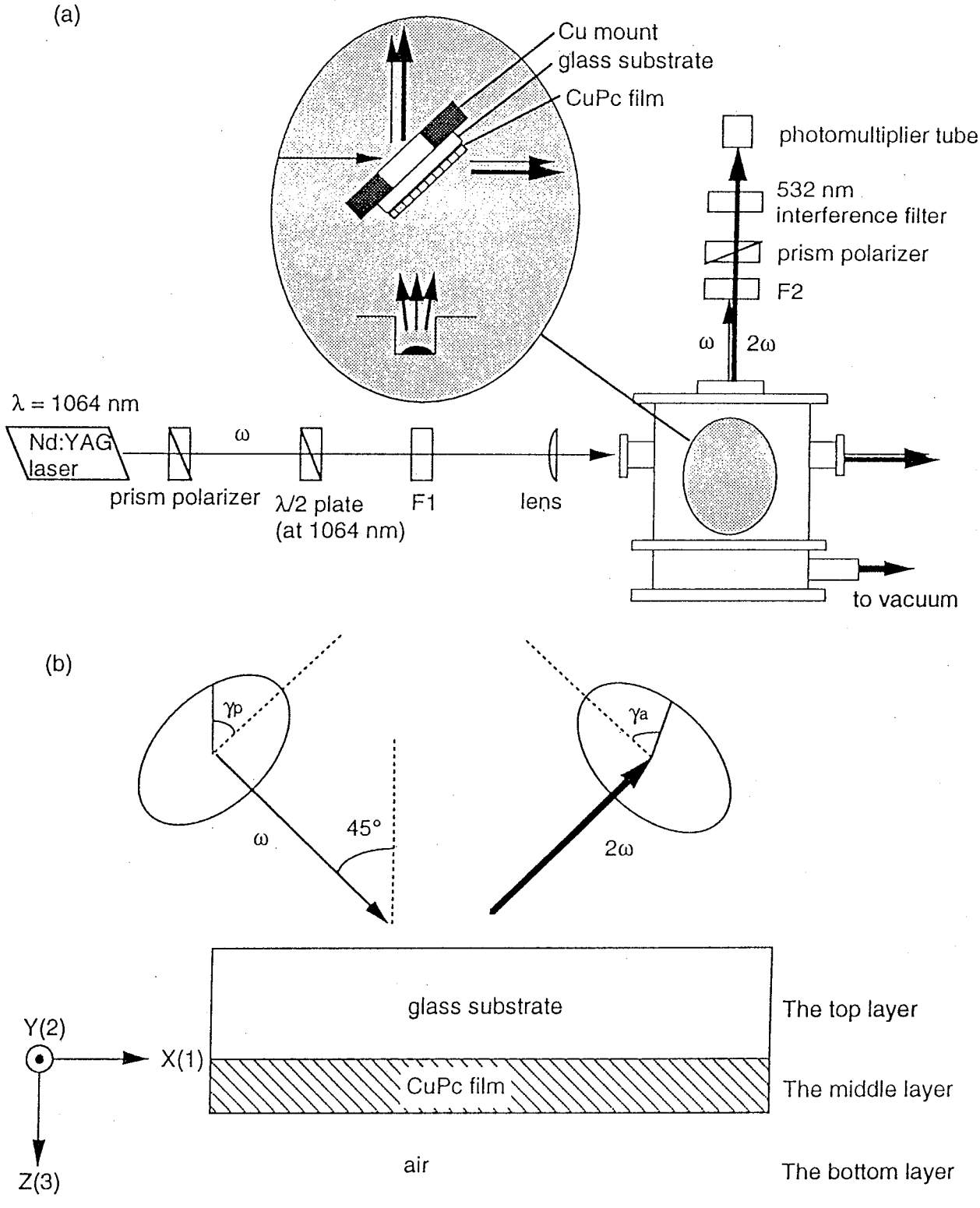

Fig. 3-2-1 (a) The optical arragement and (b) the gometry around a sample. The color filters (F1) and (F2) in the figure (a) are introduced to remove the SH light from various optical componerts and to eliminate the fundamental light, respectively.

1.2×10^{-3} Pa (1.5×10^{-5} Torr) at the rate of 1.2 nm/min. The thickness was monitored by a Leybold Inficon XTM/2 using a quartz oscillator and was calibrated by direct observation of the film thickness by means of an atomic force microscope (Seiko SPI-3700). The fundamental beam from an Nd:YAG laser (Quanta-Ray DCR-11, 1064 nm, 12 Hz) was attenuated to about 1 mJ/pulse and was focused upon the sample after passing through a polarizer, a half-wave plate (at 1064 nm), a visible cut filter to eliminate SH light from various optical components, a lens and the glass substrate. The SH light from the sample after passing through the glass substrate, an infrared cut filter to remove the fundamental light and an analyzer was detected by a photomultiplier tube (PMT Hamamatsu R955) in the reflection direction. The geometry around a sample is also shown in Fig. 3-2-1(b), where the laboratory coordinates {X(1), Y(2), Z(3)} are defined. In the figure, we find that the X(1) axis is parallel to the film surface, the Z(3) axis is perpendicular to the film surface and γ_p-polarized incident fundamental beam propagates in the XZ plane toward the positive Z(3) direction. The γ_a-polarized SH light from the film was detected in the reflection direction. The incident angle to the glass substrate was 45° which corresponds to the incident angle (28.47°) from the glass substrate to the CuPc film as described below. Absorption spectra of several samples with different film thicknesses were measured using a spectrophotometer (Hitachi U-3400), although the measurement was not *in situ* observation. It was confirmed that the spectra have the same profiles, indicating that there is no structural change within the range of the film thickness at which SHG measurement was performed.

3-3 Result and discussion

In this film preparation condition, the film has been reported to form a polycrystal of α-type-cristalline domains [3] and to have some anisotropy with respect to the surface normal [2], apart from polar ($C_{\infty v}$) or non-polar ($D_{\infty h}$). Here, we discuss contributions from higher order mechanisms and the electric dipole mechanism as a bulk for the SHG.

For s→s (γ_p=90°, γ_a=90°) and p→s (γ_p=0°, γ_a=90°) polarization conditions, the SHG should not be observed for both the electric dipole mechanism and higher order mechanisms. At first, we confirmed that this is actually the case. Figs. 3-3-1(a), 3-3-1(b) and 3-3-1(c) show the thickness dependent SHG from CuPc film for p→p (γ_p=0°, γ_a=0°), s→p (γ_p=90°, γ_a=0°) and 45°→s (γ_p=45°, γ_a=90°) polarization conditions, respectively. We can calculate the thickness dependent SHG on the presumption of the electric dipole mechanism according to the procedure described in chapter 2. In Table 2-2-1, we note that s→p and 45°→s polarization conditions in the electric dipole mechanism depend on only one parameter, respectively, and the thickness dependences are uniquely determined. Figs. 3-3-2(a) and 3-3-2(b) show the calculated thickness dependent SHG in s→p and 45°→s polarization conditions for the electric dipole mechanism, respectively. The parameters used for the calculation are

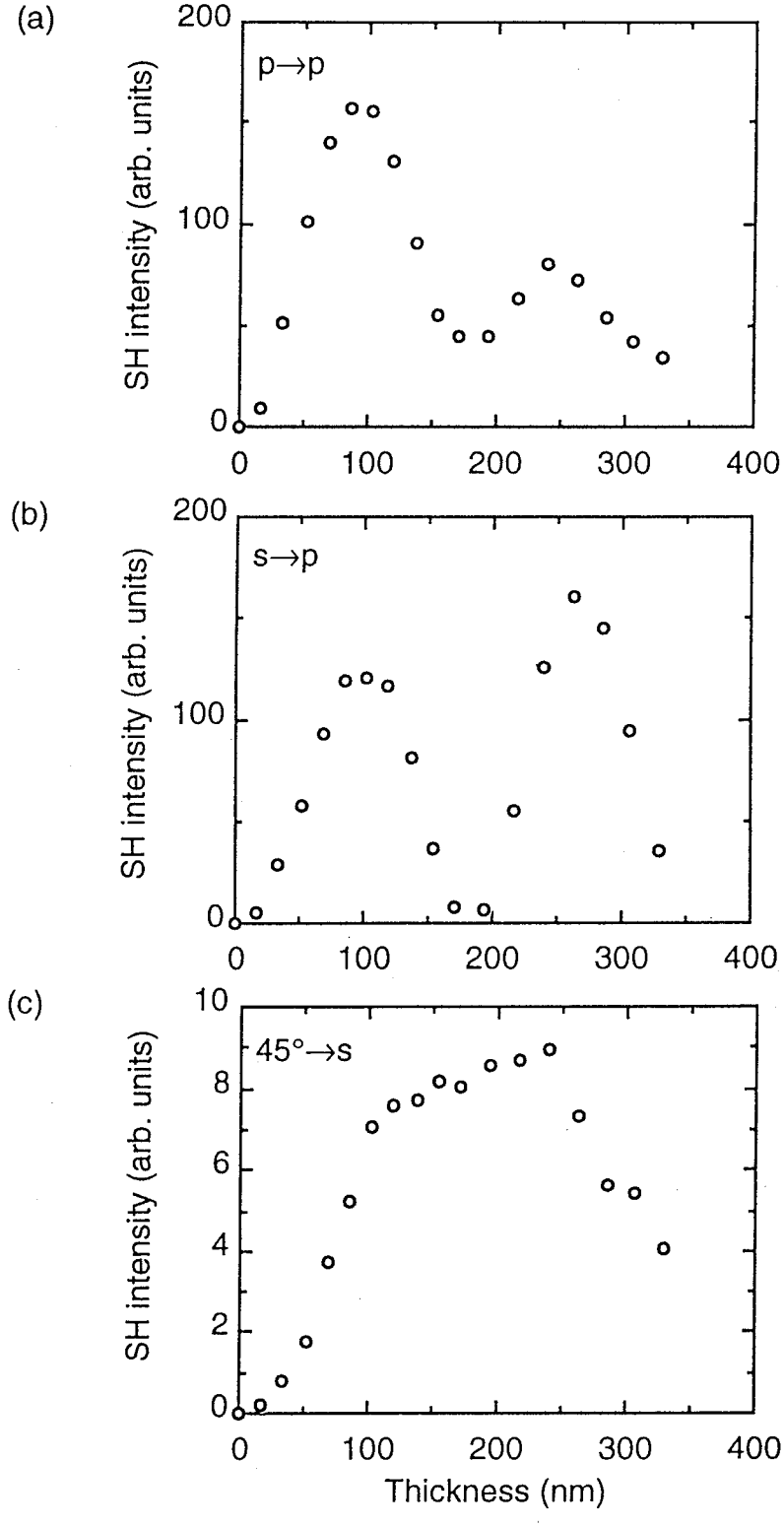

Fig. 3-3-1 The SH intensity as a function of the film thickness :
(a) p→p condition, (b)s→p condition and (c) 45°→s condition.

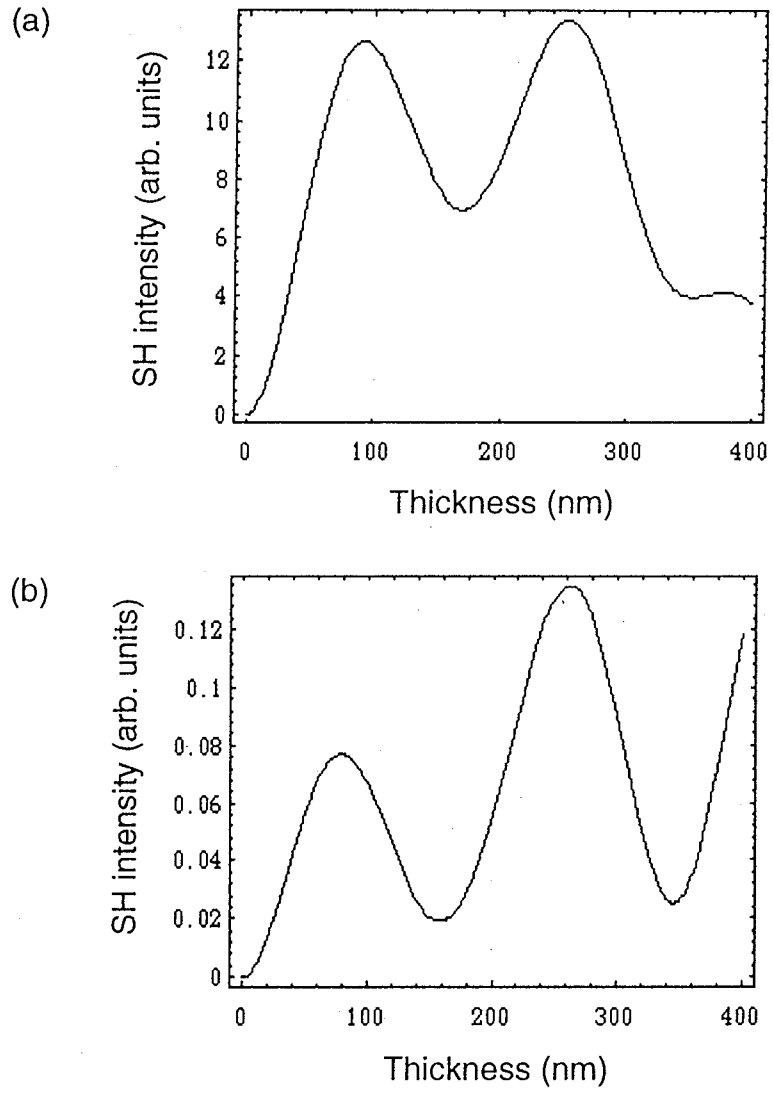

Fig. 3-3-2 The caluculation of SH intensity as a function of the film thickness assuming the electric dipole mechanism: (a)s→p condition and (b)45°→s condition.

$$\theta_0 = 28.47 \ (\sin\theta_0 = \frac{\sin 45^\circ}{\sqrt{2.2}})$$
$$\varepsilon_r = \varepsilon_R = 2.2$$
$$\varepsilon_t = \varepsilon_T = 1.0$$
$$\tilde{\varepsilon}_{m1} = 3.3$$
$$\tilde{\varepsilon}_{m3} = 4$$
$$\tilde{\varepsilon}_{M1} = 2.21 + 0.18i$$
$$\tilde{\varepsilon}_{M3} = 2.05 + 0.32i$$
$$\lambda_0 = \frac{2\pi c}{\omega} = 1064\ (nm) \qquad (3\text{-}3\text{-}1)$$

where the dielectric constants of CuPc film are those reported by Kumagai et al. We also used the ratio $\chi_{zyy}:\chi_{yzy} = 1:-0.26$ according to the result by Kumagai et al. Thus, we find the significant deviation from the electric dipole mechanism. Kumagai et al. have already observed SHG of the similar geometry. However, they mainly paid attention to the quadratic dependence of SHG on the thickness in the range thinner than 100 nm. The agreement between the experiment and the calculation on the electric dipole model in this thickness range does not allow us to conclude that the origin is due to the electric dipole mechanism, since the SHG from higher order mechanisms does show the quadratic dependence in the thickness region as illustrated below. We took advantage of *in situ* observation and could perform experiments on the precise thickness dependence of SHG up to 330 nm.

Next, we discuss the thickness dependent SHG from higher order mechanisms. In $D_{\infty h}$ and $C_{\infty v}$ symmetries, we have ten independent parameter according to eq. (2-2A-39). Moreover, the parameters should be treated as complex quantities in general. Thus, it is difficult to simulate for all polarization conditions in such systems. However, s→p polarization condition includes only two parameters (g_{1212} and g_{3232}) according to Table 2-2-1. Therefore, we discuss this polarization condition in detail.

At first, we note that g_{1212} and g_{3232} described as

$$g_{1212} = \Gamma_{1212} + \Delta_{1212} - 2\Lambda_{1122} \quad ,$$

$$g_{3232} = \Gamma_{3232} + \Delta_{3232} - 2\Lambda_{3322} \quad ,$$

using eq. (2-2A-36) and do not include nonzero components of Ξ. Therefore, the SHG should not be observed in this polarization condition, if the MD mechanism is dominant. In the present experiments, we observed the strong SHG in this condition. Thus, the MD mechanism is not a dominant origin for the present SHG.

In this film preparation condition, the film may have small anisotropy, so that we assume that the relation $g_{1212} = g_{3232}$, although we allow the anisotropic dielectric tensor. According to the procedure described in chapter 2, we can calculate the thickness dependent SHG for s→p polarization conditions using eq. (3-3-1) as shown in Fig. 3-3-3. For consistence, let us also assume the isotropic dielectric tensor for the CuPc film by taking the averaged value of $\tilde{\varepsilon}_{m1}$ and $\tilde{\varepsilon}_{m3}$ for fundamental frequency and that of $\tilde{\varepsilon}_{M1}$ and $\tilde{\varepsilon}_{M3}$ for SH frequency. The calculated result is shown in Fig. 3-3-4. Thus, the agreement between the experimental one (Fig. 3-3-1(b)) and the calculated ones (Figs. 3-3-3, and 3-3-4) is satisfactory. The slight difference may be caused by the assumption we have made.

Koopmans et al. [4,5] stated that the thickness dependent SHG in the s→p polarization condition from bulk higher order mechanisms in K_h symmetry is indistinguishable from that from surface contributions at the two interfaces (the top layer/the middle layer and the middle layer/the bottom layer) if the effective surface nonlinear susceptibilities [6,7] localized in the two interfaces have same magnitude but opposite sign each other. However, rotational dependent SHG observed in the epitaxially grown phthalocyanine films on alkali halides implies the significant contribution from bulk

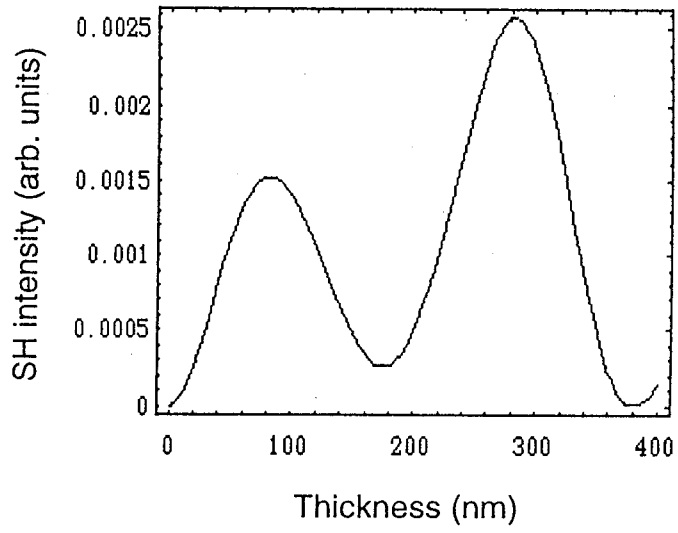

Fig. 3-3-3 The caluculation for s→p condition of SH intensity as a function of the film thickness assuming higher order mechanisms. In the calculation, we assumed the relation g1212=g3232, although we allowed the anisotropy for the dielectric tensor as described in section 3-3.

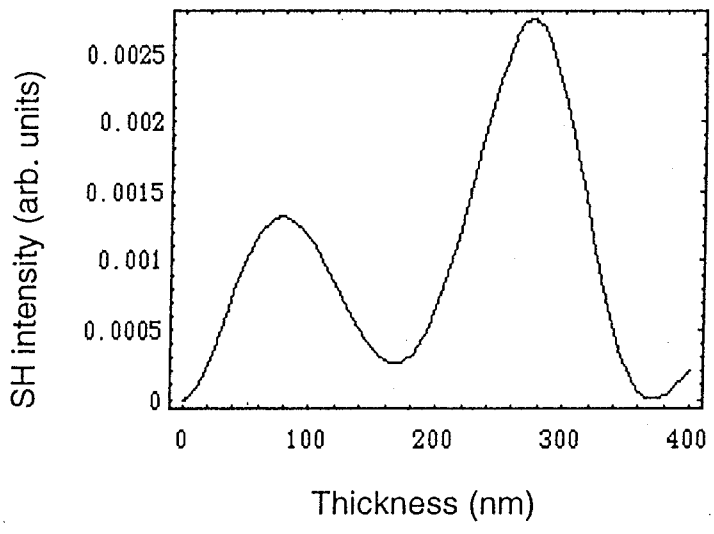

Fig. 3-3-4 The caluculation for s→p condition of SH intensity as a function of the film thickness assuming higher order mechanisms. In the calculation, we assumed the relation g1212=g3232 and the isotropy for the dielectric tensor as described in section 3-3.

higher order mechanisms (especially, EQ and EQC mechanisms), about which we will describe in chapter 4.

In the paper [7], we analyzed the thickness dependent SHG under $D_{\infty h}$ symmetry for each mechanism assuming that the SHG is off-resonant. Under such an assumption, the experimental results are successfully reproduced for all polarization conditions with EQ or EQC or MDC mechanism.

3-4 Conclusion

In conclusion, we measured thickness dependent SHG from a CuPc film in various polarization conditions by taking advantage of *in situ* observation. We attributed the SHG using 1064 nm fundamental wavelength to higher order mechanisms except for MD mechanism rather than the ED mechanism which have ever been proposed.

References

[1] P. A. Chollet, F. Kajzar, and J. Le Moigne, Proc. SPIE **1273**, 87 (1990).

[2] K. Kumagai, G. Mizutani, H. Tsukioka, T. Yamauch, and S. Ushioda, Phys. Rev. B **48**, 14488 (1993).

[3] M. Ashida, N. Uyeda, and E. Suito, J. Cryst. Growth **8**, 45 (1971).

[4] B. Koopmans, A. M. Janner, H. A. Wierenga, Th. Rasing, G. A. Sawatzky, and F. van der Woude, Appl. Phys. A **60**, 103 (1995).

[5] B. Koopmans, A. M. Janner, H. T. Jonkman, and G. A. Sawatzky, F. van der Woude, Phys. Rev. Lett. **71**, 3569 (1993).

[6] P. Guyot-Sionnest and Y. R. Shen, Phys. Rev. B **38**, 7985 (1988).

[7] J. E. Sipe, D. J. Moss, and H. M. van Driel, Phys. Rev. B **35**, 1129 (1987).

[8] H. Hoshi, T. Yamada, K. Ishikawa, H. Takezoe, and A. Fukuda, Phys. Rev. B **52**, 12355 (1995).

Chapter 4 Rotational Angle Dependence of SHG in Epitaxially Grown Phthalocyanine Films

4-1 Introduction

The molecular-beam epitaxy (MBE) technique is one of the most useful technique to control crystal growth and to produce various crystalline thin films. The systematic studies of epitaxial growth of organic system have been recently performed [1-12]. Hoshi and Maruyama et al. [5-11] succeeded in forming the epitaxially grown phthalocyanine films on alkali halide substrates. In this study, we used the CuPc film epitaxially grown on a KCl(001) substrate which has the C_4 rotational axis about the film plane normal. Ashida [13] carried out the electron diffraction measurement of the CuPc/KCl(001) film and confirmed the epitaxial structure with D_{4h} symmetry. We also investigated the VOPc epitaxial film on a KBr(001) substrate, where the stack columns of VOPc molecules are perpendicular to the substrate and form square lattices that match with the [110] direction of the KBr(001) substrate, so that the epitaxial film forms tetragonal systems apart from C_4, S_4, C_{4h}, D_4, D_{2d}, C_{4v} or D_{4h} system. Thus, there exist many possible symmetries for the epitaxial film, since a VOPc molecule has polar C_{4v} symmetry.

The epitaxial films were produced by Dr. Hoshi, a group member in Takezoe and Ishikawa laboratory. The CuPc epitaxial film on a KCl(001) substrate was obtained according to the following procedure. The base pressure of the MBE chamber was 1×10^{-9} Torr and the substrate located in the chamber was baked at 400°C before the deposition. The substrate temperature during deposition was

40°C. CuPc was sublimated at about 350°C from a Knudsen cell. The epitaxially grown VOPc film on KBr(001) substrate was obtained with the same procedure except that the substrate temperature was kept at 80°C.

Here, we have observed the rotational angle dependence [14-17] of the SH intensity by rotating the epitaxial films about the surface normal. Experiments were performed in air. The results provide us with significant informations as for the origin of the SHG from phthalocyanine thin films.

4-2 Experiment

Fig. 4-2-1(a) shows the optical arrangement to observe the rotational angle dependent SHG for an epitaxially grown CuPc film. The fundamental light from an Nd:YAG laser (BMI-compact 501/100, 1064 nm, 30 Hz, and 6 ns) was attenuated to about 1 mJ/pulse and was irradiated upon the sample after passing through a polarizer, a half-wave plate (at 1064 nm), a visible cut filter to remove SH light from various optical components and a lens. The SH light from the sample after passing through the KCl substrate, an infrared cut filter to eliminate the fundamental light, an analyzer and a 532 nm interference filter was detected by a photomultiplier tube (PMT Hamamatsu R955) in the transmission direction.

The geometry around the sample is shown in Fig. 4-2-1(b), where the laboratory coordinates {X(1), Y(2), Z(3)} are defined. In the figure, we find that the X(1) axis is parallel to the film surface, the Z(3) axis is perpendicular to the film surface and the γ_p-polarized incident fundamental beam propagates with the incident angle of 10° in the XZ plane toward the positive Z(3) direction. We observed the

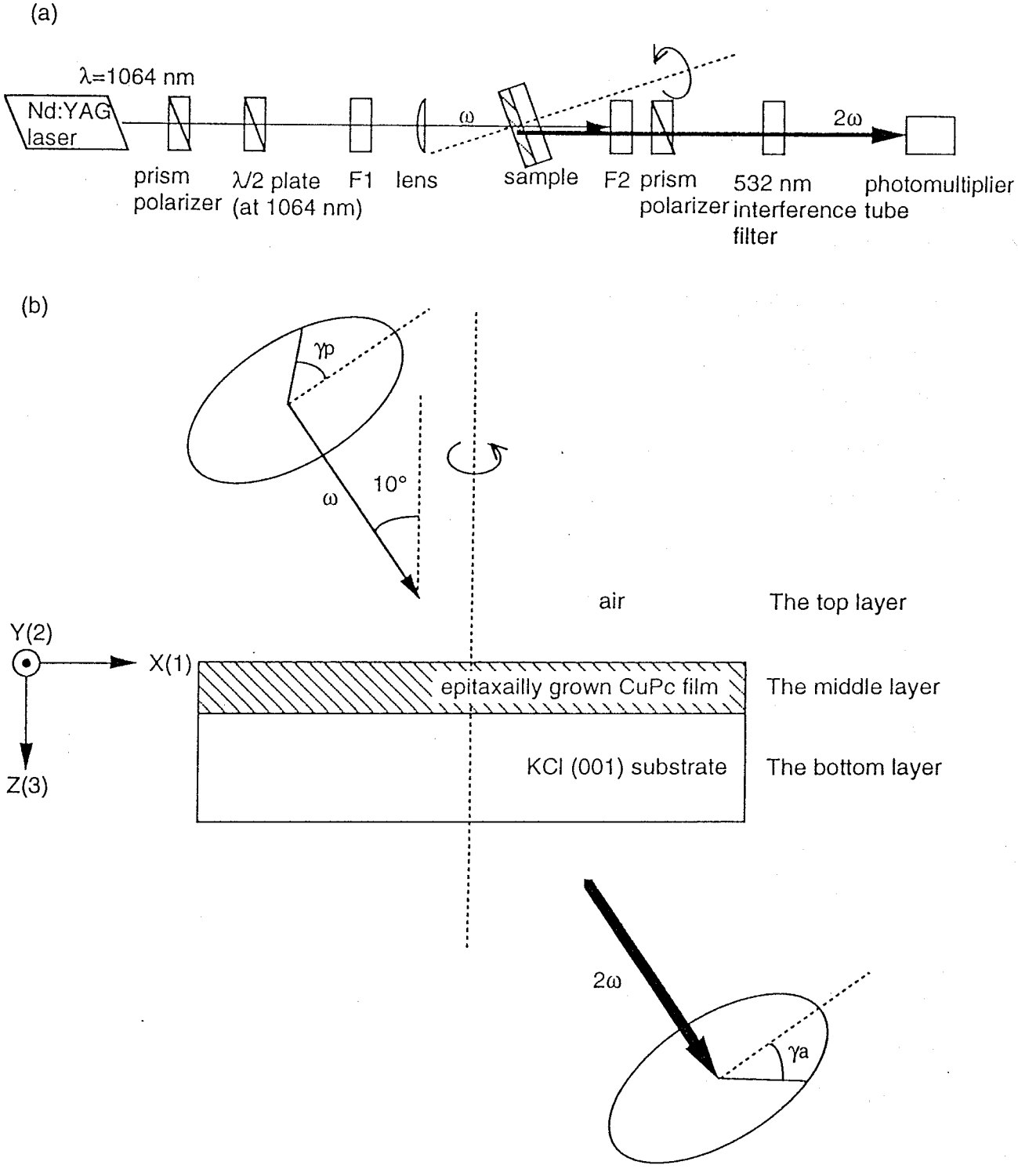

Fig. 4-2-1 (a) The optical arrangement used in the experiment for an epitaxially grown CuPc film. The color filters, (F1) and (F2) are introduced to remove the SH light from various optical components and to eliminate the fundamental light, respectively.
(b) The geometry around the sample.

rotational angle dependence of the intensity of the γ_a-polarized SH light from the sample in the transmission direction, by rotating the sample about the surface normal.

Fig. 4-2-2(a) exhibits the optical arrangement to observe the rotational angle dependence of SHG from an epitaxially grown VOPc film. The fundamental light of the wavelength 1140 nm was obtained by the optical parametric oscillation of a beta-barium-borate (BBO) crystal (BMI OP 901.355) pumped by the third harmonic light of a Nd:YAG laser (BMI 501-D.NS 710). The fundamental light of about 2 mJ/pulse ran at the repetition frequency of 10 Hz. The polarization of the fundamental light was adjusted by a combination of a phase compensator and a polarizer. The fundamental light after passing through a lens and a color filter to remove SH light from optical components was cast upon the sample. The SH light from the sample after passing through the KBr substrate was filtered by an infrared cut filter to remove the fundamental light, an analyzer, a lens and a monochromator (Ritus MC-10N) and was detected by a photomultiplier tube (PMT Hamamatsu R955) in the transmission direction.

The geometry around the sample is shown in Fig. 4-2-2(b). The laboratory coordinates in Fig. 4-2-2(b) are identical with those in Fig. 4-2-1(b). The γ_p-polarized incident fundamental beam propagates with the incident angle of 20° in the XZ plane toward the positive Z(3) direction. The rotational angle dependence of the intensity of the γ_a-polarized SH light from the sample was observed by rotating the sample about the surface normal.

We confirmed that the SHG from substrates (KCl, KBr) has negligible contribution.

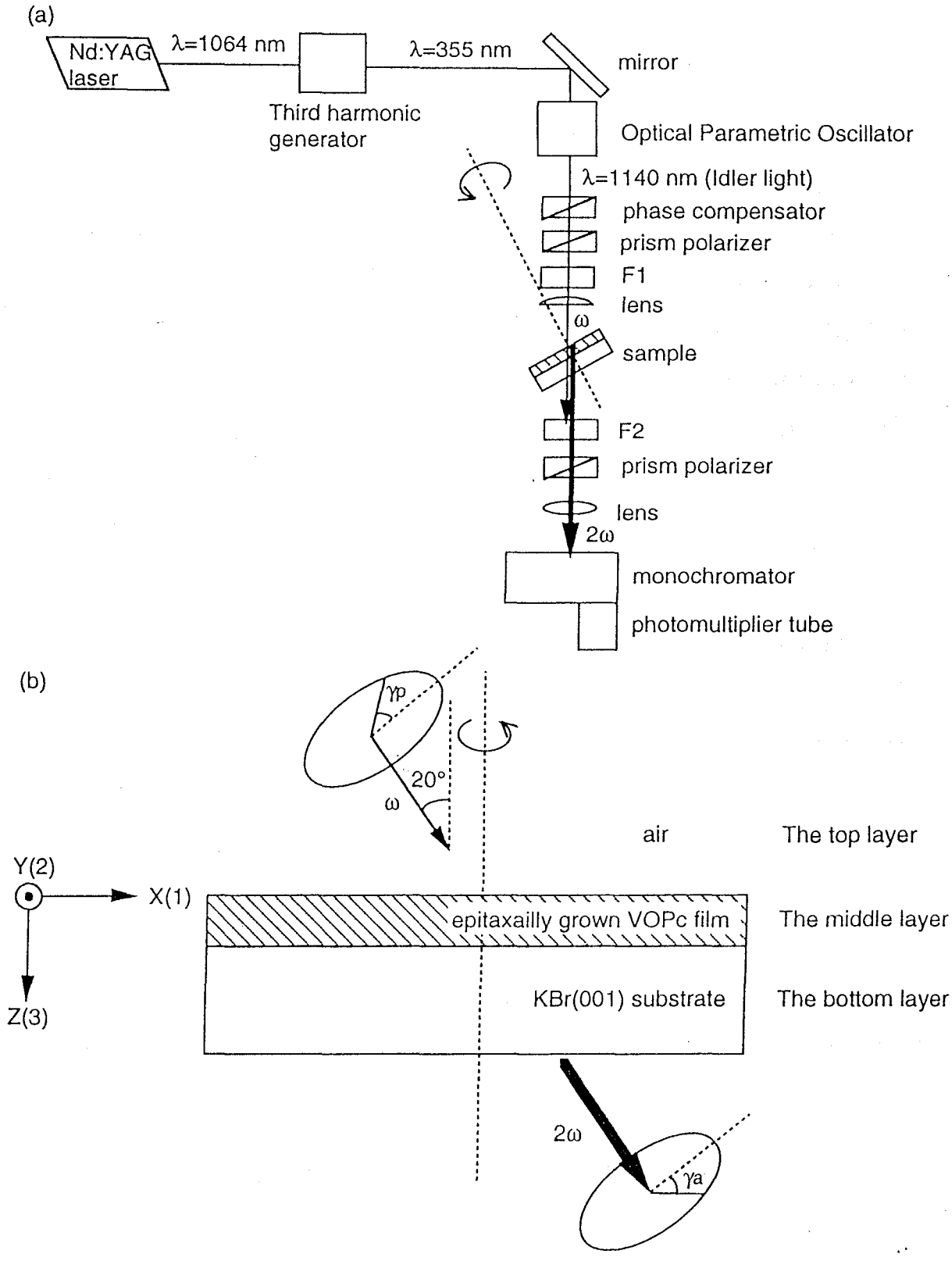

Fig. 4-2-2 (a) The optical arrangement used in the experiment for an epitaxially grown VOPc film. The color filters, (F1) and (F2) are introduced to remove the SH light from various optical components and to eliminate the fundamental light, respectively.
(b) The geometry around the sample.

4-3 Result and Discussion

At first, we consider the rotational dependent SHG from the epitaxial CuPc film (D_{4h} symmetry) on KCl(001) surface. Let us define the relation between the crystal coordinates {x(1), y(2), z(3)} for the epitaxially grown CuPc film and the laboratory coordinates {X(1), Y(1), Z(3)}. Z(3) axis is in accord with z(3) axis and the direction of x(1) axis coincides with the [100] direction in KCl(001) surface. The rotational angle φ is defined as the angle between the direction of X(1) axis and that of x(1) axis. By using the transformation matrix,

$$\begin{pmatrix} a_{11} & a_{12} & a_{13} \\ a_{21} & a_{22} & a_{23} \\ a_{31} & a_{32} & a_{33} \end{pmatrix} = \begin{pmatrix} \cos\varphi & \sin\varphi & 0 \\ -\sin\varphi & \cos\varphi & 0 \\ 0 & 0 & 1 \end{pmatrix} , \qquad (4\text{-}3\text{-}1)$$

the tensor components in the laboratory coordinates are calculated by

$$g^{L}_{\alpha\beta\gamma\delta} = \Sigma\, a_{\alpha i} a_{\beta j} a_{\gamma k} a_{\delta l} g_{ijkl} \quad . \qquad (4\text{-}3\text{-}2)$$

Here, the g components with the superscript L stand for those in the laboratory coordinates. According to the calculation, nonzero φ-dependent tensor components are,

$$g^{L}_{1111} = \frac{1}{4}(\cos 4\varphi + 3)(g_{1111} - g_{1122} - g_{1212} - g_{1221}) + (g_{1122} + g_{1212} + g_{1221}) \qquad (4\text{-}3\text{-}3)$$

for the p→p polarization condition (γ_p=0°, γ_a=0°),

$$g^L_{1212} = \frac{1}{4}(1 - \cos 4\varphi)(g_{1111} - g_{1122} - g_{1212} - g_{1221}) + g_{1212} \qquad (4\text{-}3\text{-}4)$$

for the s→p polarization condition (γ_p=90°, γ_a=0°),

$$\begin{aligned} g^L_{2111} &= -\frac{1}{4}\sin 4\varphi\,(g_{1111} - g_{1122} - g_{1212} - g_{1221}) \\ g^L_{2112} &= \frac{1}{4}(1 - \cos 4\varphi)(g_{1111} - g_{1122} - g_{1212} - g_{1221}) + g_{1221} \\ g^L_{2211} &= \frac{1}{4}(1 - \cos 4\varphi)(g_{1111} - g_{1122} - g_{1212} - g_{1221}) + g_{1122} \\ g^L_{2212} &= \frac{1}{4}\sin 4\varphi\,(g_{1111} - g_{1122} - g_{1212} - g_{1221}) \end{aligned} \qquad (4\text{-}3\text{-}5)$$

for the 45°→s polarization condition (γ_p=45°, γ_a=90°),

$$g^L_{2111} = -\frac{1}{4}\sin 4\varphi\,(g_{1111} - g_{1122} - g_{1212} - g_{1221}) \qquad (4\text{-}3\text{-}6)$$

for the p→s polarization condition (γ_p=90°, γ_a=0°),

$$g^L_{2212} = \frac{1}{4}\sin 4\varphi\,(g_{1111} - g_{1122} - g_{1212} - g_{1221}) \qquad (4\text{-}3\text{-}7)$$

for the s→s polarization condition (γ_p=90°, γ_a=90°) as summarized in Table 2-2-2.

Thus, rotational dependent tensor components in g^L for all polarization conditions are characterized by the parameter

$$(g_{1111} - g_{1122} - g_{1212} - g_{1221}) = (\Delta_{1111} - \Delta_{1122} - 2\Delta_{1212}) + (-2\Lambda_{1111} + 2\Lambda_{1122} + 4\Lambda_{1212}) \quad , \qquad (4\text{-}3\text{-}8)$$

which arises only from EQC and EQ mechanisms. Therefore, the rotational angle dependent SHG implies the significant contribution of EQC and EQ mechanisms, while MDC and MD mechanisms do not lead to the rotational dependence even in D_{4h} symmetry. It is also

noted that the ED mechanism due to the bulk and surface contributions in this sample does not lead to the rotational angle dependence, either, because the nonlinear susceptibility tensor $\chi^{(2)}$ for the ED mechanism does not distinguish C_{4v} symmetry from $C_{\infty v}$ symmetry. Since we have already ruled out the contributions of the bulk ED and MD mechanisms in chapter 3, we do not discuss them hereafter. One of the polarization conditions, such as s→p polarization condition, is enough to verify the existence of EQ and/or EQC mechanisms.

Fig. 4-3-1 shows the rotational angle dependence of SHG from the CuPc epitaxial film with the s→p polarization condition. The experiment was performed according to the procedure described in section 4-2. Thus, we find the large φ-dependent SHG with 90° periodicity. Therefore, the observed rotational dependence is the direct evidence that EQ and/or EQC mechanisms significantly contribute to SHG in CuPc films. The background signal in Fig. 4-3-1 may come from the φ-independent nature due to EQ and EQC mechanisms in g^L components, although we can not deny the contribution from the φ-independent nature due to the MDC mechanism in g^L components and due to the effective surface polarizations at two interfaces. It is also impossible to distinguish EQ mechanism from EQC mechanism based on the rotational angle dependence. However, we will show that the SHG from CuPc films originates from the EQ mechanism by the SH spectrum measurement as will be described in chapter 5.

Next, let us consider the SHG from the epitaxially grown VOPc film on KBr(001) surface. In order to proceed the analysis, we define the relation between the crystal coordinates {x(1), y(2), z(3)} for the VOPc tetragonal crystal and the laboratory coordinates {X(1),

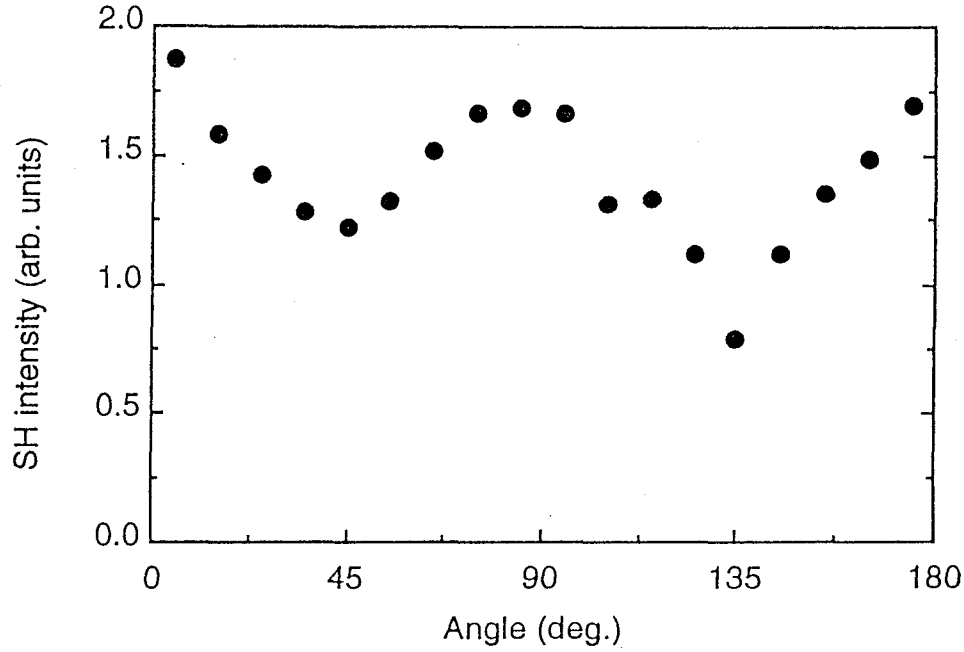

Fig. 4-3-1 Rotational angle depencence of SHG from the eptaxial CuPc film on a KCl substrate.

Y(2), Z(3)}. The Z(3) axis is in accord with the z(3) axis. The direction of the x(1) axis coincides with [110] direction in KBr(001) surface. The rotational angle φ is defined as the angle between the direction of the X(1) axis and that of the x(1) axis.

The symmetry of the film have not been known well except that the film consists in tetragonal systems. Before we show experimental results of the SHG measurement for an epitaxially grown VOPc film on the KBr(001) substrate, it is valuable to refer to the results of the third-harmonic generation (THG) measurement for the same film which was performed by Fang. et al. According to their results, we can dispel the possibility that the film has C_4, S_4 or C_{4h} symmetry as described below.

For C_4, S_4 and C_{4h} symmetry, there are 41 nonzero and 21 independent χ_{ijkl} tensor components in the crystal coordinates defined above, where χ_{ijkl}'s stand for the nonlinear susceptibility tensor components for THG. They are:

$$\begin{aligned}
&\chi_{1111} = \chi_{2222}, \chi_{3333} \\
&\chi_{3311} = \chi_{3322}, \chi_{1233} = -\chi_{2133}, \chi_{1122} = \chi_{2211}, \chi_{1112} = -\chi_{2221} \\
&\chi_{1133} = \chi_{2233}, \chi_{3312} = -\chi_{3321}, \chi_{1212} = \chi_{2121}, \chi_{1121} = -\chi_{2212} \\
&\chi_{3131} = \chi_{3232}, \chi_{1323} = -\chi_{2313}, \chi_{1221} = \chi_{2112}, \chi_{1211} = -\chi_{2122} \\
&\chi_{1313} = \chi_{2323}, \chi_{3132} = -\chi_{3231}, \qquad \chi_{2111} = -\chi_{1222} \\
&\chi_{3113} = \chi_{3223}, \chi_{3123} = -\chi_{3213} \\
&\chi_{1331} = \chi_{2332}, \chi_{1332} = -\chi_{2331}.
\end{aligned} \tag{4-3-9}$$

By using the transformation matrix,

$$\begin{pmatrix} a_{11} & a_{12} & a_{13} \\ a_{21} & a_{22} & a_{23} \\ a_{31} & a_{32} & a_{33} \end{pmatrix} = \begin{pmatrix} \cos\varphi & \sin\varphi & 0 \\ -\sin\varphi & \cos\varphi & 0 \\ 0 & 0 & 1 \end{pmatrix}, \tag{4-3-10}$$

The tensor components in the laboratory coordinates are calculated by

$$\chi^{L}_{\alpha\beta\gamma\delta} = \Sigma\, a_{\alpha i} a_{\beta j} a_{\gamma k} a_{\delta l} \chi_{ijkl} \quad . \qquad (4\text{-}3\text{-}11)$$

Here, the χ components with the superscript L stand for those in the laboratory coordinates. Fang et al. [18-20] measured the incident angle dependence of THG with the s→p polarization condition for the VOPc epitaxial film with the orientation of φ=0°, when the crystal coordinates are in accord with the laboratory coordinates. Therefore, we can remove the superscript L for χ^{L}_{ijkl}'s. The nonlinear polarization elements in the laboratory coordinates which contribute to THG with the polarization condition are described as

$$\begin{aligned} P_1 &= \chi_{1222} E_2 E_2 E_2 \\ P_3 &= 0 \end{aligned} \quad . \qquad (4\text{-}3\text{-}12)$$

Because the electric field E_2 in the film is a function of the incident angle θ, the incident angle dependence of THG should be observed provided that $\chi_{1222} \neq 0$. However, they found that the THG intensity is negligible for any incident angle, which implies that $\chi_{1222} = 0$. Therefore, the VOPc epitaxial film is not a C_4, S_4 or C_{4h} system.

Let us consider the possibility that the film has D_4, D_{2d}, C_{4v} or D_{4h} symmetry. Because D_4, D_{2d} and C_{4v} systems are polar systems, SHG due to the electric dipole mechanism should be dominant in general. Firstly, we consider the SHG from the electric dipole mechanism for D_{2d} system. For D_{2d} symmetry, nonzero χ_{ijk} components in the crystal coordinates are:

$$\chi_{123} = \chi_{213} = \chi_{132} = \chi_{231}, \chi_{312} = \chi_{321} \quad . \tag{4-3-13}$$

Using eq. (4-3-10), the tensor components in the laboratory coordinates are calculated by

$$\chi^{L}_{\alpha\beta\gamma} = \Sigma\, a_{\alpha i} a_{\beta j} a_{\gamma k} \chi_{ijk} \quad , \tag{4-3-14}$$

where the χ components with superscript L stand for those in the laboratory coordinates. The nonlinear polarization in p→p, s→p, 45°→s, p→s and s→s polarization conditions in the laboratory coordinates is summarized in Table 4-3-1. It should be noted that the SHG due to the electric dipole mechanism cannot be observed in the s→s polarization condition for any rotational angle.

Secondly, we consider the SHG from the electric dipole mechanism for D_4 system. For D_4 symmetry, nonzero χ_{ijk} components for in the crystal coordinates are:

$$\chi_{123} = -\chi_{213} = \chi_{132} = -\chi_{231} \quad . \tag{4-3-15}$$

Using eqs. (4-3-10) (4-3-14) and (4-3-15), the tensor components in the laboratory coordinates are calculated. According to the calculation, the tensor components in the laboratory coordinates coincide with those in the crystal coordinates, which imply χ_{ijk}'s in D_4 system are invariant under the transformation (eq. (4-3-10)). The nonlinear polarization in p→p, s→p, 45°→s, p→s and s→s polarization conditions in the laboratory coordinates is summarized in Table 4-3-2, where superscript L for χ components is removed because of the reason stated above.

Table 4-3-1 Expressions of nonlinear polarizations in the electric dipole mechanism for D_{2d} system in the laboratory coordinates. The relation between the crystal coordinates and the laboratory coordinates is defined in the section 4-3. Here only the elements which contribute to SHG in each polarization condition are listed.

p→p	$P_1 = (\chi^L_{113} + \chi^L_{131})E_1E_3$ $P_3 = \chi^L_{311}E_1E_1$
s→p	$P_1 = 0$ $P_3 = \chi^L_{322}E_2E_2$
45°→s	$P_2 = (\chi^L_{213} + \chi^L_{231})E_1E_3 + (\chi^L_{223} + \chi^L_{232})E_2E_3$
p→s	$P_2 = (\chi^L_{213} + \chi^L_{231})E_1E_3$
s→s	$P_2 = 0$

$\chi^L_{113} = \chi^L_{131} = \sin 2\varphi\, \chi_{123}$
$\chi^L_{311} = \sin 2\varphi\, \chi_{312}$
$\chi^L_{322} = -\sin 2\varphi\, \chi_{312}$
$\chi^L_{223} = \chi^L_{232} = -\sin 2\varphi\, \chi_{123}$
$\chi^L_{213} = \chi^L_{231} = \cos 2\varphi\, \chi_{123}$

In the calculation, we used eqs. (4-3-10), (4-3-13) and (4-3-14) in the section 4-3.

Table 4-3-2 Expressions of nonlinear polarizations in the electric dipole mechanism for D_4 system in the laboratory coordinates. The relation between the crystal coordinates and the laboratory coordinates is defined in the section 4-3. Here only the elements which contribute to SHG in each polarization condition are listed.

p→p	$P_1 = 0$ $P_3 = 0$
s→p	$P_1 = 0$ $P_3 = 0$
45°→s	$P_2 = (\chi_{213} + \chi_{231})E_1E_3$
p→s	$P_2 = (\chi_{213} + \chi_{231})E_1E_3$
s→s	$P_2 = 0$

As for C_{4v} system, we have already shown that χ in C_{4v} does not change under the transformation (eq. (4-3-10)) and the contribution appears only in p→p, s→p, 45→s polarization conditions with no rotational angle dependence as described in Table 2-2-2.

Figs. 4-3-2(a), 4-3-2(b) and 4-3-2(c) show the rotational angle dependence of SHG in the p→p, p→s and s→s polarization conditions, respectively. Thus, the observed rotational angle dependent SHG implies that the present SHG cannot be interpreted on the basis of the electric dipole mechanism for D_4, C_{4v} and D_{2d} systems. Since it is reasonable that the electric dipole mechanism should be dominant rather than the higher order mechanisms for polar D_4, C_{4v} and D_{2d} systems, we can remove the possibility of the film being D_4, C_{4v} or D_{2d} system.

Next, let us interpret the experimental results on the basis of higher order mechanisms for D_{4h} symmetry. The rotational angle dependence of SHG in D_{4h} symmetry have been described in the chapter 2. The rotational dependences observed in the experiment are consistent with those theoretically expected in D_{4h} system. The rotational dependence is caused by the parameter

$$(g_{1111} - g_{1122} - g_{1212} - g_{1221}) = (\Delta_{1111} - \Delta_{1122} - 2\Delta_{1212}) + (-2\Lambda_{1111} + 2\Lambda_{1122} + 4\Lambda_{1212}) \quad , \tag{4-3-16}$$

which include only tensor components of nonlinear susceptibilities for EQC and EQ mechanisms. Therefore, the rotational angle dependent SHG indicates the significant contribution of EQC and EQ mechanisms. Thus, we also found significant contributions of EQ and/or EQC mechanisms for the SHG from the VOPc epitaxial film using 1140 nm fundamental wavelength. In the following chapter,

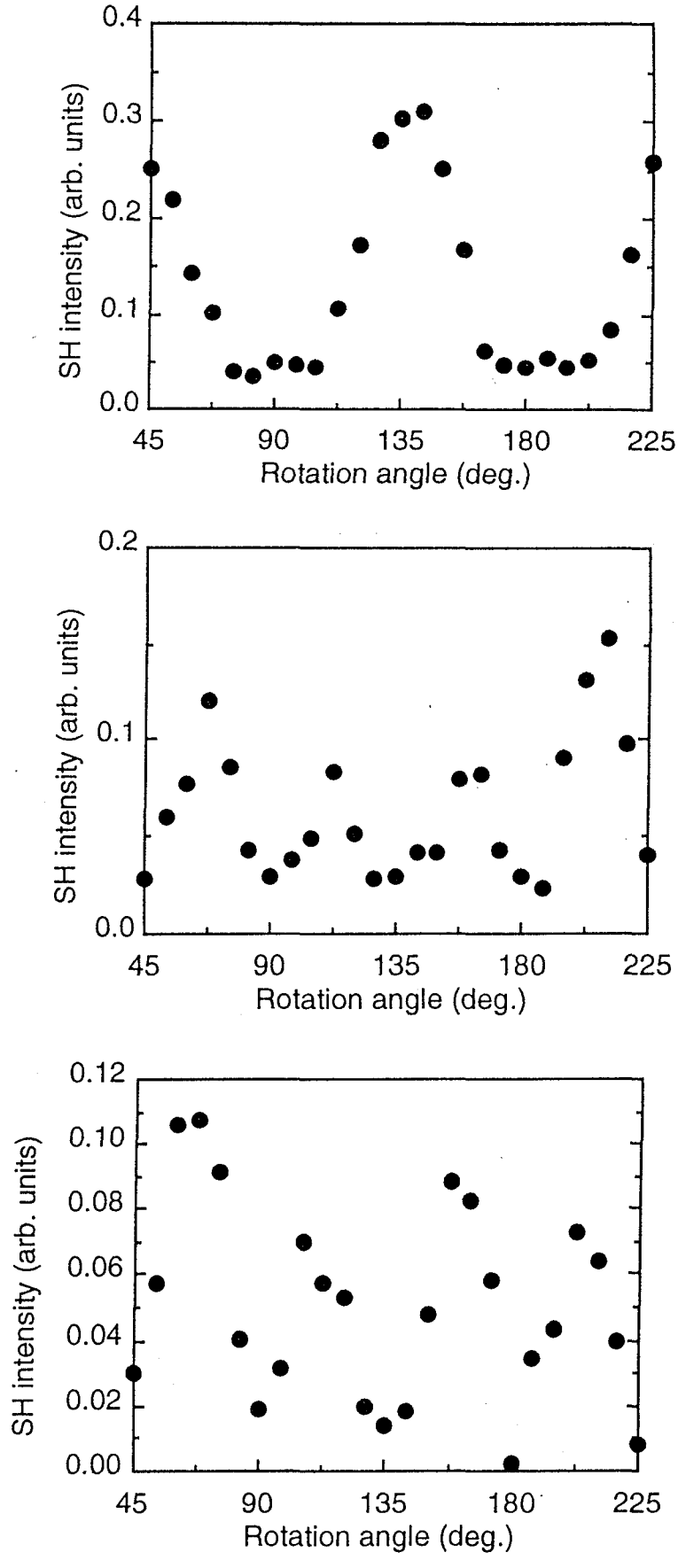

Fig. 4-3-2 Rotational angle dependence of SHG in (a) p→p polarization condition , (b) p→s polarization condition and (c) s→s polarization condition for a VOPc epitaxial film on a KBr(100) substrate.

we will show that the SHG from the VOPc epitaxial film originates from the EQ mechanism by the SH resonant spectrum measurement.

At last, we have to state that the present experimental results can also be explained on the basis of the higher order mechanisms (especially, EQ and EQC mechanisms) even in the D_4, C_{4v} and D_{2d} symmetries, if we assume that higher order mechanisms (especially, EQ and EQC mechanisms) are dominant rather than the electric dipole mechanism, because nonzero and independent tensor components of the nonlinear susceptibilities of higher order mechanisms for these symmetries are the same with those for D_{4h} symmetry.

4-4 Conclusion

We observed the rotational angle dependent SHG for the CuPc film epitaxially grown on a KCl(001) substrate and the VOPc film epitaxially grown on a KBr(001) substrate, using 1064 nm fundamental wavelength and 1140 nm fundamental wavelength, respectively. These results lead to the conclusion that the SHG from the CuPc film at 1064 nm fundamental wavelength and that from the VOPc film at 1140 nm fundamental wavelength originate from EQ and/or EQC mechanisms.

References

[1] J. C. Buchholz and G. A. Somorjai, J. Chem. Phys. **66**, 573 (1977).

[2] A. Yamada, K. Shigehara, and M. Hara, Synth. Met. **18**, 821 (1987).

[3] M. Komiyama, Y. Sakakibara, and H. Hirai, Thin Solid Films **151**, L109 (1987).

[4] M. Hara, H. Sasabe, A. Yamada, and A. F. Garito, Jpn. J. Appl. Phys. **28**, L310 (1989).

[5] A. J. Dann, H. Hoshi, and Y. Maruyama, J. Appl. Phys. **67**, 1371 (1990).

[6] H. Hoshi, A. J. Dann, and Y. Maruyama, J. Appl. Phys. **67**, 1845 (1990).

[7] H. Hoshi, A. J. Dann, and Y. Maruyama, J. Appl. Phys. **67**, 6871 (1990).

[8] H. Hoshi, Y. Maruyama, H. Masuda, and T. Inabe, J. Appl. Phys. **68**, 1396 (1990).

[9] H. Hoshi and Y. Maruyama, J. Appl. Phys. **69**, 3046 (1991).

[10] H. Hoshi, Doctoral dissertation, (Tokyo Inst. of Tech., 1992).

[11] H. Toda, K. Saiki, and A. Koma, Jpn. J. Appl. Phys. **30**, L306 (1991).

[12] H. Toda, T. Kawaguchi, and A. Koma, Appl. Phys. Lett. **61**, 2021 (1992).

[13] M. Ashida, Bull. Chem. Soc. Jpn. **39**, 2362 (1966).

[14] H. W. K. Tom, T. F. Heinz, and Y. R. Shen, Phys. Rev. Lett. **21**, 1983 (1983).

[15] J. A. Litwin, J. E. Sipe, and H. M. van Driel, Phys. Rev. B **31**, 5543 (1985).

[16] G. Lüpke and G. Marowsky, Appl. Phys. B **53**, 71 (1991).

[17] J. E. Sipe, D. J. Moss, and H. M. van Driel, Phys. Rev. B **35**, 1129 (1987).

[18] S. Fang, K. Kohama, H. Hoshi, Y. Maruyama, Chem. Phys. Lett., **234**, 343 (1995).

[19] S. Fang, H. Hoshi, K. Kohama, and Y. Maruyama, J. Phys. Chem. **100**, 4104 (1996).

[20] S. Fang, Doctoral dissertation (Inst. for Mole. Sic., 1994).

Chapter 5 Spectral Dependence of SHG in Phthalocyanine Films

5-1 Introduction

In this chapter, we describe SHG spectra for CuPc and H_2Pc films on a glass substrate which have $D_{\infty h}$ symmetry and an epitaxially grown VOPc film on KBr substrate. In order to clarify the origin of SHG, we make use of the feature that resonance conditions for each of EQC, MDC, EQ and MD mechanisms [1] differ from those for the others, as described in chapter 2. We also discuss the origin of the resonance from microscopic views.

For organic materials, sophisticated methods such as electro-absorption, two-photon absorption, electric-field-induced second-harmonic generation and third-harmonic generation spectrum have been ever used in order to investigate the electronic states including the electric dipole forbidden states, while the SHG spectrum measurement have been little concerned from such a viewpoint.

In this chapter, we have used the SHG spectrum measurement in order to clarify the origin of SHG from phthalocyanine thin films and have also obtained informations about the electric-dipole-forbidden states.

5-2 Experimental

Firstly, let us describe the experimental conditions for CuPc and H_2Pc films on a glass substrate. The sample films were prepared by vacuum evaporation in a vacuum chamber whose base pressure was 2×10^{-6} Torr. The film thickness was monitored by Leybold Inficon XTM/2 and was calibrated by a direct observation of the film

thickness by means of an atomic force microscope (Seiko SPI-3700). The film thickness for the present experiments was about 110 nm. The SHG measurement was carried out without exposing the film to atmosphere.

Figs. 5-2-1(a) and 5-2-1(b) exhibit the experimental arrangement and the geometry around the sample where the laboratory coordinates {X(1), Y(2), Z(3)} are defined. The fundamental light ranging from 1000 nm to 1400 nm was obtained by the optical parametric oscillation of a beta-barium-borate crystal (BMI OP 901.355/70) pumped by the third harmonic light of a Nd:YAG laser (Quanta Ray DCR-11). The fundamental light of 3~5 mJ/pulse ran at the repetition frequency of 10 Hz. The polarization of fundamental light was adjusted by a combination of a phase compensator and a polarizer to obtain p- (γ_p=0°) or s- (γ_p=90°) polarized fundamental light. The fundamental light after passing through a lens and a color filter to remove SH light from optical components was cast upon the film. The fundamental light was impinged on the film side with the incident angle of 45°. The p-polarized SH light (γ_a=0°) filtered through a color filter to remove the fundamental light, an analyzer, a lens and a monochromator (Ritsu MC-10N) was detected by a photomultiplier (Hamamatsu R955) in the transmission direction. The frequency and the polarization dependence of the effective efficiency for the detector system was calibrated using a standard halogen lamp. The frequency dependence of the fundamental light power was calibrated using a power-meter (Gentec TPM-310 or Gentec EM-1).

Next, let us describe the experimental conditions for epitaxially grown VOPc film on a KBr(001) substrate. The sample is the same with that described in chapter 4. The thickness was about

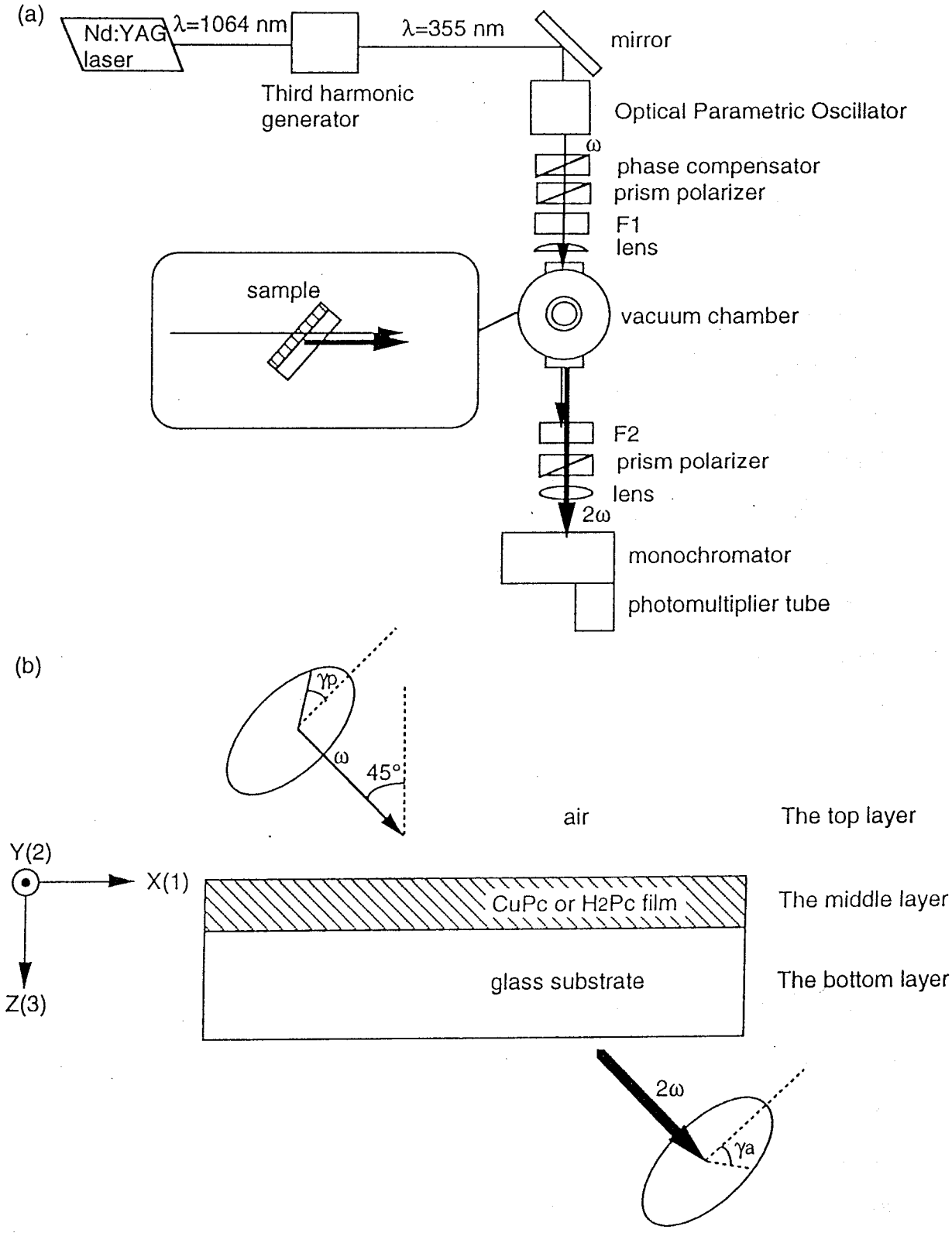

Fig. 5-2-1 (a) The optical arrangement used in the experiment for a CuPc or a H2Pc film on a glass substrate. The color filters, (F1) and (F2) are introduced to remove the SH light from various optical components and to eliminate the fundamental light, respectively. (b) The geometry around the sample.

160 nm. The experimental arrangement was the same with that in Fig. 5-2-1(a) except that a Nd:YAG laser (BMI 501D.NS 710) and a optical parametric oscillator (BMI OP901.355) were used. The SHG spectrum measurement was performed with the p→s polarization condition (γ_p=0°, γ_a=90°) at the incident angle of 45° in air. Fig. 5-2-2(a) shows the geometry around the sample where the laboratory coordinates {X(1), Y(2), Z(3)} are defined. The relation between the laboratory coordinates {X(1), Y(2), Z(3)} and the crystal coordinates {x(1), y(2), z(3)} is defined as follows. Z(3) axis is in accord with z(3) axis and the direction of x(1) axis coincides with the [110] direction in a KBr(001) surface. The rotational angle φ is defined as the angle between the direction of X(1) axis and x(1) axis and φ=22.5° was chosen for the present experiment as illustrated in Fig. 5-2-2(b).

The linear absorption spectra for CuPc and H_2Pc films on a glass substrate and the epitaxial VOPc film on KBr(100) surface were measured using a spectrophotometer (Hitach U-3400).

5-3 Result and Discussion

Let us discuss the experimental results for CuPc and H_2Pc films on a glass substrate which have $D_{\infty h}$ symmetry. In general, a bulk optical nonlinear polarization in centrosymmetric $D_{\infty h}$ symmetry is written in the form $P_i = g_{ijkl} E_j \partial_k E_l$ and the nonzero g components are characteristic in the four mechanisms as described in chapter 2. Here, we describe the resonant terms of microscopic expressions for four mechanisms. The EQC mechanism or the MDC mechanism is due to an EQ transition or a MD transition at one input field, respectively, and an ED transition at the other input field and an ED transition at the output field as illustrated in Figs. 5-3-1(a) and 5-3-

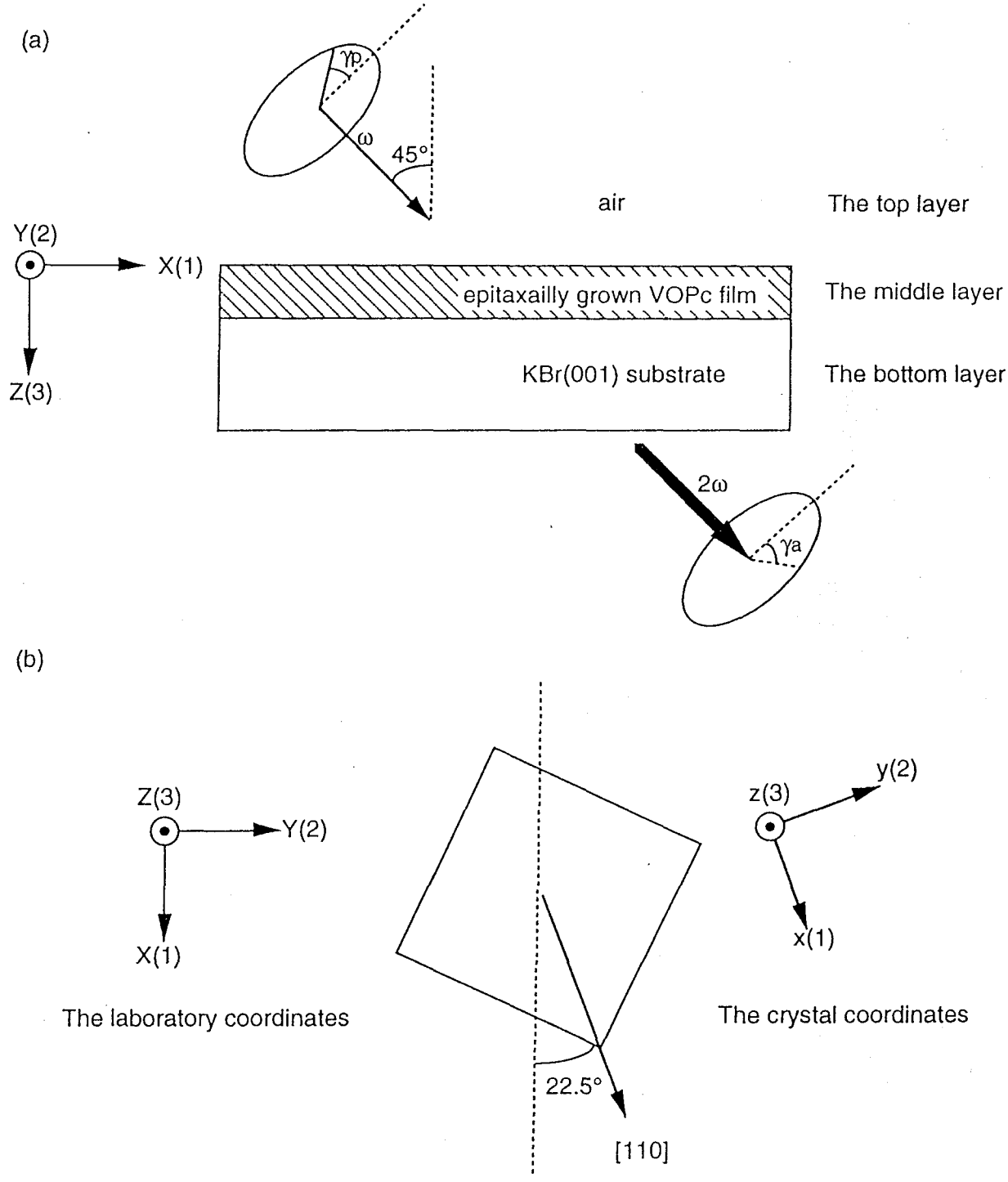

Fig. 5-2-2 (a) The goermetry around a VOPc epitaxial film.
(b) The relation between the laboratory coordinates and the crystal coordinates.

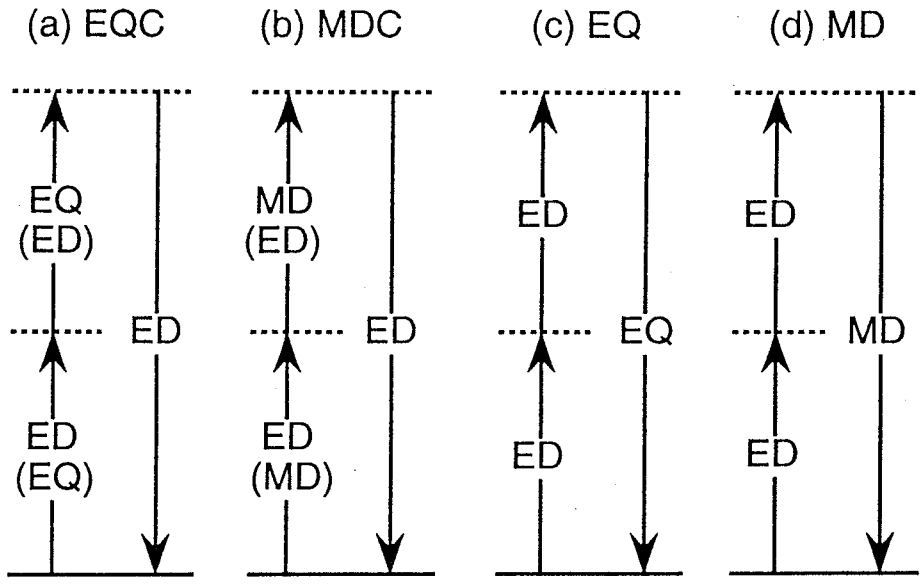

Fig. 5-3-1. Schematic illustration of microscopic views of four SHG processes, (a) the electric quadrupole coupling (EQC) mechanism, (b) the magnetic dipole coupling (MDC) mechanism, (c) the electric quadrupole (EQ) mechanism and (d) the magnetic dipole (MD) mechanism.

1(b). The EQ mechanism or the MD mechanism is due to ED transitions at both the input fields and an EQ transition or a MD transition at the output field, respectively, as illustrated in Figs. 5-3-1(c) and 5-3-1(d). Among them, the MD mechanism can be ruled out from a symmetrical consideration.

The SH spectra and the absorption spectra for a CuPc film and a H_2Pc film are displayed in Figs. 5-3-2 and 5-3-3, respectively, where $I^T(s \rightarrow p)$, for example, stands for p-polarized SH intensity under the incidence of s-polarized fundamental light. It was confirmed that $I^T(p \rightarrow s)$ and $I^T(s \rightarrow s)$ are negligible as expected from a symmetrical consideration. A sharp resonance peak was observed at high energy edge (550 nm) of the Q-absorption band in both films.

Let us first examine the effect of the absorption on the SH intensity. Not only the frequency dispersion of the nonlinear susceptibility but also the dispersion of a dielectric constant influence the SH intensity. Debe et al. [2] measured a dielectric dispersion in visible region for a CuPc film. We estimated the influence of dielectric dispersion using their values as follows. For the polarization condition of $I^T(s \rightarrow p)$, the bulk nonlinear polarization P involves P_1 and P_3, where 3-axis is along the film surface normal and 1-axis is parallel to the film surface and to the optic plane illustrated in Fig. 5-2-1(b). They are expressed as

$$
\begin{aligned}
P_1 &= \Delta_{1212}E_2\partial_1E_2 + \Gamma_{1212}E_2\partial_1E_2 - \Lambda_{1122}\partial_1E_2^2 \\
&= (\Delta_{1212} + \Gamma_{1212} - 2\Lambda_{1122})E_2\partial_1E_2 \\
&= g_{1212}E_2\partial_1E_2 \\
P_3 &= \Delta_{3232}E_2\partial_3E_2 + \Gamma_{3232}E_2\partial_3E_2 - \Lambda_{3322}\partial_3E_2^2 \\
&= (\Delta_{3232} + \Gamma_{3232} - 2\Lambda_{3322})E_2\partial_3E_2 \\
&= g_{3232}E_2\partial_3E_2
\end{aligned}
$$

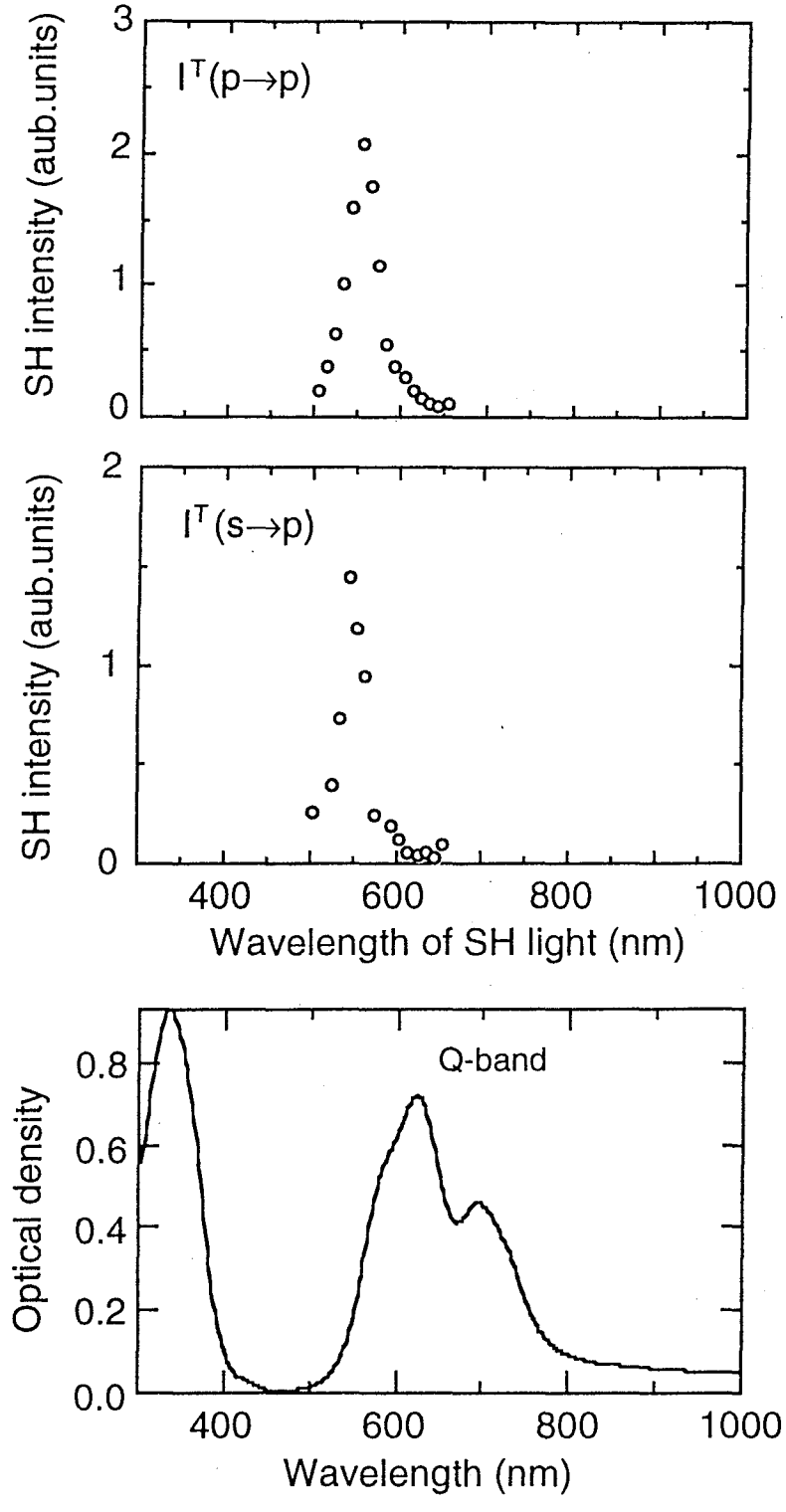

Fig. 5-3-2 The SH spectra and the linear absorption spectrum in a CuPc film. The SH intensities, $I^T(p\rightarrow p)$ and $I^T(s\rightarrow p)$, are plotted for the SH wavelength.

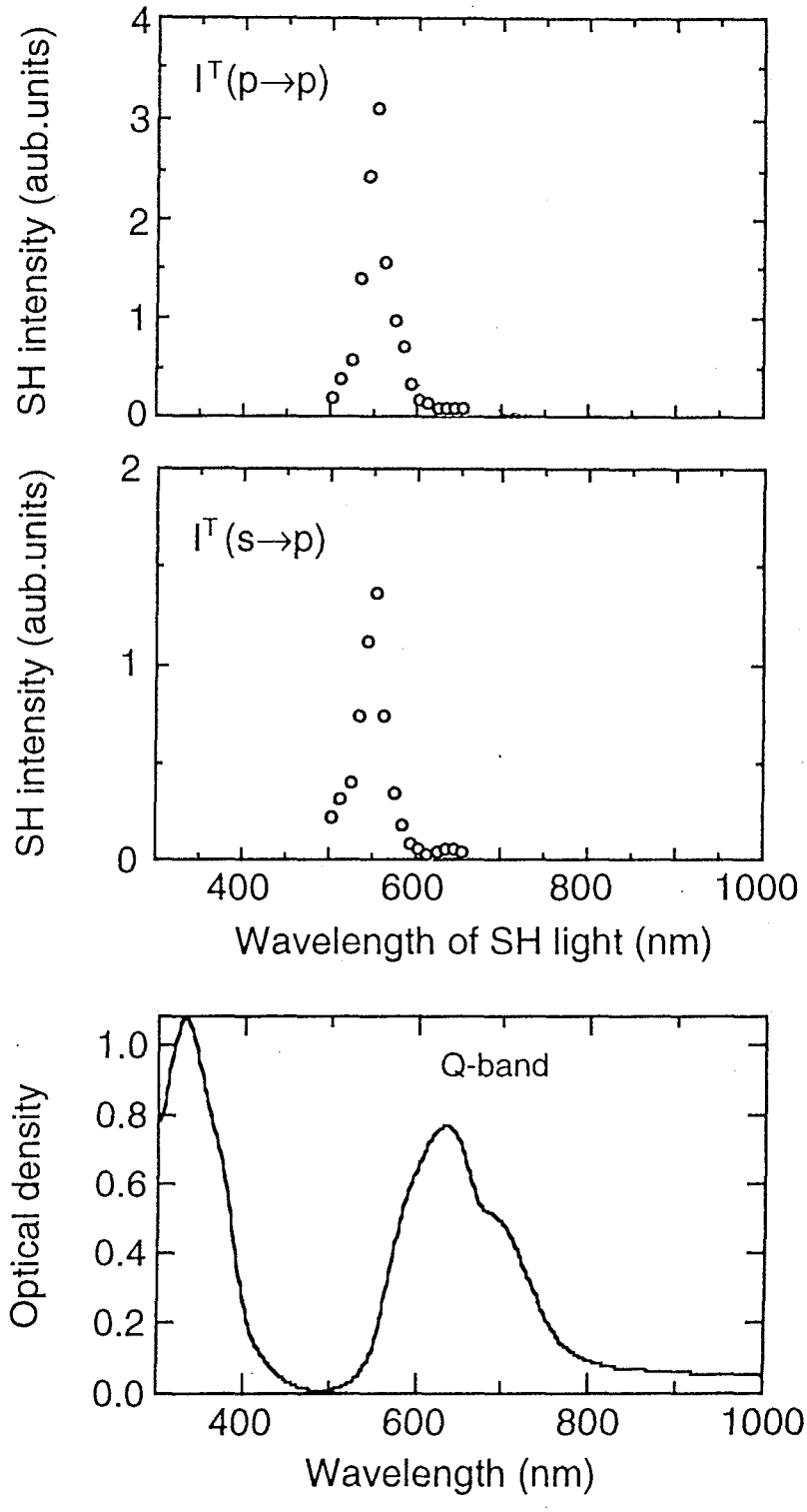

Fig. 5-3-3 The SH spectra and the linear absorption spectrum in a H_2Pc film. The SH intensities, $I^T(p\rightarrow p)$ and $I^T(s\rightarrow p)$, are plotted for the SH wavelength.

where Δ, Γ, and Λ are nonlinear susceptibilities for the EQC, MDC, and EQ mechanisms, respectively. The electric field E of fundamental light in the film is expressed as a sum of the forward and the backward waves, that is

$$E_2 = E_2^{mf} + E_2^{mb}$$

In order to examine the effect of the dielectric dispersion, we assumed the relation $g_{1212}=g_{3232}$. We calculated $I^T(s \rightarrow p)$ at two wavelengths, 550nm (SH resonance peak) and 620 nm (absorption peak), only by taking account of the dielectric dispersion assuming that g has no frequency dependence. The calculation was performed by solving the wave equations at ω and 2ω subject to the Maxwell boundary conditions [3]. In the calculation, we used the values, $\tilde{\varepsilon}_{M1}$ (550 nm)=2.3+0.3i, $\tilde{\varepsilon}_{M3}$ (550 nm)=1.9+0.7i, $\tilde{\varepsilon}_{M1}$ (620 nm)=2.0+1.6i and $\tilde{\varepsilon}_{M3}$ (620 nm)=3.4+4.2i. For dielectric constants at 1100 nm and 1240 nm, a value at 1064 nm ($\tilde{\varepsilon}_{m1}$ (1064 nm)=3.3) obtained by Kumagai et al. [4] was used. The calculation leads to $I^T(s \rightarrow p, 620\,nm) / I^T(s \rightarrow p, 550\,nm) = 0.65$ for the film of 110 nm thickness. The value 0.65 is solely caused by the dielectric dispersion. However, $I^T(s \rightarrow p, 620\,nm) / I^T(s \rightarrow p, 550\,nm) = 0.036$ obtained by the experiment is much smaller than the simulation. This fact indicates that the influence of the absorption in the film exists but is not serious since the film is not thick, and that a frequency dispersion of the nonlinear susceptibility plays an important part in the present SH spectra.

Let us discuss the SH spectra based on an orientation gas model in which optical properties of a free molecule directly reflect to a bulk optical properties through a molecular orientation

distribution function. The energy diagram for a free CuPc molecule is shown in Fig. 5-3-4(a). The relative energy intervals between the levels correspond to the energy diagram given in ref. [5]. Although one electron is located on the metal dominant $b_{1g}(d_{x^2-y^2})$ level according to their results, this level has no influence upon the present SH optical process, since the SH resonance peak appears at the same wavelength in a H_2Pc film as that in a CuPc film. Since the Q-absorption band originates from the lowest π-π^* transition, ($^2B_{1g}$(ground state)-^2E_u ($a_{1u}(\pi)\rightarrow e_g(\pi^*)$)) for CuPc, there are no energy levels which contribute to the resonance in the fundamental frequency region used in this experiment, including MD, EQ and ED transitions. Furthermore, the resonance wavelength 550 nm is far from the peak of the Q-absorption band, indicating that the resonant excited state must be for the ED forbidden transition. Judging from the energy diagram, the EQ and MD allowed transitions, $b_{2g}(Np\sigma)\rightarrow e_g(\pi^*)$ and $a_{1g}(Np\sigma)\rightarrow e_g(\pi^*)$, are the candidates for the resonance at the SH frequency, since $b_{2g}(Np\sigma)$ and $a_{1g}(Np\sigma)$ levels exist near $a_{1u}(\pi)$ level. However, the energy level calculation for the $Np\sigma$ orbitals in various phthalocyanines has poor reliability [5]. In fact, such σ-orbitals exist lower than $a_{2u}(\pi)$ level according to a recent calculation for magnesium phthalocyanine (MgPc) [6]. Moreover, it is questionable whether the large nonlinearity occurs in the optical process which includes the localized σ-orbital electron excitation. The EQ allowed transition ($^2B_{1g}$(ground state)-$^2A_{1g}$ ($a_{1u}(\pi)\rightarrow b_{1u}(\pi^*)$)) or ($^2B_{1g}$(ground state)-$^2A_{2g}$ ($a_{1u}(\pi)\rightarrow b_{2u}(\pi^*)$)) can contribute to the resonance at SH frequency, since the $b_{1u}(\pi^*)$ and $b_{2u}(\pi^*)$ levels exist at a reasonable position according to the recent calculation [6].

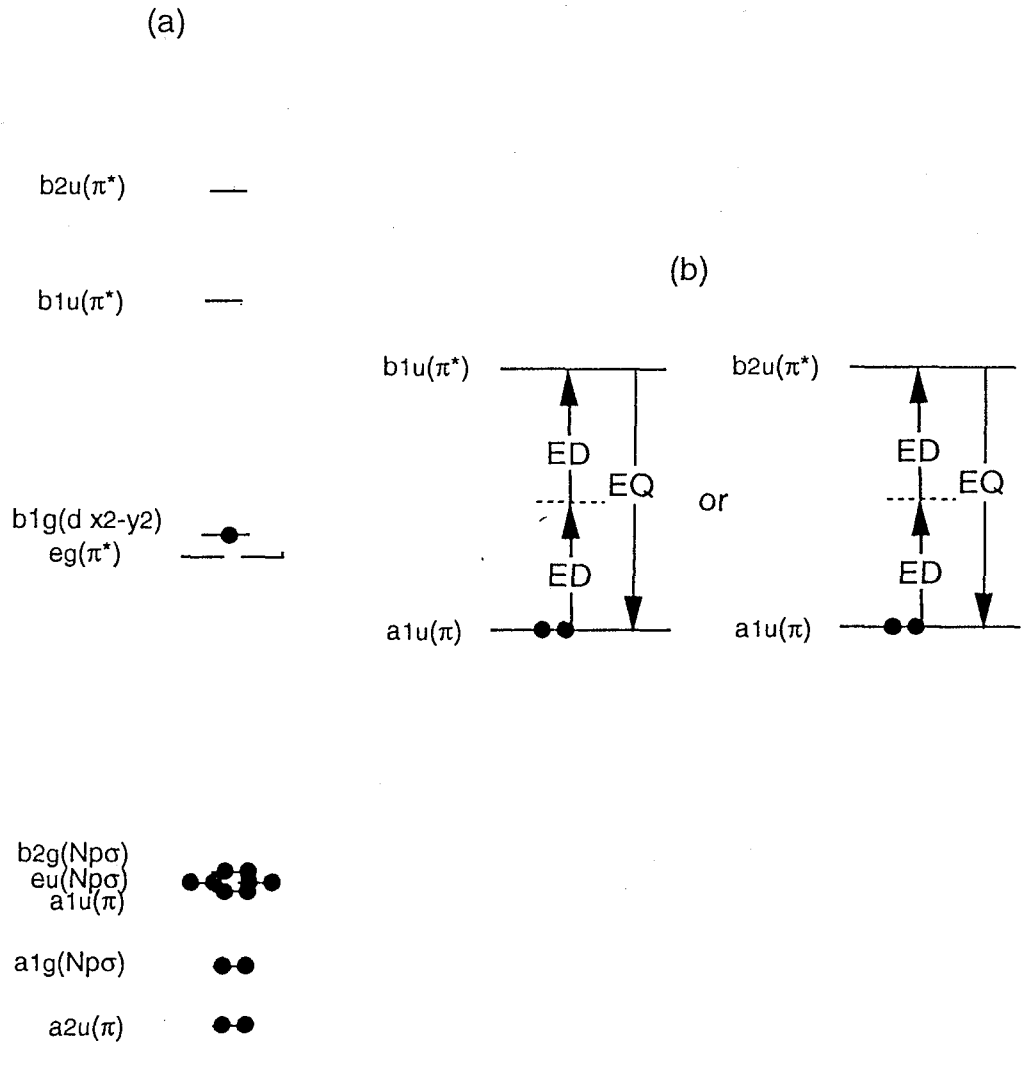

Fig. 5-3-4 (a) The energy diagram for a free CuPc, which is quoted from ref. [5].
(b) The resonance conditions using 1100 nm fundamental wavelength.

An alternative interpretation for the resonance peak is the one based on charge transfer (CT) excitons [7,8] in phthalocyanine crystals. Tokura et al. [9,10] measured an electro-absorption (EA) spectrum and suggested the existence of an antisymmetric CT exciton state. Since this state is ED-transition-forbidden and lies above the main absorption band, the observed resonance SHG may be attributed to the EQ transition to this state. However, this idea can be ruled out by the observation of in-plane anisotropy of SHG in CuPc films epitaxially grown by molecular beam epitaxy, as briefly mentioned in the following.

Epitaxial CuPc films on KCl (001) substrate surface have D_{4h} symmetry [11]. In D_{4h} symmetry, $I^T(s \rightarrow p)$ is expressed as a sum of φ-independent and φ-dependent terms in g^L, where φ is a rotation angle about the film surface normal. In the experiment using 1064 nm fundamental wavelength, we observed large φ-dependent SHG with 90° periodicity as described in chapter 4. It should be also noted that the SH wavelength 532 nm is within resonance band. According to the analysis described in chapter 4, the parameter

$$(g_{1111} - g_{1122} - g_{1212} - g_{1221}) = (\Delta_{1111} - \Delta_{1122} - 2\Delta_{1212}) + (-2\Lambda_{1111} + 2\Lambda_{1122} + 4\Lambda_{1212}) \quad ,$$

where in-plane components of Λ and/or Δ in the crystal coordinates are included, plays an important role in the rotational anisotropy of the SHG. The plane-like CuPc molecules tend to lie parallel to KCl (001) plane, so that in-plane components in the crystal coordinate system are related to in-plane components of the molecular coordinate system. The resonance at SH frequency due to the EQ allowed transition ($^2B_{1g}$(ground state)-$^2A_{1g}$ ($a_{1u}(\pi) \rightarrow b_{1u}(\pi^*)$)) illustrated in Fig. 5-3-4(b) produces dominant tensor components

($\lambda_{11qq}=\lambda_{22qq}$ (q=1, 2, or 3)), where λ_{ijkl}'s are microscopic susceptibility tensor components for EQ mechanism, while the resonance at SH frequency due to the EQ allowed transition ($^2B_{1g}$(ground state)-$^2A_{2g}$ ($a_{1u}(\pi)\rightarrow b_{2u}(\pi^*)$)) illustrated in Fig. 5-3-4(b) produces dominant tensor components ($\lambda_{1212}=\lambda_{1221}$). For $I^T(s\rightarrow p)$, the terms $\lambda_{1111}=\lambda_{2222}$ and $\lambda_{1122}=\lambda_{2211}$, or $\lambda_{1212}=\lambda_{1221}$ mainly contribute to the angle dependence. Thus, rotational angle dependent SHG is also consistent with the interpretation of the SH spectrum based on the orientation gas model. In case of CT-exciton states, on the other hand, out-of-plane components must play a role, since CT exciton states have large anisotropy to the direction of stack axis.

In the case of a H_2Pc film, the resonance at the SH frequency originates from the quadrupole transition (^1A_g(ground state)-^1A_g ($a_u(\pi)\rightarrow a_u(\pi^*)$)) or ($^1A_g$(ground state)-$^1B_{1g}$ ($a_u(\pi)\rightarrow b_{1u}(\pi^*)$)) if we refer to Figs. 5-3-5(a) and 5-3-5(b), which is also quoted from ref. [12], and consider with the simmilar procedure.

Next, let us discuss the experimental results for a VOPc epitaxial film on a KBr(001) substrate. The SH spectrum in the p→s polarization condition at $\varphi=22.5°$ and the absorption spectra for the film are displayed in Fig. 5-3-6. A sharp resonance peak (570 nm) and a shoulder structure (650 nm) were observed at the high energy edge of the Q-absorption band for the VOPc film. It is reasonable that a frequency dispersion of the nonlinear susceptibility plays an important part in the SH spectrum for the VOPc film since the film is thin. We have already shown the rotational anisotropy of the SHG using 1140 nm fundamental wavelength in the p→s polarization condition as illustrated in Fig. 4-3-2(b). The rotational anisotropy is caused by the parameter.

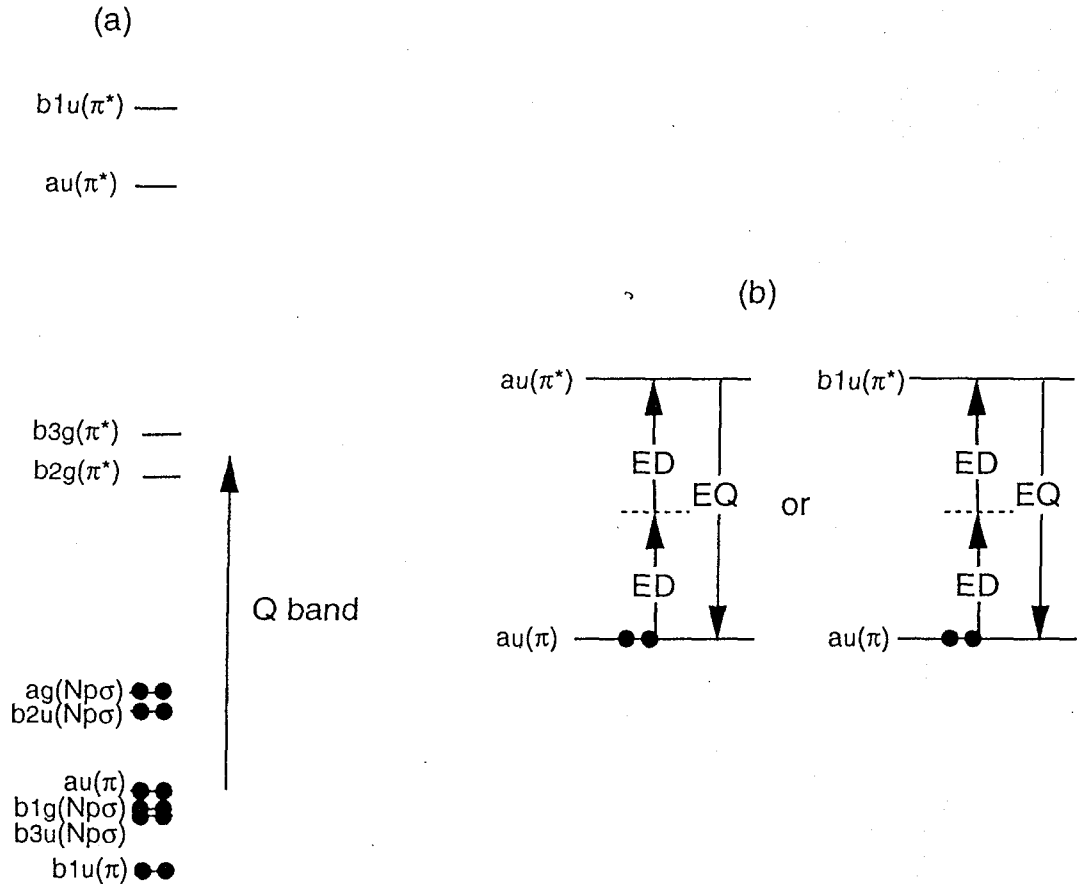

Fig. 5-3-5 (a)The energy diagram for a free H_2Pc, which is quoted from ref. [12].
(b) The resonant condtions using 1100 nm fundamental wavelength.

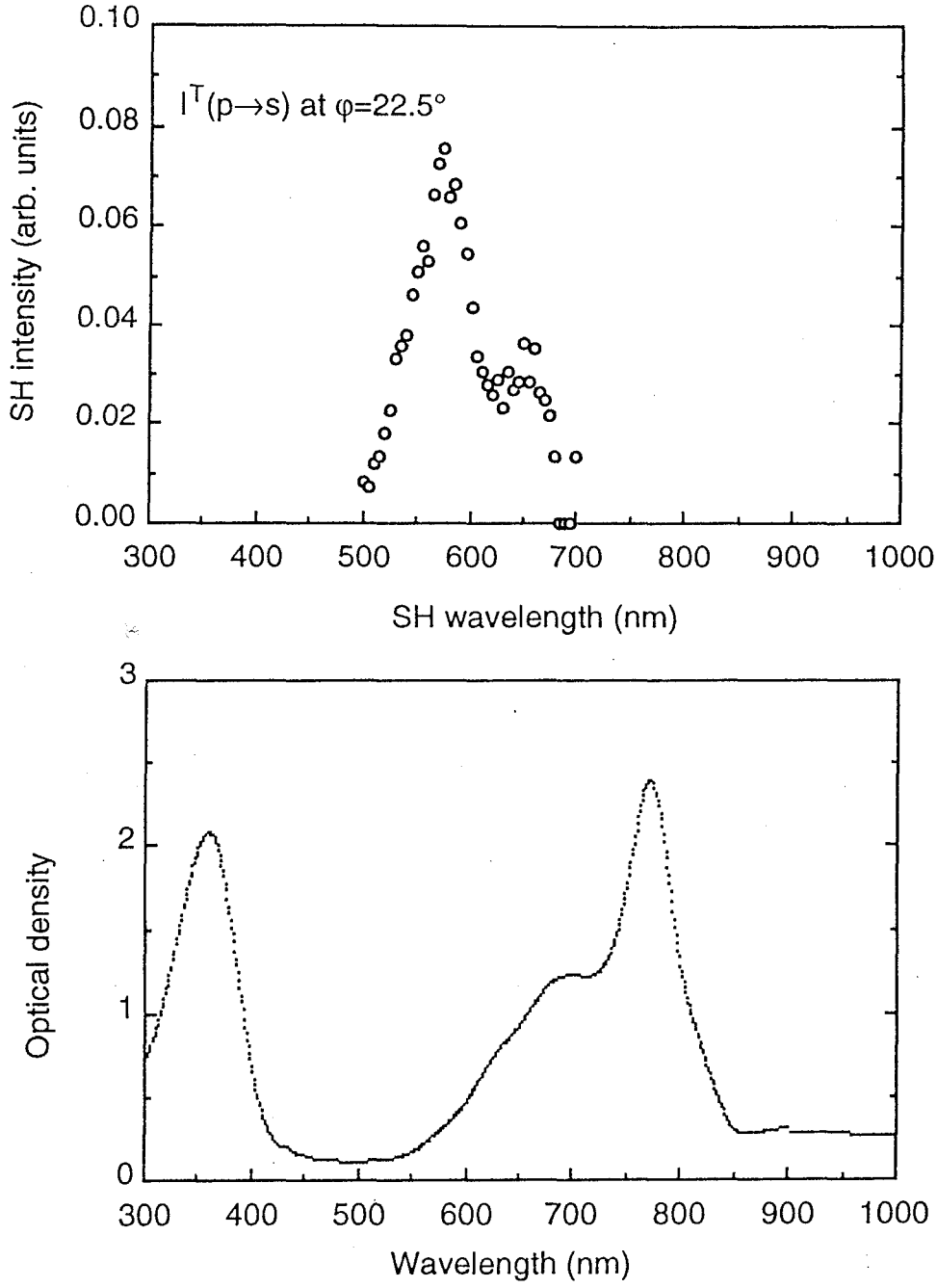

Fig. 5-3-6 The SH spectrum and the absorption spectrum in a VOPc epitaxial film on a KBr(100) substrate.

$$(g_{1111} - g_{1122} - g_{1212} - g_{1221}) = (\Delta_{1111} - \Delta_{1122} - 2\Delta_{1212}) + (-2\Lambda_{1111} + 2\Lambda_{1122} + 4\Lambda_{1212}) \quad ,$$

where in-plane components of Λ and/or Δ in the crystal coordinates are included apart from D_{4h}, C_{4v}, D_{2d}, or D_4 system, macroscopically. Since the stack columns for VOPc molecules are perpendicular to the substrate, VOPc molecules lie parallel to KBr (001) plane. Therefore, in-plane components in the crystal coordinate system are related to in-plane components of the molecular coordinate system. It seems reasonable to suppose that levels ($b_2(\pi^*)$ and $b_1(\pi^*)$ in C_{4v} point group) such as $b_{1u}(\pi^*)$ and $b_{2u}(\pi^*)$ in a CuPc molecule also exists in a VOPc molecule, since they are not metal dominant molecular orbitals. According to the simmilar consideration with CuPc and H_2Pc films, we attribute the peak at 570 nm to the resonance at SH frequency due to the EQ allowed transition, where the in-plain components of melecular nonlinear susceptibility of the EQ mechanism significantly cotributes to the SHG.

5-4 Conculusion

Second harmonic generation (SHG) spectra were measured in thin films of CuPc and H_2Pc and an epitaxially grown VOPc film. A sharp resonant peak was observed at the high energy edge of the Q-absorption band using 1100 nm fundamental light for H_2Pc and CuPc films and using 1140 nm fundamental light for the VOPc epitaxial film, respectively, and was attributed to the resonant enhancement of the electric quadrupole transition at SH frequency. We discussed the origin based on an orientation gas model.

References

[1] E. Adler, Phys. Rev. **134**, A728 (1964).

[2] M. K. Debe, J. Vac. Sci. Technol. A **10**, 2816 (1991).

[3] N. Bloembergen and P. S. Parshan, Phys. Rev. **128**, 606 (1962).

[4] K. Kumagai, G. Mizutani, H. Tsukioka, T. Yamauchi, and S. Ushioda, Phys. Rev. B **48**, 14488 (1993).

[5] A. M. Schaffer, M. Gouterman, and E. R. Davidson, Theoret. chim. Acta (Berl.) **30**, 9 (1973).

[6] M. G. Cory, H. Hirose, and M. C. Zerner, Inorg. Chem. **34**, 2969 (1995).

[7] J. P. Hernandez and S. Choi, J. Chem. Phys. **50**, 1524 (1969).

[8] W. L. Pollans and S. Choi, J. Chem. Phys. **52**, 3691 (1970).

[9] Y. Tokura, T. Koda, Y. Iyechika, and H. Kuroda, Chem. Phys. Letters **102**, 174 (1983).

[10] H. Yoshida, Y. Tokura, and T. Koda, Chem. Phys. **109**, 375 (1986).

[11] M. Ashida, Bull. Chem. Soc. Jpn. **39**, 2632 (1966).

[12] A. M. Schaffer and M. Gouterman, Theoret. chim. Acta (Berl.) **25**, 62 (1972).

Chapter 6 Concluding Remarks

This thesis was undertaken to clarify the origin of the relatively strong SHG from phthalocyanine thin films. For this purpose, we performed the thickness, rotational, and spectral dependent SHG measurements for phthalocyanine films on glass substrates and epitaxially grown phthalocyanine on alkali halides. Especially, we noticed that SHG spectrum measurement provide us with a useful tool for studying electric dipole forbidden and electric quadrupole and/or magnetic dipole allowed states.

In chapter 1, we stated an overview of SHG from centrosymmetric system and described briefly electronic structures of phthalocyanine molecules, including samples studied. We also stated purpose of this study.

In chapter 2, we described the expressions of the nonlinear susceptibilities from higher order mechanisms and the analysis under various systems and geometries, which include systems used in this study. The expressions and the analysis are used in the following chapters.

In chapter 3, we have measured thickness dependent SHG for CuPc films on a glass substrate by taking advantage of in situ observation. The experimental results exhibited the significant deviation from the ED mechanism as a bulk which has ever been proposed. We attributed the SHG using 1064 nm fundamental wavelength to higher order mechanisms except for MD mechanism.

In chapter 4, we have investigated in-plane anisotropic SHG for CuPc films epitaxially grown on KCl and VOPc films epitaxially grown on KBr using 1064 nm fundamental wavelength and 1140 nm fundamental wavelength, respectively. The periodic signals were observed for both films, which implies the significant contribution of EQ and/or EQC mechanisms for the present SHG. We also discussed the symmetry of a VOPc epitaxial film.

In chapter 5, spectral dependent SHG for CuPc and H_2Pc films on a glass substrate and an epitaxially grown VOPc film have been studied. A sharp peak was observed at the high-energy edge of the Q-absorption band for both of CuPc and H_2Pc films on the glass substrate at 1100 nm fundamental wavelength, which implies the dominance of the EQ mechanism due to the EQ resonant transition at SH frequency. We discussed the origin with the orientation gas model, which was supported by rotational anisotropic SHG described in chapter 4. A sharp resonant peak was observed at the high-energy edge of the Q-absorption band for the epitaxially grown VOPc film using 1140 nm fundamental wavelength. We also attributed the SHG to the resonant enhancement of the electric quadrupole transition at SH frequency.

At last, we describe extensions to the work presented in this thesis. The immediate application of SHG spectrum measurement to various systems (ex. polydiacetylene and polyacetylene) is very interesting, which will help to understand the electronic structure for each system.

If we can use two wavelength-tunable beams as pump beams, we can measure the SFG spectrum which originates from higher

order mechanisms. The doubly resonance may be possible by adjusting ω_p and ω_q. The SFG measurement also provides us with a variety of polarization dependences, since we can choose the polarization conditions of two pump beams, independently. These advantages may allow us to probe various excited states.

According to experiments for C_{60} and phthalocyanines, the effective $\chi^{(2)}$ values under the resonance conditions due to higher order mechanisms are an order of magnitude larger than the non-resonant $\chi^{(2)}$ value (1.9×10^{-9} esu) of quartz. From application viewpoints, it may be possible to produce SHG devices by making use of resonances with forbidden states at fundamental or SH frequency and the phase matching condition. For such devices, non-centrosymmetric structures are not needed.

Appendix

In many papers [1-9], the vector notations are used in order to describe the nonlinear electric polarization from higher order mechanisms for K_h and O_h symmetries. Here, we obtain the vector notations from the general tensor expressions.

For K_h symmetry, the P_1 component of the nonlinear electric polarization is expressed with the general tensor expressions as follows.

$$\begin{aligned} P_1 &= g_{1111}E_1\partial_1E_1 \\ &+ g_{1122}E_1\partial_2E_2 + g_{1133}E_1\partial_3E_3 \\ &+ g_{1212}E_2\partial_1E_2 + g_{1313}E_3\partial_1E_3 \\ &+ g_{1221}E_2\partial_2E_1 + g_{1331}E_3\partial_3E_1 \quad . \end{aligned} \tag{A-1}$$

Using the relations which are satisfied for K_h symmetry,

$$g_{1122} = g_{1133} = g_{iijj},\ g_{1212} = g_{1313} = g_{ijij},\ g_{1221} = g_{1331} = g_{ijji},\ g_{1111} = g_{iiii} = g_{iijj} + g_{ijij} + g_{ijji} \quad , \tag{A-2}$$

eq. (A-1) is expressed as

$$\begin{aligned} P_1 &= g_{iijj}E_1(\partial_1E_1 + \partial_2E_2 + \partial_3E_3) \\ &+ g_{ijij}(E_1\partial_1E_1 + E_2\partial_1E_2 + E_3\partial_1E_3) \\ &+ g_{ijji}(E_1\partial_1 + E_2\partial_2 + E_3\partial_3)E_1 \\ &= g_{iijj}E_1(\partial_1E_1 + \partial_2E_2 + \partial_3E_3) \\ &+ \frac{1}{2}g_{ijij}\partial_1(E_1E_1 + E_2E_2 + E_3E_3) \\ &+ g_{ijji}(E_1\partial_1 + E_2\partial_2 + E_3\partial_3)E_1 \quad . \end{aligned} \tag{A-3}$$

According to the same procedure, the P_2 and P_3 components can be also obtained, so that we get the vector notation

$$P_v = g_{iijj}E_v(\nabla \cdot \boldsymbol{E}) + \frac{1}{2}g_{ijji}\partial_v(\boldsymbol{E} \cdot \boldsymbol{E}) + g_{ijji}(\boldsymbol{E} \cdot \nabla)E_v \quad . \qquad \text{(A-4)}$$

In many papers, P_V is expressed with the form.

$$P_v = \beta E_v(\nabla \cdot \boldsymbol{E}) + \gamma\partial_v(\boldsymbol{E} \cdot \boldsymbol{E}) + (\delta - \beta - 2\gamma)(\boldsymbol{E} \cdot \nabla)E_v$$
$$(\beta = g_{iijj},\ \gamma = \frac{1}{2}g_{ijji},\ \delta - \beta - 2\gamma = g_{ijji}) \quad . \qquad \text{(A-5)}$$

In this expression, each of the three terms gives us a vector multiplied by a constant. Therefore, these three terms do not depend on the orientation of the material, which reflects K_h symmetry. We summarized expressions of the nonlinear polarization from higher order mechanisms for K_h system in the laboratory coordinates defined in Figs. 2-2-1(a) and 2-2-2(b), in Table A-1.

In the standard coordinates for O_h symmetry, the P_1 component of the nonlinear electric polarization is expressed with the general tensor expressions as follows.

$$P_1 = g_{1111}E_1\partial_1E_1$$
$$+ g_{1122}E_1\partial_2E_2 + g_{1133}E_1\partial_3E_3$$
$$+ g_{1212}E_2\partial_1E_2 + g_{1313}E_3\partial_1E_3$$
$$+ g_{1221}E_2\partial_2E_1 + g_{1331}E_3\partial_3E_1 \quad . \qquad \text{(A-6)}$$

It is worthwhile recalling that the forth rank tensor for O_h symmetry can be distinguished from that for K_h symmetry due to the relation.

$$g_{iijj} + g_{ijij} + g_{ijji} \neq g_{iiii}$$

Therefore, we introduce a parameter g^a which express the deviation from K_h symmetry as follows.

$$g_{iiii} = (g_{iiii} - g_{iijj} - g_{ijij} - g_{ijji}) + g_{iijj} + g_{ijij} + g_{ijji} = g^a + g_{iijj} + g_{ijij} + g_{ijji}$$
$$(g^a = g_{iiii} - g_{iijj} - g_{ijij} - g_{ijji}) \qquad \text{(A-7)}$$

Using the relations which are fulfilled in O_h symmetry,

$$g_{1122} = g_{1133} = g_{iijj},\ g_{1212} = g_{1313} = g_{ijij},\ g_{1221} = g_{1331} = g_{ijji},\ g_{1111} = g_{iiii} = g_{iijj} + g_{ijij} + g_{ijji} + g^a \qquad \text{(A-8)}$$

eq. (A-7) is expressed as

$$\begin{aligned}
P_1 &= g_{iijj}E_1(\partial_1 E_1 + \partial_2 E_2 + \partial_3 E_3) \\
&+ g_{ijij}(E_1\partial_1 E_1 + E_2\partial_1 E_2 + E_3\partial_1 E_3) \\
&+ g_{ijji}(E_1\partial_1 + E_2\partial_2 + E_3\partial_3)E_1 \\
&+ g^a E_1\partial_1 E_1 \\
&= g_{iijj}E_1(\partial_1 E_1 + \partial_2 E_2 + \partial_3 E_3) \\
&+ \frac{1}{2}g_{ijij}\partial_1(E_1E_1 + E_2E_2 + E_3E_3) \\
&+ g_{ijji}(E_1\partial_1 + E_2\partial_2 + E_3\partial_3)E_1 \\
&+ g^a E_1\partial_1 E_1
\end{aligned} \qquad \text{(A-9)}$$

According to the same procedure, the P_2 and P_3 components can be also obtained, so that we get the expression

$$P_\nu = g_{iijj}E_\nu(\nabla \cdot \boldsymbol{E}) + \frac{1}{2}g_{ijij}\partial_\nu(\boldsymbol{E} \cdot \boldsymbol{E}) + g_{ijji}(\boldsymbol{E} \cdot \nabla)E_\nu + g^a E_\nu\partial_\nu E_\nu \qquad \text{(A-10)}$$

In many papers [1-9], P_ν is expressed with the form

$$P_\nu = \beta E_\nu(\nabla \cdot \boldsymbol{E}) + \gamma\partial_\nu(\boldsymbol{E} \cdot \boldsymbol{E}) + (\delta - \beta - 2\gamma)(\boldsymbol{E} \cdot \nabla)E_\nu + \zeta E_\nu\partial_\nu E_\nu$$
$$(\beta = g_{iijj},\ \gamma = \frac{1}{2}g_{ijij},\ \delta - \beta - 2\gamma = g_{ijji},\ \zeta = g^a) \qquad \text{(A-11)}$$

In this expression, the first three terms have an isotoropic character, while the last term depends on the crystal orientation. We consider the transformation about the last term from the crystal

to the laboratory coordinates defined in Figs. 2-2-1(a) and 2-2-1(b), since the first three term are invariant under this transformation because of the isotoropic character. Therefore, we rewrite eq. (A-10) or (A-11) as

$$P_v = g_{iijj}E_v(\nabla \cdot \boldsymbol{E}) + \frac{1}{2}g_{ijij}\partial_v(\boldsymbol{E} \cdot \boldsymbol{E}) + g_{ijji}(\boldsymbol{E} \cdot \nabla)E_v + g^a \kappa E_v \partial_v E_v \qquad \text{(A-12)}$$

$$(P_v = \beta E_v(\nabla \cdot \boldsymbol{E}) + \gamma\partial_v(\boldsymbol{E} \cdot \boldsymbol{E}) + (\delta - \beta - 2\gamma)(\boldsymbol{E} \cdot \nabla)E_v + \zeta\kappa E_v\partial_v E_v) \quad , \qquad \text{(A-13)}$$

where κ is a forth rank tensor defined for the crystal coordinates which have only the components

$$\kappa_{1111} = \kappa_{2222} = \kappa_{3333} = 1 \quad . \qquad \text{(A-14)}$$

If we treat the SHG from the (001) surface in the laboratory coordinates illustrated in Figs. 2-2-1(a) and 2-2-1(b), the tansformation matrix is described as

$$\begin{pmatrix} a_{11} & a_{12} & a_{13} \\ a_{21} & a_{22} & a_{23} \\ a_{31} & a_{32} & a_{33} \end{pmatrix} = \begin{pmatrix} \cos\varphi & \sin\varphi & 0 \\ -\sin\varphi & \cos\varphi & 0 \\ 0 & 0 & 1 \end{pmatrix} \quad , \qquad \text{(A-15)}$$

and the tensor components in laboratory coordinates $\kappa^L_{\alpha\beta\gamma\delta}$ are calculated by

$$\kappa^L_{\alpha\beta\gamma\delta} = \Sigma\, a_{\alpha i}a_{\beta j}a_{\gamma k}a_{\delta l}\kappa_{ijkl} \quad , \qquad \text{(A-16)}$$

so that we obtain the expressions in the laboratory coordinates

$$P_\alpha = g_{iijj}E_\alpha(\nabla \cdot \boldsymbol{E}) + \frac{1}{2}g_{ijij}\partial_\alpha(\boldsymbol{E} \cdot \boldsymbol{E}) + g_{ijji}(\boldsymbol{E} \cdot \nabla)E_\alpha + g^a \Sigma\, \kappa^L_{\alpha\beta\gamma\delta}E_\beta\partial_\gamma E_\delta \quad . \qquad \text{(A-17)}$$

$$(P_\alpha = \beta E_\alpha(\nabla \cdot \boldsymbol{E}) + \gamma \partial_\alpha(\boldsymbol{E} \cdot \boldsymbol{E}) + (\delta - \beta - 2\gamma)(\boldsymbol{E} \cdot \nabla)E_\alpha + \zeta \Sigma \kappa^L_{\alpha\beta\gamma\delta} E_\beta \partial_\gamma E_\delta)$$

(A-18)

We summarized the expressions of the nonlinear polarization in higher order mechanisms for O_h system in the laboratory coordinates in Table A-2.

Table A-1 Expressions of nonlinear polarizations in higher order mechanisms for K_h system in the laboratory coordinates illustrated in Figs 2-2-1(a) and 2-2-1(b). Here only the elements which contribute to SHG in each polarization condition are listed.

p→p	$P_1 = g_{iijj}E_1(\partial_1 E_1 + \partial_3 E_3) + \frac{1}{2}g_{ijij}\partial_1(E_1^2 + E_3^2) + g_{ijji}(E_1\partial_1 + E_3\partial_3)E_1$
	$P_3 = g_{iijj}E_3(\partial_1 E_1 + \partial_3 E_3) + \frac{1}{2}g_{ijij}\partial_3(E_1^2 + E_3^2) + g_{ijji}(E_1\partial_1 + E_3\partial_3)E_3$
s→p	$P_1 = \frac{1}{2}g_{ijij}\partial_1(E_2^2)$
	$P_3 = \frac{1}{2}g_{ijij}\partial_3(E_2^2)$
45°→s	$P_2 = g_{ijji}(E_1\partial_1 + E_3\partial_3)E_2$
p→s	$P_2 = 0$
s→s	$P_2 = 0$

In this caluculation, we used only the relation $\partial_2=0$. However, further transfigurations which are also dependent on the geometries (Figs. 2-2-1(a) and 2-2-1(b)) can be made as described in the section 2-2C.

Table A-2 Expressions of nonlinear polarizations in higher order mechanisms for O_h system in the laboratory coordinates illustrated in Figs. 2-2-1(a) and 2-2-1(b). The relation between the crystal coordinates and the laboratory coordinates is defined in the section 2-2-B. Here only the elements which contribute to SHG in each polarization condition are listed.

p→p	$P_1 = g_{iiij}E_1(\partial_1 E_1 + \partial_3 E_3) + \frac{1}{2}g_{ijij}\partial_1(E_1^2 + E_3^2) + g_{ijji}(E_1\partial_1 + E_3\partial_3)E_1$ $+ g^a\kappa^L_{1111}E_1\partial_1 E_1$
	$P_3 = g_{iiij}E_3(\partial_1 E_1 + \partial_3 E_3) + \frac{1}{2}g_{ijij}\partial_3(E_1^2 + E_3^2) + g_{ijji}(E_1\partial_1 + E_3\partial_3)E_3$ $+ g^a\kappa^L_{3333}E_3\partial_3 E_3$
s→p	$P_1 = \frac{1}{2}g_{ijij}\partial_1(E_2^2) + g^a\,\kappa^L_{1212}E_2\partial_1 E_2$
	$P_3 = \frac{1}{2}g_{ijij}\partial_3(E_2^2)$
45°→s	$P_2 = g_{ijji}(E_1\partial_1 + E_3\partial_3)E_2$ $+ g^a\,(\kappa^L_{2111}E_1\partial_1 E_1 + \kappa^L_{2211}E_2\partial_1 E_1 + \kappa^L_{2112}E_1\partial_1 E_2 + \kappa^L_{2212}E_2\partial_1 E_2)$
p→s	$P_2 = g^a\,\kappa^L_{2111}E_1\partial_1 E_1$
s→s	$P_2 = g^a\,\kappa^L_{2212}E_2\partial_1 E_2$

$$\kappa^L_{1111} = a_{11}a_{11}a_{11}a_{11}\kappa_{1111} + a_{12}a_{12}a_{12}a_{12}\kappa_{2222} = \frac{1}{4}(\cos 4\varphi + 3)$$
$$\kappa^L_{3333} = \kappa_{3333} = 1$$
$$\kappa^L_{1212} = a_{11}a_{21}a_{11}a_{21}\kappa_{1111} + a_{12}a_{22}a_{12}a_{22}\kappa_{2222} = \frac{1}{4}(1 - \cos 4\varphi)$$
$$\kappa^L_{2111} = a_{21}a_{11}a_{11}a_{11}\kappa_{1111} + a_{22}a_{12}a_{12}a_{12}\kappa_{2222} = -\frac{1}{4}\sin 4\varphi$$
$$\kappa^L_{2112} = a_{21}a_{11}a_{11}a_{21}\kappa_{1111} + a_{22}a_{12}a_{12}a_{22}\kappa_{2222} = \frac{1}{4}(1 - \cos 4\varphi)$$
$$\kappa^L_{2211} = a_{21}a_{21}a_{11}a_{11}\kappa_{1111} + a_{22}a_{22}a_{12}a_{12}\kappa_{2222} = \frac{1}{4}(1 - \cos 4\varphi)$$
$$\kappa^L_{2212} = a_{21}a_{21}a_{11}a_{21}\kappa_{1111} + a_{22}a_{22}a_{12}a_{22}\kappa_{2222} = \frac{1}{4}\sin 4\varphi$$

In this caluculation, we used only the relation $\partial_2=0$. However, further transfigurations which are also dependent on the geometries (Figs. 2-2-1(a) and 2-2-1(b)) can be made as described in the section 2-2C.

References

[1] N. Bloembergen, R. K. Chang, S. S. Jha, and C. H. Lee, Phys. Rev. **174**, 813 (1968).

[2] H. W. K. Tom, T. F. Heinz, and Y. R. Shen, Phys. Rev. Lett. **51**, 1983 (1983).

[3] J. A. Litwin, J. E. Sipe, and H. M. van Driel, Phys. Rev. B **31**, 5543 (1985).

[4] G. Lüpke and G. Marowsky, Appl. Phys. B **53**, 71 (1991).

[5] J. E. Sipe, D. J. Moss, and H. M. van Driel **35**, 1129 (1987).

[6] B. Koopmans, A. M. Janner, H. T. Jonkman, G. A. Sawatzky, and F. van der Woude, Phys. Rev. Lett. **71**, 3569 (1993).

[7] B. Koopmans, A. M. Janner, H. A. Wierenga, Th. Rasing, G. A. Sawatzky, F. van der Woude, Appl. Phys. A **60**, 103 (1995).

[8] H. W. K. Tom, G. D. Aumiller, and C. H. Brito-Cruz, Phys. Rev. Lett. **60**, 1438 (1988).

[9] G. Mizutani, Y. Sonoda, S. Ushioda, T. Maeda, and J. Murota, Jpn, J. Appl. Phys. **34**, L119 (1995).

List of Publications

Related to this thesis

1) "In-Situ Observation of SHG and Its Origin in Vacuum Deposited Copper Phthalocyanine Film"
H. Hoshi, T. Yamada, K. Kajikawa, K. Ishikawa, H. Takezoe, and A. Fukuda.
Mol. Cryst. Liq. Cryst. **267**, 1-6 (1995).

2) "Origin of Second-Harmonic Generation in Vacuum-Evaporated Copper Phthalocyanine Film"
T. Yamada, H. Hoshi, K. Ishikawa, H. Takezoe, and A. Fukuda.
Jpn. J. Appl. Phys. **34**, L299-L302 (1995).

3) "Second-harmonic generation in centrosymmetric molecular films: Analysis undar anisotropic condition"
H. Hoshi, T. Yamada, K. Ishikawa, H. Takezoe, and A. Fukuda.
Phys. Rev. B **52**, 12355-12365 (1995).

4) "Second Harmonic Generation from Various Phthalocyanine Film and its Spectral Dependence"
T. Yamada, T. Manaka, H. Hoshi, K. Ishikawa, H. Takezoe, and A. Fukuda.
Nonlinear Optics **15**, 193-196 (1996).

5) "Second Harmonic Generation From Centrosymmetric Phthalocyanines"
T. Yamada, H. Hoshi, K. Ishikawa, H. Takezoe, and A. Fukuda.
Nonlinear Optics **15**, 131-138 (1996).

6) "Anisotropic second harmonic generation of electric quadrupolar origin in copper phthalocyanine films epitaxially grown by molecular beam epitaxy"
H. Hoshi, T. Yamada, K. Ishikawa, H. Takezoe, and A. Fukuda.
Phys. Rev. B **53**, 12663 (1996).

7) "Resonant Enhancement of Second-Harmonic Generation of Electric Quadrupolar Origin in Copper Phthalocyanine Films"

T. Yamada, H. Hoshi, T. Manaka, K. Ishikawa, H. Takezoe and A. Fukuda.
Phys. Rev. B **53**, R13314 (1996).

Others

1) "Selective Dissociation of Merocyanine J-aggregate with Linealy Polarized Laser Light Studied by Optical Second Harmonic Generation"
T. Yamada, K. Kajikawa, K. Ishikawa, H. Takezoe, and A. Fukuda.
Thin Solid Films **226**, 173-177 (1993).

2) "L film of Dye-attached Polyamic Acid and the Imidization Process of its LB Film Studied by Second-Harmonic Generation"
T. Yamada, S. Yokoyama, K. Kajikawa, K. Ishikawa, H. Takezoe, A. Fukuda, M. Kakimoto, and Y. Imai.
J. Photopolymer Sci. and Tech. **6**, 197-200 (1993).

3) "Second Harmonic Generation in a Langmuir Monolayer of the New Amphiphilic Coordination Compound Pentacyano(4-octadecylaminopyridine)-ferrate(III)"
F. Armand, H. Sakuragi, K. Tokumaru, T. Yamada, K. Kajikawa, H. Takezoe, S. Okada, H. Matuda, and H. Nakanishi.
Molecular Engineering **2**, 315-324 (1993).

4) "Various Orientation of Pendant Dye Attached to Polyamic Acid Langmuir and Langmuir-Blodgett Films Studied by an Optical Second-Harmonic Generation Interferometry Technique"
T. Yamada, S. Yokoyama, K. Kajikawa, K. Ishikawa, H. Takezoe, A. Fukuda, M. Kakimoto, and Y. Imai.
Thin Solid Films **244**, 754-757 (1994).

5) "Imidization Process in a Dye-Labeled Poly(amic acid) Langmuir-Blodett Film Studied by Optical Second-Harmonic Generation"
T. Yamada, S. Yokoyama, K. Kajikawa, K. Ishikawa, H. Takezoe, A. Fukuda, M. Kakimoto, and Y. Imai.
Langmuir **10**, 1160-1163 (1994).

6) "Novel Orientation of Azobenzene Pendant Group in Hybrid Monolayers Composed of Polyimide Langmuir-Blodgett Film and Alkyl Polysiloxane Self-Assembled Monolayer"
S. Yokoyama, T. Yamada, K. Kajikawa, M. Kakimoto, Y. Imai, H. Takezoe, and A. Fukuda.
Langmuir **10**, 4599-4605 (1994).

7) "Thickness Dependence of the Epitaxial Structure of Vanadyl Phthalocyanine Film"
H. Hoshi, K. Hamamoto, T. Yamada, K. Ishikawa, H. Takezoe, A. Fukuda, S. Fang, K. Kohama, and Y. Maruyama.
Jpn. J. Appl. Phys. **33**, L1555-L1558 (1994).

8) "Helicoidal distributed-feedback cavity action in a ferroelectric liquid crystal"
T. Furukawa, T. Yamada, K. Ishikawa, H. Takezoe, and A. Fukuda.
Applied Physics B **60** 485-487 (1995).

9) "Phase of Second Harmonic Generation in Ultra Thin Films"
K. Kajikawa, T. Isoshima, H. Sasabe, W. Knoll, T. Yamada, and H. Takezoe.
Nonlinear Optics **15**, 127-130 (1996).

10) "Absolute Orientation of Pendant Chromophore Attached to Polymer Backbone in Monolayers at Interfaces Studied by Phase Measurement of Second-Harmonic Generation"
K. Kajikawa, T. Yamada, S. Yokoyama, S. Okada, H. Matsuda, H. Nakanishi, M. Kakimoto, Y. Imai, H. Takezoe, and A. Fukuda.
Langmuir **12**, 580-583 (1996).

11) "Observation of the Electric-Dipole-Forbidden States in Polydiacetylene by Means of Resonance Second-Harmonic Generation Spectroscopy"
T. Manaka, T. Yamada, H. Hoshi, K. Ishikawa, H. Takezoe, and A. Fukuda.
Jpn. J. Appl. Phys. **35**, L831 (1996).

12) "Orientation of Liquid Crystal Molecules on Side-Chain Polyimide Alignment Layer Studied by Second Harmonic Generation Interferometry"

T. Sakai, K. Shirota, T. Yamada, H. Hoshi, K. Ishikawa, H. Takezoe, and A. Fukuda
Jpn. J. Appl. Phys. **35**, 296 (1996).

13) "Surface Structure and Orientation of Polyamic Acid Alkylamine Salt Langmuir-Blodgett Films Having An Azobenzene Pendant Unit"
S. Yokoyama, M. Kakimoto, Y. Imai, T. Yamada, K. Kajikawa, H. Takezoe, and A. Fukuda
Thin Solid Films **273**, 254 (1996).

Acknowledgments

I would like to express my deep gratitude to Professor Hideo Takezoe for his helpful advice, careful concern and encouragement throughout this work. I am sincerely grateful to Professor Atsuo Fukuda and Professor Ken Ishikawa for their guidance and thoughtful comments not only about this work but also about various topics. I gratefully wish to thank Professor Takehiko Mori, Professor Youkoh Kaizu and Professor Fujio Minami for their kindest efforts concerning this dissertation.

I gratefully acknowledge helpful discussions and collaboration with Dr. Hajime Hoshi. I also acknowledge valuable discussions with Mr. Takahiro Nishioka and collaboration with Mr. Takaaki Manaka. I am thankful to Dr. Kotaro Kajikawa (Nagoya University) who gave me his technique on SHG experiment. I am indebted to all the member in our laboratory for their kindness and cooperation.

Finally, I would like to thank my parents and sister for their continuous support and understanding.

This work was supported by Japan Society for the Promotion of Science.

Toshiki Yamada

September, 1996